Natland, J.H., Dick H.J.B., Miller, D.J., and Von Herzen, R.P. (Eds.)
Proceedings of the Ocean Drilling Program, Scientific Results Volume 176

11. Magnetic Susceptibility as an Index of the Lithology and Composition of Gabbros, ODP Leg 176, Hole 735B, Southwest Indian Ridge[1]

James H. Natland[2]

ABSTRACT

During Leg 176, magnetic susceptibility was measured at a 4-cm spacing on all gabbroic rock recovered from Hole 735B using a Bartington sensor attached to the shipboard multisensor track. The instrument was particularly sensitive to the presence of magmatic magnetite, which is consistently intergrown with more abundant ilmenite. These oxide minerals together range from trace amounts to >30% of the rocks. The log of magnetic susceptibility thus produced a pattern of abrupt and pronounced spikes whenever oxide-bearing and oxide-rich gabbros were encountered. It provides a detailed, precise, *high-resolution* means of evaluating this aspect of gabbro lithology. The log reveals a far more intricate pattern of oxide gabbros cross-cutting and intruding primitive olivine gabbros and troctolites with low magnetic susceptibility than was possible to discern by eye during preparation of the shipboard core descriptions. Magnetic susceptibility confirms and reinforces the observation that oxide gabbros are typically more strongly deformed than olivine gabbros and troctolites, and it also shows that late-stage felsic veins are very strongly associated with oxide gabbros.

Because magmatic magnetite is always intergrown with ilmenite, there is a strong correlation between magnetic susceptibility and the bulk TiO_2 contents of rocks with >0.7% TiO_2, which represents ~1% by volume of oxide minerals in the rock. Among olivine gabbros and troc-

[1]Natland, J.H., 2002. Magnetic susceptibility as an index of the lithology and composition of gabbros, ODP Leg 176, Hole 735B, Southwest Indian Ridge. *In* Natland, J.H., Dick, H.J.B., Miller, D.J., and Von Herzen, R.P. (Eds.), *Proc. ODP, Sci. Results*, 176, 1–69 [Online]. Available from World Wide Web: <http://www-odp.tamu.edu/publications/176_SR/VOLUME/CHAPTERS/SR176_11.PDF>. [Cited YYYY-MM-DD]
[2]Rosenstiel School of Marine and Atmospheric Science, University of Miami, Miami FL 33149, USA.
jnatland@rsmas.miami.edu

Initial receipt: 12 October 2000
Acceptance: 6 August 2002
Web publication: 24 October 2002
Ms 176SR-008

tolites, which have <0.7% TiO_2 contents, the correlation is weaker and is not significantly influenced by tiny variations in the proportions of magmatic oxides; instead, magnetic susceptibility among these rocks correlates more strongly with extent of differentiation, as marked by a decrease in bulk-rock MgNo. The correlation may indicate a higher proportion of exsolved magnetite in the somewhat more iron-rich ferromagnesian silicates and plagioclases of the olivine gabbros. The shipboard-based conclusion that the section cored consists of several sequential plutons, each more differentiated upward, breaks down in light of the magnetic susceptibility log. The upper parts of the three so-called plutons cored during Leg 176 instead are places where late-stage, intrusive disseminated oxide and oxide gabbros are particularly concentrated. The olivine gabbros and troctolites that they intrude have a different, unrelated pattern of compositional variability. In many cases, iron-rich melts penetrated the fine-scale porosity structure of crystallizing primitive gabbros, enriching them in oxide minerals but not modifying compositions of preexisting olivine. Several zones where particularly magnesian olivine gabbros and troctolites with very low magnetic susceptibilities are concentrated may represent places where the lower crust was significantly inflated by intrusion of primitive basalt at or near the ridge axis, before the oxide gabbros were emplaced and before significant crystal-plastic deformation occurred. The body of rock beneath a fault zone at 1100 meters below the seafloor is distinct, with more primitive olivine gabbros and troctolites than in the rocks above, far fewer seams of oxide gabbro, much less deformation, and far more widely separated felsic veins.

INTRODUCTION

This paper deals with a new nondestructive technique for evaluating the igneous stratigraphy, structure, and composition of cores of gabbroic rock. I illustrate its utility by comparing the measurement to observations on cores recovered from Ocean Drilling Program (ODP) Hole 735B, Southwest Indian Ridge, during Leg 176 and to the bulk compositions of the rocks. The technique is one previously applied to problems in high-resolution stratigraphy of marine sediments obtained by hydraulic piston coring from *JOIDES Resolution.* It provides results of comparable detail and quality on continuously cored gabbro.

During ODP Leg 118, downhole logging of magnetic susceptibility in Hole 735B recorded variations between gabbros rich in the magmatic oxides, ilmenite, and magnetite, which produced sharp peaks, and oxide-poor olivine gabbros and troctolites, which produced the intervening lows (Pariso et al., 1991). The peaks, or high-susceptibility spikes, were most numerous near the top and bottom of the 490 m logged, and there was one longer interval between ~220 and 280 meters below the seafloor (mbsf) with systematically high magnetic susceptibility (Fig. F1). The pattern of peaks accords well with the placement of oxide gabbros in descriptions of the recovered core (Shipboard Scientific Party, 1989).

The logging tool sensed the presence of magnetite. Pure magnetite has a very high magnetic susceptibility (κ = 3 SI units) (Collinson, 1983; Hunt et al., 1995), as does pyrrhotite, whereas the susceptibilities of other ferrimagnetic minerals likely to be in the rocks (e.g., ilmenite and hematite) are one to three orders of magnitude smaller, and silicate minerals have κ = 0.001 SI. Of the oxide minerals and sulfides, ilmenite

F1. Leg 118 downhole log magnetic susceptibility vs. depth, p. 33.

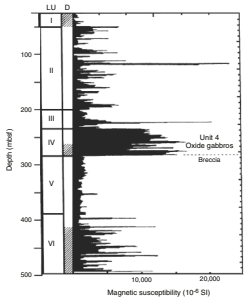

(κ = ~0.009 SI) is the only one besides magnetite that is volumetrically significant in any of the rocks. It is always intergrown with magnetite and in many rocks with tiny amounts of globular magmatic sulfide, which includes pyrrhotite (Natland et al., 1991; Natland and Dick, 2001). Ilmenite and magnetite together comprise between ~2% and 30% of the mode of oxide gabbros and gabbronorites, ~1%–2% of disseminated oxide gabbros and gabbronorites and <1% (oftentimes <<1%) of olivine gabbros, troctolitic gabbros, and troctolites. Only the latter rocks may contain more magmatic pyrrhotite than magnetite. Measurements of magnetic susceptibility on minicores of these lithologies decrease by about two orders of magnitude in that order.

There are at least three types of magnetite in the gabbros (Natland et al., 1991; Shipboard Scientific Party, 1999b). The most abundant is magmatic in origin. It is actually a solid solution of magnetite ($Fe^{2+}Fe_2^{3+}O_4$) and ulvöspinel ($Fe_2^{2+}TiO_4$) or Mt-Usp_{ss} (Natland et al., 1991). The ilmenite intergrown with it is a solid solution of ilmenite ($FeTiO_3$) and hematite (Fe_2O_3), or Il-Hem_{ss}, and it is usually several times more abundant than magnetite in the intergrowths. The two minerals are present as platelike intergrowths; rarely is ilmenite exsolved from magnetite (Shipboard Scientific Party, 1989).

The second variety is almost pure magnetite. It is much finer grained and forms during alteration along with secondary amphibole and layer-lattice silicates replacing olivine and pyroxenes. A third variety is also nearly pure Mt, and it formed by exsolution from olivine, pyroxenes, and plagioclase during high-temperature subsolidus recrystallization of the rocks (Shipboard Scientific Party, 1999b). Such magnetite is not volumetrically important in oxide gabbros, but it may be the most important magnetic mineral in olivine gabbros and troctolites, especially in the usual case where the rocks are very little altered. Because magmatic oxides crystallize late during the differentiation of basaltic magma and often have particular relationships to gabbroic textures (Natland et al., 1991; Natland and Dick, 1996, 2001), any systematic nondestructive measure of the abundance of magmatic oxides is potentially a very useful petrogenetic index.

Although there was no magnetic logging during Leg 176, magnetic susceptibility was routinely and systematically measured on recovered rock, which amounted to >86% of the 1003.2 m cored during the leg, using a Bartington MS2C sensor integrated with the multisensor track (MST). This is the same instrument that is used to detect fluctuations in magnetic susceptibility of marine sediments obtained by piston coring. During Leg 176, measurements were almost always at 4-cm spacing and were made as the rock was carried along a moving track through the instrument, in the same way and at the same scale as measurements on sediments. The measurements were obtained on whole-round core immediately after the pieces of rocks were spaced in half liners, thus are directly related to curated depth, the measure by which cores are described, photographed, and sampled. Additional measurements were made on 339 minicore samples at an average spacing of ~3 m. The MST, on the other hand, was able to resolve local concentrations of magmatic iron-titanium oxides on the scale of only a few centimeters, and these could later almost always be identified visually in the cores (Shipboard Scientific Party, 1999b). The measurements show that the pattern of spikes originally seen in the downhole log of Leg 118 persists into deeper rock and exists on the scale of the individual piece of rock measured in a single section of core. Several hundred large and small spikes in magnetic susceptibility, each spike only a few centimeters to a few

tens of centimeters in length, were thus recorded between 504 and 1008 mbsf. MST magnetic susceptibility data therefore provide a novel and potentially extremely precise means to evaluate gabbro lithology in cores. The recovery during Leg 176 was also sufficiently high that the measurements provide a statistically valid assessment of the proportion of rocks with high magnetic susceptibility, thus with high concentrations of iron-titanium oxides, throughout the long section cored.

In this paper, I illustrate some of the ways in which spikes in magnetic susceptibility coincide with lithologic features of the core. I also demonstrate that there are strong correlations between magnetic susceptibility and chemical attributes of the rocks related to the abundance of ilmenite and magnetite, thus that magnetic susceptibility is a useful and quantitative geochemical log. It can even provide information about the dispersed and low, but nevertheless varying, concentrations of magnetite in olivine gabbros and troctolites. Combining the logging results from Leg 118 with the MST data from Leg 176 provides the only nondestructive log pertaining to the bulk composition of the rocks obtained over the entire core. It provides a means of refining estimates of the bulk composition of the entire section.

CONVENTIONS, PROTOCOLS, AND EDITING OF THE DATA FILE

Magnetic susceptibility (κ) is given in dimensionless SI (Système Internationale) units. Minicore measurements made during Leg 176 are listed as volume-normalized SI units $\times 10^{-6}$ (Shipboard Scientific Party, 1999b, table T11), whereas output from the MST is recorded in machine units (MU $\times 10^{-6}$), but these measurements are not volume normalized. Conversion to SI units requires multiplication by a geometric calibration constant (C) that depends on the core diameter. For a whole core of diameter 66 mm, C = 0.66, and this is conventionally applied to MST measurements of magnetic susceptibility of sediments. However, spot measurements of full-round gabbro core during Leg 176 gave diameters of 58.5 to 59.5 mm, thus application of this constant is not quite correct.

As noted in the site report (Shipboard Scientific Party, 1999b), MST data for magnetic susceptibility recorded during Leg 176 were degraded by three other factors: (1) in some cases, the spacing of rock in the liners meant that there was no rock in the core as it passed through the instrument; (2) in other cases, the rock was either rubble or had less than full core diameter; and (3) the readings from the MST saturate and wrap around at machine values over 10,000 (e.g., a true value of 10,500 would appear as 500 in the data set). To use the data set in more than a qualitative way means that it should be edited to remove measurements made on core not having a full-round core diameter and that instances of machine saturation should be identified.

I have accordingly screened the data set in the following ways. First, all measurements not made on full-round core were deleted. Second, measurements within 2–4 cm of ends of whole-round pieces separated by plastic dividers were also deleted. During Leg 176, the half-width of the peak produced by a point-element of susceptible material (a nail) was found to be 5 cm. "For a rock of even the nominal 6.6 cm diameter to yield its true volume-normalized value requires a sample at least ten

centimeters long" (Shipboard Scientific Party, 1999a, p. 77). Measurements within 10 cm of the end of a piece are degraded.

Two factors mitigate this effect, however. The first is that highly susceptible zones of core are rarely point sources; they are seams of rock rich in magnetite dispersed over some centimeters and they are usually inclined. The second is that except at the ends of sections, gaps containing plastic spacers between pieces are usually only 1–3 cm. Such narrow gaps do not produce the same drop-off in measured susceptibility as the abrupt end of a section. Thus rocks of low susceptibility usually have no obvious drops in susceptibility within 2 cm of the ends of pieces, as long as those pieces are closely spaced.

However, examination of several narrow but strong peaks in the data showed full drop-offs to background levels within 4 cm of maxima produced by very narrow oxide-rich seams. Predicted measurements are higher (Fig. F2). In the case of Sample 176-735B-139R-1 (Piece 7) shown in Figure F2, the apparent drop-off was such that the measurement should have exceeded 10,000 × 10^{-6} MU, and the next underlying measurement was also too low because it came at the end of Section 139R-1. The predicted values are indicated by the blue dashed line. Some uncertainty exists in the vicinity of a felsic vein that obliquely crosses the core at the end of the section and beginning of the next. This is indicated by question marks. The appropriate response is exhibited by the lower drop-off to the peak centered at 872.64 mbsf at the top of Section 176-735B-139R-2. Using this type of evaluation, I therefore usually chose to delete two measurements at spacer gaps between full-round pieces, the one at or nearest the spacer and the one measurement closest to it in the rock on either side. This was always done by comparison of the listed location of the measurements to the graphic representation of the core on the site report barrel sheets and, sometimes, to core photographs. Of the 22,678 original measurements, this left 18,971 measurements at 4-cm spacing on full-round core, representing 758.84 m of rock (18.08 m of this was at 2-cm spacing). This is 75.6% of the 1003.2 m drilled in Hole 735B during Leg 176. In the annals of attempts to recover whole-round core of igneous rock by rotary coring from a wave-tossed platform in deep water, this is an extraordinarily high figure.

Finally, in the midst of 15 high-susceptibility peaks, a single value abruptly drops to levels no greater than the nearest background measurements—too much of a drop-off. I assume these to be values above the saturation limit and have added 10,000 × 10^{-6} MU to them.

With all of these adjustments, I then compared minicore measurements of magnetic susceptibility (Shipboard Scientific Party, 1999b, table T11) to the nearest MST measurements (Fig. F3). Linear and power-law regressions fit the data similarly, both having standard deviations $r > 0.8$. The slope on the linear regression gives a value for C of 0.62. However, the regression does not fit values with low magnetic susceptibility particularly well. Forcing the regression through the origin increases C to 0.71 with little change in standard deviation. The slope of the data field is better matched, but the bulk of the data are offset from the regression. The power-law regression matches the log-log linearity of the data well, is not offset, and has a higher correlation coefficient than either variant of the linear regression.

My main interest here, however, is in the relative differences of values measured on whole-round core. To the extent that core diameters are consistent to within a small error, the machine units, which are not volume normalized, are perfectly adequate to describe variations in the core and to compare with geochemical or other data obtained on the

F2. Effects of gaps at piece edges and machine saturation on magnetic susceptibility, p. 34.

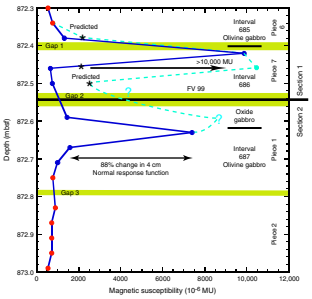

F3. Magnetic susceptibility of minicores vs. MST, p. 35.

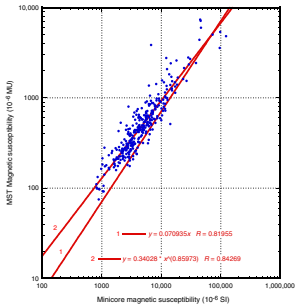

same rocks. In most of the following, I consequently use machine units ($\times 10^{-6}$ MU). Comparison to the susceptibility well log obtained during Leg 118, however, requires the geometrical correction. The correction factor, C = 0.66, splits the difference between the two values for C given by the different ways of calculating the linear regression, and I use this to provide consistency with the way the data were plotted in the site report (Shipboard Scientific Party, 1999b). The power-law relationship works better for high values of magnetic susceptibility, but since these represent only a small percentage of minicores, the relationship may be an artifact of sampling. The differences between this and applying the simple correction affect only a small percentage of the core and are not sufficient to affect general relationships.

What explains the scatter about any of the regressions? Besides the imprecision inherent in the repeatability of any measurement, the objects being compared are not identical. First, the Bartington sensor loop samples a volume with a 5-cm half-width, and oxide minerals usually are unevenly distributed in whole-round core. Minicores are much smaller and sample the oxides in the working half in a different way. Over some hundreds of comparisons between MST and minicore measurements, however, this effect should even out. Similarly, X-ray fluorescence (XRF) bulk compositions were determined either on slab samples or on quarter-round samples obtained from the working half of the core. These also sampled oxide minerals in a different way than did the Bartington sensor. Once again, however, over many samples, the effect should even out.

The final editing procedure was to separate peaks from background. This involved an assumption that there were sharp boundaries to intervals bearing magmatic iron-titanium oxides. This certainly is the case for the rocks themselves, for which the presence and abundance of magmatic oxides is a critical aspect of the lithologic identification (Shipboard Scientific Party, 1999a). In almost all cases, abrupt spikes in susceptibility, even small ones of a few hundred machine units above a definable background, are the norm. However, as shall be demonstrated, background values themselves shift around, and maximum values for small peaks at one place can be the same as background levels elsewhere. The range of background measurements is from just below 100×10^{-6} to 800×10^{-6} MU, with fluctuations occurring on a scale of several to several tens of meters. Within this range, there can be oscillations of ~200×10^{-6} MU from one measurement to the next; these are still in excess of the sensitivity of the Bartington sensor. Rather than choosing an arbitrary value to separate peaks from background, I therefore examined plots of the data at 50-m intervals, in each case separating individual peaks from whatever their immediate background happened to be. On this basis, 62.8% of full-round measurements are at background levels, representing oxide-poor lithologies, mainly olivine gabbros and troctolites, and 37.2% are peaks representing oxide-bearing and oxide-rich lithologies, mainly disseminated oxide and oxide gabbros, gabbronorites, and olivine gabbronorites. Some gabbronorites, however, have low magnetic susceptibility, and some olivine gabbros have relatively high magnetic susceptibility, a factor we shall have to consider more carefully later on. Measurements of susceptibility >2000×10^{-6} MU comprise 8.6% of the total and represent prominent seams of oxide gabbro.

The following is illustrated with images scanned from whole-round core, split core, slab samples, thin sections, photomicrographs, and core

photos. Usually, I have somewhat sharpened the contrast of these images by computer, and in some cases I have expanded the horizontal scale, but otherwise I have left them alone. Details of image adjustments will be found in the figure captions. Of the various image types, only those obtained from whole-round core may be unfamiliar to the reader. Whole-round images were obtained on every cylindrical piece obtained during Leg 176 using a DMT Digital Color CoreScan system by rotating the core around its cylindrical axis with the camera line scan positioned so that it is parallel to the axis of rotation (see Shipboard Scientific Party, 1999a). Core pieces were placed consistently in the liner using a reference line drawn by one of the structural geologists using a wax marker. This line was always drawn to maximize the apparent dip of inclined fabric in the rock on split surfaces of the core. This is the basis for the "Core Reference Frame," against which variations in the orientation of all structural elements and magnetic declination were compared in the site report (Shipboard Scientific Party, 1999b). The result is an "unrolled" image, from 0° to 360°, oriented left to right, in which planar features such as fractures and joints have a sinusoidal pattern, the amplitude of which increases with the dip of the feature. The images were intended to augment borehole images from the Formation MicroScanner and to allow full reorientation of the core. I use them here simply to depict features of the core related to fluctuations in magnetic susceptibility.

I have also tried to relate magnetic susceptibility and the features imaged to core descriptions, whether from the barrel sheets in the site report or itemized in spread sheets included as supplemental material to the site report (Shipboard Scientific Party, 1999b). The principal descriptive unit during both Legs 118 (Dick et al., 1991) and 176 was the "lithologic interval," which is taken to be any length of core >5 cm in thickness that consists of a single rock type that is distinguishable from its surroundings in mineralogy (principally, presence or absence of olivine or oxide minerals), grain size, or texture. Igneous intervals have sharp, diffuse, or sutured contacts that variously represent tectonic or intrusive relationships. Textures can be magmatic, thus undeformed, or they may exhibit brittle or ductile deformation, including cataclastic, gneissic, porphyroclastic, mylonitic, and ultramylonitic fabrics. An exception to the 5-cm lower limit to describable lithologic intervals is leucocratic, or *felsic* veins, of which 203 are annotated in the igneous veins spreadsheet in the supplemental material to the site report. These were millimeters to a few centimeters wide. I have numbered these sequentially downward in annotations on the figures. The term "felsic" was chosen as the primary descriptor because starkly white sodic plagioclase is the most abundant mineral in the veins, which have low color index. However, the veins range from diorite to granodiorite in composition, most being trondhjemite, and contain quartz, sodic plagioclase, minor green amphibole, and, in some cases, traces of magnetite, apatite, and zircon. Most felsic veins have sharp contacts, thus are intrusive, but some are dispersed or diffuse. Shipboard descriptions indicate a common association between felsic veins and intervals of oxide gabbro. Data for magnetic susceptibility provide a means of investigating this relationship.

PRINCIPAL RESULTS

Figure F4 is a plot of the edited measurements vs. depth, and it supplants figure F120 of the site report (Shipboard Scientific Party, 1999b). Scales for both MU and volume-corrected SI units are provided on the bottom and top of the figure, respectively. There are 476 individual peaks and peak regions with values of susceptibility >2000 × 10^{-6} MU, with the frequency of these spikes diminishing generally but sporadically downward. There are few such peaks below 1100 mbsf. Peak regions are collections of peaks spaced over several tens of centimeters that oscillate at high values of several thousand × 10^{-6} MU and that have no intermediate background values. Almost all of these were identified as intervals of oxide gabbro or oxide olivine gabbro in the core descriptions, although their internal fluctuations in magnetic susceptibility suggest that they have uneven internal concentrations of oxide minerals. In some cases, the internal oscillations are at average high values of magnetic susceptibility (Fig. F5), and in others, the fluctuations are more extreme (Fig. F6). In some places, individual peaks, some of them quite pronounced, are fairly widely spaced (Fig. F7). Some lithologic intervals have only small oscillations in magnetic susceptibility above background (e.g., gabbronorite interval 562 in Fig. F6). In all of these instances, there are at least some measurements, even within oxide gabbro intervals at background levels (red portions of the susceptibility variations shown in Figs. F5, F6, and F7). This attests to the presence of minor amounts of relatively primitive gabbro crosscut by, or perhaps occurring as xenoliths in, oxide gabbro at a very fine scale in these rocks.

Defining the width of the peak or peak region as the span of measurements having >2000 × 10^{-6} MU, and in this way clipping fall-offs representing the tail ends of the point-source response function, the average peak width is 13.4 cm, with a high standard deviation reflecting a range of widths between 176 and 4 cm. The true average is probably less than this because 4 cm is the lower limit of resolution of the MST and there are many narrow seams of oxide gabbro <1 cm in width. Some of these cross the core obliquely and are recorded in two or three consecutive measurements. Nevertheless, the lower 1000 m of core from Hole 735B is dominated by olivine gabbros and troctolites; these lithologies provide the background measurements of magnetic susceptibility. The olivine gabbros and troctolites are crosscut by a great many seams of oxide gabbro, *the largest of which* is <2 m thick in the portion of the hole cored during Leg 176.

Most of the wider peak regions between 500 mbsf and the bottom of the hole having widths of >50 cm are between 504 and 710 mbsf (Fig. F8). The percentage of core represented by peaks also diminishes downward in the section (Fig. F9). The region of core between 600 and 700 mbsf has >80% oxide-bearing and oxide-rich gabbro because many of the peak regions are fairly wide and closely spaced. The MST susceptibility measurements reveal that there is scarcely an interval of relatively primitive olivine gabbro or troctolite that is utterly without some proportion of rock enriched in oxide minerals, even if that material causes only small fluctuations in susceptibility.

Assuming that all peaks in magnetic susceptibility in some measure represent late-stage intrusive rocks, then there should be an underlying and possibly unrelated variability in the more primitive olivine gabbros and troctolites that magnetic susceptibility might reveal. Figure F10

F4. Edited MST magnetic susceptibility, p. 36.

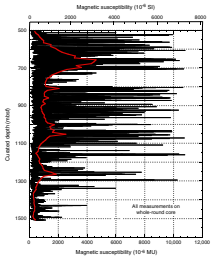

F5. Magnetic susceptibility for a typical peak region, 70–706.5 mbsf, p. 37.

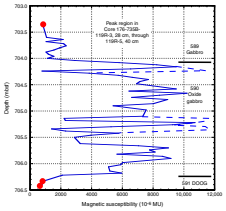

F6. Magnetic susceptibility for two peak regions, 652–662 mbsf, p. 38.

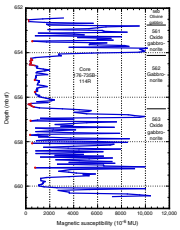

F7. Magnetic susceptibility, 1071–1084 mbsf, p. 39.

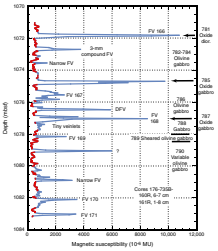

F8. Thicknesses of peaks and peak regions, 500–1500 mbsf, p. 40.

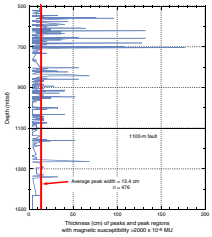

shows that there are indeed variations beyond the general oscillation in background measurements. Fluctuations are indicated by two smoothing curves fit to the data. The black curve is a weighted fit, one of the standard ones provided by the plotting program, Kaleidagraph. This fit encompasses a data point and 10% of the surrounding data and intrinsically produces discontinuities at either end of the plot, where data are tied to the terminal data points. It reveals fluctuations in magnetic susceptibility, thus proportion of oxide minerals, at a fairly coarse scale of perhaps 100 m, assuming that there are approximately the same numbers of measurements in each 100 m of the core depicted. There are five oscillations, delimited at their minima by dashed horizontal lines, and numbered to the right.

The second curve with more spikes is an interpolated function that passes through sequential data points and matches the slopes at those points. There are 23 small peaks on this curve, defining fluctuations in slope presumably marking shifts in composition. This curve effectively indicates the preponderance of background measurements within intervals of ~20 m length. Finally, downward spikes on the overall susceptibility curve with values <250 × 10^{-6} MU indicate where the most primitive gabbroic rocks, olivine gabbros and troctolites, were detected.

The most important feature of Figure **F10** is an abrupt offset in background magnetic susceptibility to lower values downcore at 1100 mbsf. This corresponds to a fault zone over ~30 m of the core, in which there are numerous small faults having both normal and reversed senses of displacement (Shipboard Scientific Party, 1999b). Background susceptibilities are, on the whole, higher above this fault than below it, and there are only two maxima at the 100-m scale of variability above the fault, whereas there are four lesser maxima, shifted to lower values, below it. There is also no strong correspondence between the coarse maxima in background susceptibility and those portions of the core having high proportions of oxide-rich seams, represented by peaks and peak regions in the downhole susceptibility trend.

Another way to consider these data is to assume that the material recovered in each core is fully representative of the interval cored, even if recovery was fairly low. Figure **F11** thus shows the average background magnetic susceptibility by core plotted vs. depth, with another 10% weighted curve, this time smoothing many fewer data points. Nevertheless, the weighted curves in Figures **F10** and **F11** are very similar, and the core-by-core fluctuations in Figure **F11** resemble the interpolated curve in Figure **F10.**

Of greatest interest is whether the shifts in background magnetic susceptibility reveal the pattern of cryptic variation in mineral compositions among the principal gabbroic facies cored in Hole 735B. The issue is complicated because the rocks are cumulates, and in such rocks the proportions of oxide minerals may vary not merely because one rock is more differentiated than another, but also because the percentage of intercumulus melt, from which the oxides crystallized, can vary because of differences in the amount of postcumulus overgrowth on surrounding silicates, expulsion of intercumulus melt by compaction and deformation, and even reintroduction of differentiated melt into the fine-scale porosity structure of the crystallizing rocks (Natland et al., 1991). A second possibility is that among these rocks, magmatic oxides may be present in such small abundance that they do not matter at all. If so, then another cause for variations in magnetic susceptibility must be sought. A correlation between magnetic susceptibility and the general extent of differentiation of rocks *lacking* magmatic oxides then becomes

F9. Percent peaks and percent background measurements, 500–1500 mbsf, p. 41.

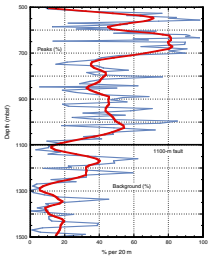

F10. Background magnetic susceptibility, 500–1500 mbsf, p. 42.

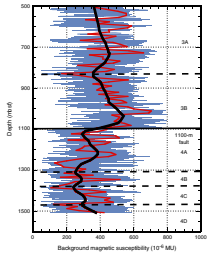

F11. Average background magnetic susceptibility by core, 500–1500 mbsf, p. 43.

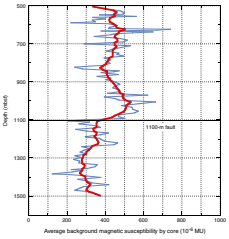

of unusual importance, no matter how it is caused. This would tie magnetic susceptibility to what petrologists have usually termed the *cryptic variation* (Wager and Deer, 1939) of intrusive bodies, namely the variation in composition of silicate minerals, which tracks differences of temperature of the magmas that produced the minerals (e.g., Usselman and Hodge, 1978). Then the fluctuations in magnetic susceptibility in Figures **F10** and **F11,** whether construed as 2, 5, 23, or more in number, could reflect the volume and frequency of magma injection and the fluctuations in magma temperature that prevailed when this bit of ocean crust was accreting. This whole topic requires attention to the relationship between magnetic susceptibility and the bulk compositions and silicate mineralogy of the gabbros, which will be considered toward the end of this paper.

COMBINING RESULTS OF LEGS 118 AND 176

Figure **F12** compares results from downhole measurement of magnetic susceptibility obtained during Leg 118 (Pariso et al., 1991) with the edited MST measurements on Leg 176 rocks, both transformed to SI units. There is a small data gap between the deepest downhole measurement at 490 mbsf and the first MST measurement at 504 mbsf. The chief difficulty in making this comparison is that the logging tool and the Bartington sensor sampled different volumes of rock in different geometrical relationships. The downhole log looked outward, sensing rock in the wall of the hole. It was sensitive, among other things, to borehole diameter. The Bartington sensor looked inward, toward a column of core 6.6 cm in diameter. Its measurements were very refined by comparison. To ameliorate this a bit, I coarsened the line thickness for the plot of MST measurements in order to merge oscillations in high-magnetic susceptibility spikes to a scale of ~2 m. My intention, however, is primarily to show *where* there are concentrations of high-susceptibility spikes and to derive some sense of their amplitudes. On this basis, the entire core can be divided into several distinctive "susceptibility regions," (Fig. **F12**) with lithologic inferences based on core descriptions, as follows:

F12. Merged magnetic susceptibility log, Hole 735B, p. 44.

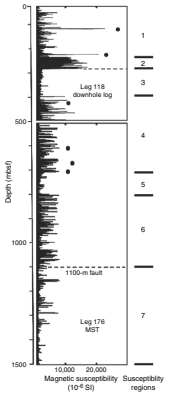

0–220 mbsf. This has numerous oscillations between background measurements recording olivine gabbros and spikes with moderately high magnetic susceptibility recording oxide gabbros, with one of these having very high magnetic susceptibility.

220–280 mbsf. Principally oxide gabbros with very high magnetic susceptibility.

280–400 mbsf. A zone with virtually no high-susceptibility spikes, made up of olivine gabbros and troctolites.

400–690 mbsf. Another zone with rock alternating between low susceptibility and narrow seams with moderately high magnetic susceptibility.

680–770 mbsf. Another zone of fairly primitive gabbro and few high-susceptibility oxide gabbros.

770–1100 mbsf. A third zone of high-susceptibility spikes alternating with background gabbros, with the fault mentioned earlier at its base.

1100–1504 mbsf. The longest zone of primitive gabbro, having low susceptibility, with few high-susceptibility spikes.

Gabbros with the highest magnetic susceptibility are concentrated in the upper 500 m of the core drilled during Leg 118. These include the two very strong, but narrow, spikes detected by the downhole log and the entire interval of oxide gabbros constituting lithologic Unit IV, from 220 to 280 mbsf. For comparison, I have also plotted the three highest minicore measurements of magnetic susceptibility obtained during each of Legs 118 (Kikawa and Pariso, 1991) and 176 (Shipboard Scientific Party, 1999b). These all exceed the logged measurement of magnetic susceptibility at their corresponding intervals, as might be expected when oxide-rich rock can be directly sampled by a paleomagnetist drilling a small minicore. On the other hand, corrected background measurements by MST and on minicores are very similar. Below 700 mbsf, however, almost all minicore measurements were obtained on olivine gabbros and troctolites; only two of the large spikes in MST magnetic susceptibility have corresponding minicores, indicating the preference of shipboard paleomagnetists to sample representative core rather than narrow intervals of unusual material.

Figure F13 compares the susceptibility measurements in 20-m intervals, whether on minicores above 500 mbsf or using the MST below that. Proportions of measurements both above background and above 2000×10^{-6} MU are given in the right panel, with the proportion of core in the same intervals described as oxide gabbro in the shipboard descriptions in the left. Bear in mind that only 6–12 measurements of magnetic susceptibility on minicores were made in each 20 m of the upper 500 m of core, whereas there are usually >200 measurements per 20 m from the MST. There is a strong correspondence between the curves for strong peaks ($>2000 \times 10^{-6}$ MU) and proportions of oxide gabbros, indicating the approximate equivalence of the human eye and the MST at detecting obvious seams of oxide gabbro. The proportions of oxide gabbro fluctuate strongly throughout the core but are clearly higher upward in each 500-m portion of the core, with the substantial zone of oxide gabbros (lithologic Unit IV) flaring out at 250 mbsf. The fault at 1100 mbsf is not evident in the distribution of strong spikes in magnetic susceptibility, but it is apparent as an abrupt drop in the sum of measurements above background, given by the red curve. There is no way as yet to extend this curve to the upper 500 m of the core.

F13. Oxide gabbro, oxide gabbronorite, and oxide olivine gabbro, p. 45.

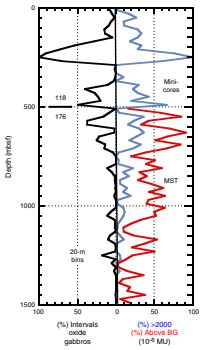

EXAMPLES OF LITHOLOGY LINKED TO MAGNETIC SUSCEPTIBILITY

Several different features of the core can be linked to peak regions and narrow spikes in magnetic susceptibility. These include oxide concentrates or seams—some of them deformed, felsic veins, and vein nets associated with oxide gabbros and other types of igneous breccias. I provide a sampling here, not an inventory.

Peak Regions

Figure F14 depicts a peak region in Sections 176-735B-114R-1 and 11R-2; the several prominent spikes in magnetic susceptibility correspond to lithologic interval 561, an oxide gabbronorite. In the core photograph in the site report, oxide-rich material is systematically darker than rock composed mainly of silicate minerals. I have enhanced the contrast of a portion of the core photograph strongly to highlight

F14. Magnetic susceptibility, 652.5–654.5 mbsf, p. 46.

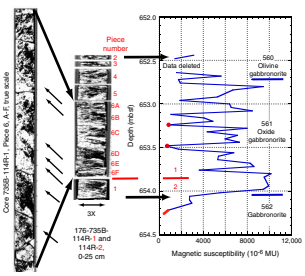

the incidences of oxide-rich material. These appear as irregular patches in the true-scale image on the left, with a suggestion of a steeply dipping preferred orientation to some of them (arrows). Apart from this suggestion, the rocks are not described as being deformed in the core description, nor do they contain felsic veins (Shipboard Scientific Party, 1999b). A weaker orthogonal pattern of boundaries to the oxide-rich patches is probably shadowing along curving rock-saw marks. The left image is that of a single piece of rock that is in several subpieces (Section 176-735B-114R-1 [Pieces 6A–F]). These together comprise only a portion of the lithologic interval. I have compressed the image and widened it by a factor of three in the central image, including as well the rest of the core in the interval, to provide a direct correlation to the plot of magnetic susceptibility on the right. Each of the several shaded regions rich in oxide minerals corresponds to one of the spikes in magnetic susceptibility. The inclined boundaries to the oxide-rich patches are actually easier to see in the compressed image. In Section 176-735B-114R-1 (Pieces 2–5), the inclined pattern is not apparent, probably because the cores were split in a different orientation. This is because the rocks themselves are not foliated, and foliation was the principal criterion by which whole-round core was oriented in the core reference frame.

Figure **F15** shows an unrolled image of a portion of Section 176-735B-154R-3. The entirety of lithologic interval 730, a disseminated oxide gabbro, was recovered within a single, unbroken piece of whole-round core. It corresponds to a peak region in magnetic susceptibility ~50 cm long, in which there are two spikes of 4000×10^{-6} MU. The unrolled image reveals that there are five fairly sharp planar boundaries with low dip paralleling the planar boundaries of the interval and three others that are more diffuse (solid and dashed lines in the sketch to the left). The upper and lower planar boundaries were identified as contacts in the site report, but not the intervening ones. Brackets therefore indicate six previously undetected subintervals, bounding darker or lighter rock that is coarser or finer grained or more leucocratic. The rock beneath is identified as a seventh subinterval on the scale of the scanned image. Susceptibility spikes correspond to subintervals 3 and 6. There are also two more steeply inclined fractures 95–118 cm from the top of the section, both clearly unrelated to the contacts above. Most of lithologic interval 730 is described as weakly foliated (degree of deformation = 1), but subinterval 6 and the top few centimeters of the olivine gabbro beneath it are more strongly deformed (degree of deformation = 3 and 2, respectively).

F15. Magnetic susceptibility, 1008.1–1009.1 mbsf, p. 47.

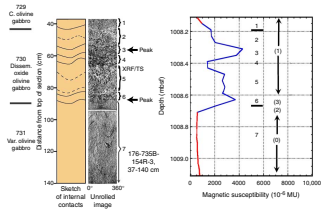

Figure **F16** shows a peak region in Section 156-735B-156R-7 having similar but mostly more strongly deformed subintervals. The peak region corresponds to lithologic interval 742, an oxide gabbro that is variably deformed but again having rock that is darker and lighter or with variable grain size and extent of deformation. The maximum susceptibility is almost $10{,}000 \times 10^{-6}$ MU, nearly the saturation limit of the Bartington detector. The extent of deformation is somewhat higher than in the core shown in Figure **F15.** There are 10 subintervals indicated in the sketch, with the lower interval boundary, described as a planar tectonic contact in the core descriptions, present at the base of the ninth. The upper boundary at the top of this piece of rock (and placed at the top of this section) was evidently not entirely recovered, although it is described as planar in the core descriptions.

F16. Magnetic susceptibility, 1032.6–1033.3 mbsf, p. 48.

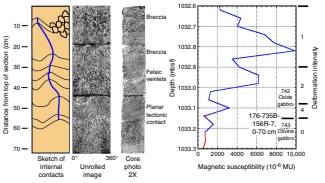

The subinterval planar contacts are not parallel, as indicated by the shifting of their sinusoidal patterns in the unrolled image and sketch,

although this is not so apparent in the core photograph. The upper two subinterval boundaries warp beneath a coarse-grained breccia. There are two igneous breccias and one interval with narrow felsic veinlets, with the most prominent peaks in magnetic susceptibility corresponding to one of the breccias (subinterval 3) and the veinlets (subinterval 5). Lithologic interval 742 is ~23 m below interval 730 shown in Figure F15. Interval and subinterval contacts have similar low dips in both.

The last three figures in sequence fairly characterize the range in lithologic variability represented by peak regions in magnetic susceptibility in the core recovered during Leg 176. The internal spikes and troughs of peak regions clearly represent variable lithologies and extents of deformation that have actually been imaged, although they were not described in detail during the leg. The planar subinterval boundaries of Figures F15 and F16 are almost certainly tectonic in origin because they parallel tectonic interval contacts, are distorted around breccias, and subdivide the rock into zones of different extents of deformation. Adjacent olivine gabbro in these two instances is undeformed except near the interval contacts, and this relationship is a common one at peak regions elsewhere.

A general impression is that peak regions with oxide gabbros having a diffuse or patchy distribution of oxides (e.g., Fig. F15) are more prevalent from 700 to 900 mbsf, whereas the narrower peak regions below that are more extensively deformed. The narrower bands of differentiated rock in the rocks beneath therefore seem to have served to concentrate deformation in narrow subintervals, whereas in portions of the section where oxide gabbros are wider and more abundant, it was more widely distributed or dispersed. Even at that, the oxide-rich zones in the rock shown in Figure F15 have the suggestion of planar boundaries about them, so that the rocks were probably not completely undeformed.

Whether oxide gabbros consistently served to localize high-temperature deformation, perhaps because they retained some melt at the time, was strongly debated during Leg 176. An *association* was noted between portions of core containing oxide gabbros and zones of highly deformed rock (Dick et al., 2000). This meant that although oxide gabbros might be close to deformed rock, and even themselves somewhat deformed, they were often not the most deformed rock in a zone of gradationally increasing or variable deformation fabric. This is borne out by the two examples of Figures F15 and F16. However, within these two lithologic intervals, described, respectively, as disseminated-oxide gabbro and oxide gabbro, the intervals themselves overall are more deformed than surrounding rock, and the most oxide-rich portions of them—revealed by individual peaks in magnetic susceptibility and contrast-enhanced images—are subintervals bounded by planar, tectonic, internal contacts. Deformation was clearly concentrated *at* each of the two more oxide-rich intervals, but it was not necessarily *most* concentrated where oxide minerals are most abundant in the rocks. Instead, in both cases, it is at the basal contacts, where differences in the rheological responses of the rocks to deformation presumably were greatest. The *association* between oxide gabbros and deformation therefore is not coincidental at all. It is intimate, if not precisely corresponding in degree.

Felsic Veins

A total of 203 felsic veins are sufficiently prominent to have been annotated in a vein-log spreadsheet (I-vein.xls) that is supplemental to the

core descriptions (Shipboard Scientific Party, 1999b). These usually have sharp, planar contacts at high angles to full-round cored surfaces; however, some are irregular or form complicated vein networks. There are some inconsistencies between the core descriptions and the vein log. In particular, some veins are intimately bound with zones of deformation, and some of these are noted on the core barrel sheets but not included in the vein log. In some cases, the associated oxide gabbro seams are not noted, although they are evident in core photos, especially when the contrast is somewhat enhanced, and were detected by measurement of magnetic susceptibility.

The leading petrogenetic question concerning these veins is how they might be related to the next most differentiated rocks in the section, namely the oxide-bearing and oxide-rich gabbros. Magnetic susceptibility provides much information on this score and shows that the connection to oxide gabbros is extremely strong. Most of the veins are associated with oxide gabbros and, indeed, are present within oxide-rich peak regions that have, on the whole, the greatest magnetic susceptibilities in the section. However, there are many instances where the veins reached into primitive rock and modified them both physically and chemically.

The first large felsic vein encountered during Leg 176 is one of the latter (Fig. **F17**). The vein itself is almost 4 cm wide. It is embedded in olivine gabbro and contains aligned fragments of the host rock in its center. There is a bleached corona of reacted material on its margins. Above and below the vein, just out of the range of the photograph, the olivine gabbro has magnetic susceptibility at a background level given by the gray background on the plot next to the core photo. Within the piece of rock traversed by the vein, magnetic susceptibility is slightly higher than background, but it is just below background where the vein was most strongly detected by the Bartington sensor in whole-round core.

In Figure **F18,** a larger and more complicated vein network is shown using an unrolled image. A portion of the vein network is also shown in a close-up core photograph. The vein fills an array of vertical and inclined fractures. The associated magnetic susceptibility exceeds 2000 × 10^{-6} MU, with the peak corresponding to a slightly darker patch of oxides in the center of the unrolled image, between 33 and 38 cm from the top of the section.

Figure **F19** depicts a 1-cm felsic vein in a deformation zone. The vein bisects a deformed seam of oxide gabbro that was detected as a sharp doublet in magnetic susceptibility, with a peak in excess of 6000 × 10^{-6} MU centered just above the vein and rising above background (see inset). The larger peak of the doublet lies just above the region of the inset, which shows only the lower of the two peaks. The deformation intensity is strongest right at the vein, although the vein itself is undeformed. The seam is not described as oxide gabbro, but was included within lithologic interval 693, olivine gabbro. Nevertheless the oxide minerals are plainly visible in the close-up core photograph. In Figure **F18,** to make this more apparent, I have expanded a portion of the photograph in the lower two images and both enhanced the contrast in the first enlargement and then selected only the oxides in the second. Adjusting the contrast brightens the specular reflection of the visible light spectrum from the alkalic feldspars in the vein more than from the calcic plagioclases in the surrounding olivine gabbro. The oxide minerals in the vein are part of the gabbroic host rock that the vein has engulfed.

F17. Prominent felsic vein, p. 49.

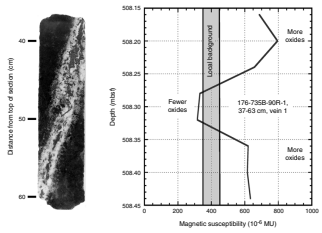

F18. Felsic material filling fractures and surrounding angular fragments, p. 50.

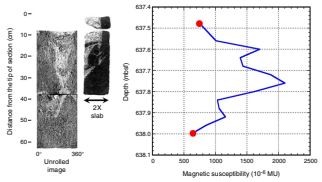

F19. Felsic vein with oxide-rich gabbro, p. 51.

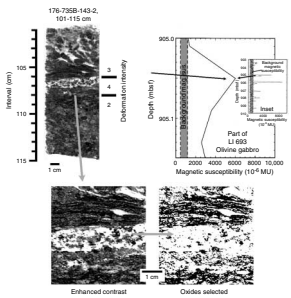

Figure F20 depicts a similarly deformed zone in troctolite (lithologic interval 718) about 58 m farther down the core. Once again, a seam of foliated oxide gabbro with an extremely strong spike in magnetic susceptibility has the highest deformation intensity. Enhancing the contrast of the scan of a close-up photograph brings out its presence. Some brighter felsic material is distributed in the deformed rock above the seam, and there is an irregular lozenge—a deformed felsic vein—about 20 cm farther up. It is clearly caught up in the foliated fabric of the rock. Once again, neither the lithology of the felsic lozenge nor of the oxide-rich seam was noted in the core descriptions, although the deformation of both was depicted graphically. Thus, instead of being an example of strong deformation in rock other than oxide gabbro, this is a deformed oxide gabbro that incorporated a preexisting felsic vein.

The difficulty of identifying oxide-bearing and oxide-rich gabbro in deformed rock carried down to some very narrow zones of deformation. Figure F21 shows a strongly deformed band ~8 cm thick that was simply described as a shear zone in lithologic interval 550, an olivine gabbro. The extent of deformation is strongest at both contacts. Contrast enhancement of both the unrolled image and the scanned split surface of the core (slab) reveals streaks of felsic material in the deformed rock. The deformed zone also corresponds to a small but unmistakable peak in magnetic susceptibility, indicating a concentration of magmatic oxides at the basal, most deformed contact. Gabbro above and below the shear zone is very coarse grained, with that beneath almost appearing to be brecciated.

Felsic material in oxide-rich rock corresponding to some of the wider and undeformed peak regions is not always distributed in veins. Instead, it can be as patchy as the oxide minerals. Figure F22 shows four different images of the same portion of Section 176-735B-131R-1, taken from the core photograph and corresponding to lithologic interval 648, oxide gabbro. The swirly pattern of the felsic material is more distinctly contrasted against dark gray silicate minerals, mainly clinopyroxene, and black oxides in the adjacent image (Fig. F21). The oxides and felsic swirls are separately selected (black), respectively, in Figure F21. An analyzed sample from between 10 and 15 cm below the top of the section has very high TiO_2 and enough Zr to show the influence of the felsic swirls (Snow et al., Chap. 12, this volume). This rock appears to exemplify imperfect segregation of felsic material from the oxide gabbro in which it differentiated.

Net Veins and Vein Breccias

A number of felsic vein networks (or net veins) and vein breccias are in the core recovered during Leg 176. These are rocks in which angular fragments of gabbro are bounded by fine, millimeter-scale felsic veins. In vein networks, the fragments are still in their original relative positions. In vein breccias, they are disrupted. The small size of the veins and their dispersed arrangement in the rocks meant that many of these were not noted in the igneous vein log. I have not investigated magmatic breccias with felsic veins systematically but provide examples showing a close connection between some of them and zones of high magnetic susceptibility in the core.

Figure F23A–F23F, is a gallery of net veins and vein breccias in slab samples, arranged in order of depth. Narrow and irregularly distributed felsic veinlets show up as light gray to nearly white, and the veins in each sample contain quartz, based on examination with a hand lens.

F20. Deformed oxide gabbro seam, p. 52.

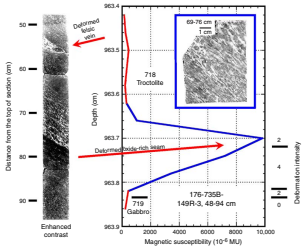

F21. A narrow mylonite/ultramylonite zone, p. 53.

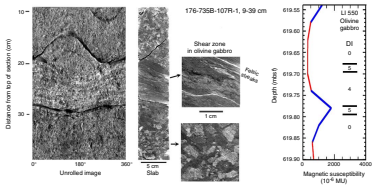

F22. Oxide gabbro with three magnetic susceptibility peaks, p. 54.

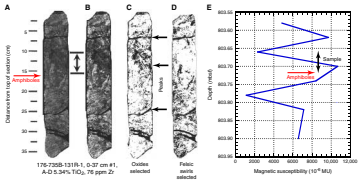

F23. Slab samples with felsic veinlets or vein nets cementing breccias, p. 55.

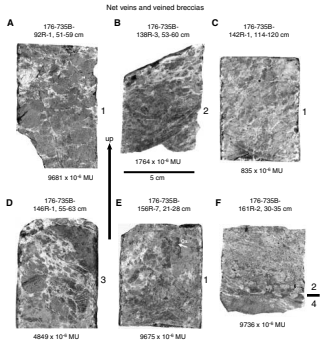

The maximum of magnetic susceptibility is indicated below each image. The extent of plastic deformation in the darker matrix, ranging from slightly deformed (1) to mylonitic (4) is indicated to the right of each image. None are undeformed. Only one of these samples, shown in Figure F23C, has low magnetic susceptibility. The host rock is olivine gabbro. The breccias shown in Figure F23B and F23D were also identified as olivine gabbro, but this is inconsistent with the high magnetic susceptibility measured in the same intervals. The sample shown in Figure F23A was identified as a disseminated oxide olivine gabbro in the core descriptions, but again the same interval has the very high magnetic susceptibility of a much more oxide-rich gabbro. In the sample shown in Figure F23D, fragments of the host rock clearly constitute a disrupted breccia. Although the sample in Figure F23E appears almost equally brecciated, in fact most of the fragments are conformal to the direction of relatively weak foliation in the rock on either side. The sample in Figure F23F is olivine gabbro with gneissic fabric, coarsening downward to an abrupt contact with a fine-grained mylonitic oxide gabbro. Felsic veinlets are dispersed parallel to the gneissic fabric and into the mylonite.

In each case, formation of felsic veinlets followed plastic deformation. In each case, a drop in temperature accompanying magmatic differentiation was attended by a shift from plastic to brittle deformation. In each case, variably foliated rocks were then irregularly disrupted and infiltrated by the extreme late differentiates forming in the section. All of this occurred at high temperature, above the liquidus temperature for differentiates of basaltic parents (~1000°C for anhydrous liquids according to Dixon and Rutherford, 1979). Veining of deformed rock also occurred higher in the section, in the thick interval of oxide gabbros (lithologic Unit IV), where trondhjemite intrusion breccias crosscut foliated oxide gabbros (Dick et al., 1991a, plate 5.1). Near the top of the hole, trondhjemite, or fluids from which a felsic leucosome precipitated, intruded amphibole gneiss in the plane of foliation, possibly in the manner of lit-par-lit injection (Dick et al., 1991, plate 5.2). In every case, there is a strong association between felsic veins and oxide gabbros, which during Leg 176 were without exception indicated by high magnetic susceptibility.

Other Magmatic Breccias

The cores of Hole 735B contain dozens of magmatic breccias in oxide gabbros with few or no felsic veinlets. I show one example. Figure F24 depicts unrolled and slabbed images of a single piece of core entirely spanning lithologic interval 555, gabbro, and portions of the intervals above and below. Two fracture surfaces bound the breccia (sinusoidal patterns in the unrolled image), the upper of which appears to be magmatically annealed. The breccia fragments are extremely coarse grained and evidently were originally part of a pegmatitic gabbro. Now they are twisted and bent. Lithologic interval 555 also spans a strong spike in magnetic susceptibility, exceeding 7000 × 10^{-6} MU, although no corresponding concentration of oxide minerals was noted in the core descriptions. A second spike is in undeformed rock below the breccia. Some contrast enhancement applied to the unrolled image suggests that felsic material may have concentrated in porosity structure near the bounding fracture surfaces of the breccia.

F24. Coarse pegmatitic breccia with high magnetic susceptibility, p. 56.

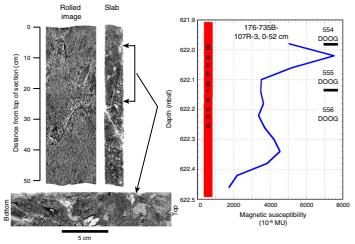

SUMMARY OF THE RELATIONSHIP BETWEEN FELSIC VEINS AND OXIDE GABBROS

Although felsic veins crosscut all rock types, they appear most frequently to be associated with oxide gabbros. Magnetic susceptibility allows this relationship to be assessed quantitatively. Figure F25 is a histogram of magnetic susceptibility intensities for the 196 felsic veins that crosscut whole-round core at the intervals where they occur in the core, out of 203 altogether. Nearly 60% of the veins have values of magnetic susceptibility >800 × 10^{-6} MU at the precise intervals where they were sampled and thus have susceptibilities clearly higher than background olivine gabbros and troctolites; 26.5% of them have values >2000 × 10^{-6} MU and thus correspond to seams of oxide gabbro.

The immediate value of magnetic susceptibility at a vein, however, does not indicate the overall susceptibility of the peak region cut by the vein, which might be more appropriate to consider. Accordingly, I divided peak regions into two types: (1) those containing one or more felsic veins and (2) those without felsic veins. Figure F26 shows weighted variations of each of these plotted vs. depth. Between 500 and 1100 mbsf, peak regions with veins have greater magnetic susceptibility than those without veins. Deeper than 1100 mbsf, there are fewer peak regions, these have lower magnetic susceptibility, and there are fewer felsic veins. Throughout the core, there is no correspondence between peak regions with or without veins and fluctuations in background magnetic susceptibility. Most significantly, magnetic susceptibility data show that felsic veins are most abundant amid oxide gabbros with *the highest* concentrations of oxide minerals. The intimate association of the veins and very oxide-rich rocks supports the interpretation that granitic liquids were the products of extreme high iron differentiation involving the prior precipitation of oxide minerals, the well-known Fenner trend of igneous differentiation (Fenner, 1929, 1931; Bowen and Schairer, 1935). That many of the oxide gabbros have variable, sometimes extensive, degrees of crystal-plastic deformation, whereas most granitic veins that cross them are undeformed, indicates that the molten material that froze in the veins was squeezed or expelled from nearly crystalline host oxide gabbros while they were being deformed. Some veins were later deformed themselves. This is one aspect of the process of differentiation by deformation described by Bowen (1920), or the synkinematic differentiation of Dick et al. (1991).

The fault at 1100 m in Figure F14 is also seen in a difference in vein frequency above and below it (Fig. F27A). The fairly even distribution of veins in the two portions of the core is surprising, given the uneven distribution of oxide gabbros that are the most important host of felsic veins. Vein volume per 10 m of core (Fig. F26B) is a better indication of where felsic material is concentrated, with peaks corresponding to local flattenings of the slope of the curve (its derivative) in Figure F27A. Differences between the crustal blocks above and below 1100 mbsf are still apparent, and the spikes in vein volume correlate in general with the distribution of oxide gabbros with high magnetic susceptibility (Fig. F4).

F25. Histogram of number of veins vs. magnetic susceptibility, p. 57.

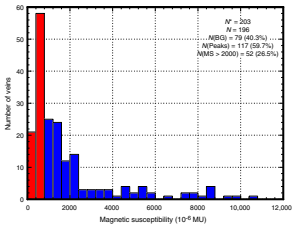

F26. 10% least-squared weighted curves of magnetic susceptibility vs. depth, p. 58.

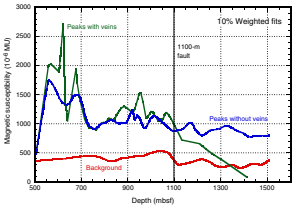

F27. Vein-log spreadsheet information, p. 59.

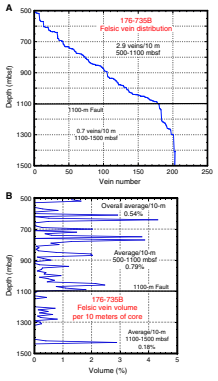

RELATIONSHIP BETWEEN OXIDE GABBROS AND DEFORMATION

Magnetic susceptibility also allows precise comparison between zones of deformation and occurrences of oxide gabbro. Evaluation of this for the entire core would provide substance for an entire paper on its own. At this time, I consider only a small 19.5-m segment of core, which provides some guidance on this score (Fig. F28). Core between 944.5 and 964 mbsf comprises the longest single interval obtained during Leg 176 in which rock is continuously deformed. The great majority of the segment has at least gneissic texture (crystal/plastic deformation grade 2). Much of it is porphyroclastic (grade 3), and there are seven intervals in which the rock is mylonitic or ultramylonitic (grades 4 and 5). Dips are consistent and relatively steep, averaging ~40° in the core reference frame.

The segment spans nine lithologic intervals, the thickest of which are gabbros and olivine gabbros. There are three narrow intervals of oxide gabbro plus an olivine microgabbro and a troctolite at the base of the sequence. Contacts between intervals dip conformably to the deformation. There are three felsic veins. This short segment thus spans almost the entire lithologic variability of rock from Hole 735B in the complicated, alternating pattern that is characteristic of the entire core.

The magnetic susceptibility log is given on the right side of Figure F28 and the deformation log on the left. The fluctuations in magnetic susceptibility reveal far more complexity to the 19.5 m of rock than is represented by the lithologic intervals. More of the rock is oxide rich and a great deal more of it is at least oxide bearing, than is suggested by the presence of only three narrow intervals of oxide gabbros (709, 711, and 715). Indeed, there are 27 peak regions in magnetic susceptibility rising above background levels in this single short sequence of rocks, 16 of which have magnetic susceptibilities exceeding 2000 × 10^{-6} MU. Most of these, obviously, went undetected by visual inspection of the core. Probably this has to do with the difficulty of recognizing fine-grained and dispersed oxide minerals in hand specimens of deformed rock unless their abundance is very high. In strongly foliated gabbros, ilmenite and magnetite tend to be dispersed around elongate silicates and are aligned parallel to the fabric (Fig. F29A). In oxide gabbros, they are concentrated in more visible bands where the oxides form shadow zones between aligned pyroxene porphyroclasts (Fig. F29B). The actual proportion of "background" olivine gabbro and troctolite, given by the gray portions of the susceptibility curve in Figure F28, is only 35.3%, whereas peak regions comprise 64.7% of the deformed segment.

All rocks with at least porphyroclastic texture coincide with either peak regions or narrow spikes in magnetic susceptibility. One ultramylonite and six mylonites are present at contacts between oxide gabbros (blue susceptibility peaks) and more primitive olivine gabbro or troctolite (gray background). In each case, the more deformed rock has higher magnetic susceptibility. The upper and lower contacts of the 19.5-m segment are both deformed and oxide rich. The lower contact is the mylonitic oxide-rich seam at ~77 cm from the top of the section shown in Figure F20. It was not accorded the status of a lithologic interval. The upper contact is shown in Figure F30. Interval 710, olivine gabbro, has gneissic fabric, and the pegmatitic oxide gabbro of lithologic interval 709 above it is described as porphyroclastic, although its crystal/plastic deformation grade is 0. The unrolled image and the core photograph

F28. Comparison of magnetic susceptibility with crystal-plastic deformation intensity, p. 60.

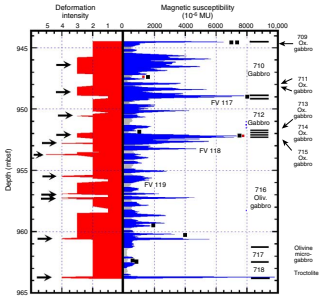

F29. Scans of oversized thin sections from deformed rock, p. 61.

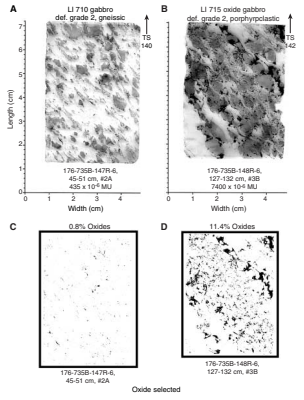

F30. Upper contact of deformed region, p. 62.

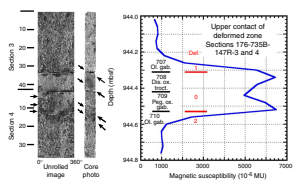

both show that there is a 2- to 3-cm seam of dark oxide gabbro, corresponding to the lower peak in the strong doublet in magnetic susceptibility plotted on the right. On the barrel sheet describing the core, this seam was included in interval 710, olivine gabbro, rather than in interval 709, the pegmatitic oxide gabbro. Interval 708 is an unusual fine-grained lithology, termed leucocratic disseminated-oxide troctolite, and it produced the upper peak of the high-susceptibility spike. Its contact with the olivine gabbro above it is inclined and parallel to several other contacts and deformation fabric just beneath, as indicated by the arrows next to the core photo, and farther downsection. The unrolled image suggests that pegmatitic material in interval 709 is actually distributed unevenly in fine-grained rock resembling that of interval 708, most of which wound up in the archive half of the core, whereas the working half was used for the core description.

The relationship between the distribution of oxide gabbros and deformation in this short segment of core epitomizes the principal structural problem of Hole 735B. The zones of greatest deformation coincide strongly with oxide gabbros where they are juxtaposed with more primitive olivine gabbros and troctolites. This can be asserted more confidently in light of correlations with magnetic susceptibility than it can just using visual descriptions of the core alone. Those provide only nine lithologic intervals without much clue about their relationships. However, this 19.5-m segment is a coherent structural entity in the core, bounded by a particular highly deformed oxide-rich lithology at both the top and bottom and with the same lithology internally punctuating the sequence at equivalently strongly deformed intervals at numerous points within. The intimate relationship between zones of deformation and oxide gabbros in this segment cannot be denied. The deformed oxide gabbros at the upper and lower contacts suggest that strongly differentiated, iron-rich magmas played a role in the structural emplacement of the entire segment, perhaps in the manner of lubricants, greatly reducing effective stress at the upper and lower shear boundaries.

The structural problem comes down to the question of whether deformation followed crystallization of strongly differentiated, iron-rich magmas that intruded more primitive rock or whether it facilitated migration of those differentiated magmas along dilatant zones of shear, the magmas then crystallizing while deformation was occurring (e.g., Natland et al., 1991; Natland and Dick, 2001). The choice depends in part on how closely zones of deformation correspond to occurrences of oxide gabbro. Obviously, if deformed rocks are not discerned visually as carrying oxide minerals, then the correspondence between deformation and oxide gabbros will be considered either weak or nonexistent. Magnetic susceptibility provides a great deal of additional information, more firmly demonstrating a connection between zones of deformation and the distribution of oxide gabbros.

As to the general case, Figure **F31** is a histogram for the number of magnetic susceptibility measurements (N = 1342) of different intensities that correspond to crystal/plastic deformation grades 2–5 (gneissic to ultramylonitic fabrics). Fully 65.9% of all such whole-round core recovered during Leg 176 occurs in peaks or peak regions, leaving 34.1% in background olivine gabbros and troctolites. Seams of oxide gabbro with magnetic susceptibility >2000 × 10^{-6} MU constitute 32.4% of the measurements. Given the different proportions of rock in the core, oxide gabbros are approximately six times more likely to have gneissic or greater deformation fabric than olivine gabbro and troctolite. Leaving out gneissic rocks, the association of deformation and oxide gabbros is

F31. Magnetic susceptibility histogram for strongly deformed rock, p. 63.

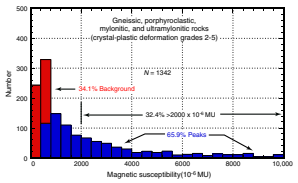

even more pronounced. Some 78% of porphyroclastic, mylonitic, and ultramylonitic rocks (deformation grades 3–5) are present at peaks and peak regions. Much of the remaining 22% is present in immediately adjacent olivine gabbros and troctolites, a consequence of the shear couple across contacts with strongly deformed oxide gabbros. An oxide gabbro (>2000 × 10^{-6} MU) is almost exactly 15 times more likely to have these strongly deformed fabrics than olivine gabbro or troctolite.

RELATIONSHIPS BETWEEN MAGNETIC SUSCEPTIBILITY AND ROCK COMPOSITIONS

Oxides and sulfides were lumped together as opaque minerals in point counts of gabbros from Hole 735B (Shipboard Scientific Party, 1989, 1999b); therefore, proportions of ilmenite to magnetite in the rocks were not determined by this means. In reflected light, the proportion of ilmenite to magnetite in oxide gabbros was estimated (not point counted) to be at least 3:1 but it reaches 5:1 in some samples. Since the oxides are coarse grained in many of these rocks, no great stock should be taken in this variance; only the high proportion of ilmenite to magnetite is important. At the extreme, a few oxide gabbros are extensively hydrothermally altered. In these cases, all, even secondary, magnetite is completely replaced by green amphibole but ilmenite remains in grids, relict from an original oxyexsolution intergrowth with magnetite.

Ignoring such altered samples, however, how consistent is the proportion of the two minerals? Among oxide gabbros, bulk-rock compositions show that the proportion is very consistent. In the ternary of Figure **F32A,** the proportion of the two minerals in oxide gabbros can be estimated from the ratio of TiO_2 to FeO, using samples in which the latter was measured by titration (Shipboard Scientific Party, 1989; 1999b). The third component in the ternary, SiO_2 that is combined in silicate minerals, behaves simply as a dilutant with respect to the oxide minerals, in which TiO_2 and FeO are so concentrated. Samples plotted are least-altered gabbros, having either positive or small negative loss on ignition (LOI > –2%). This procedure screens out samples with high Fe_2O_3/FeO, which were oxidized during alteration, plus those that have abundant secondary amphibole containing structural Fe_2O_3. Positive LOI indicates weight gain, mainly by addition of oxygen to FeO, for example, that is present in the oxide minerals, during ignition at 1000°C—the first step in preparation of rock powders for XRF analysis. Such samples are extremely fresh, and many oxide gabbros analyzed on board ship have positive LOI.

Least-altered olivine gabbros and troctolites (234 samples with FeO determined by titration) have so little TiO_2 that they plot very close to the SiO_2-FeO sideline in Figure **F32A,** as do average clinopyroxenes and amphiboles, taken from electron-probe analyses of minerals compiled by Dick et al. (**Chap. 10,** this volume). Almost all oxide gabbros fall along a single trend pointing toward the basal TiO_2-FeO sideline between the plotted positions of average ilmenite and magnetite (data from Natland et al., 1991). The dashed sides of the shaded triangle define simple mixing trends between the pure oxide minerals and an apex olivine gabbro with few or no oxide minerals. The apex corresponds to the intersection of the trend for oxide gabbros with the sideline trend for olivine gabbros and troctolites. The lever rule applied to this triangle indicates that the proportion of ilmenite to magnetite in the oxide gab-

F32. Chemical relationships between gabbros and minerals, p. 64.

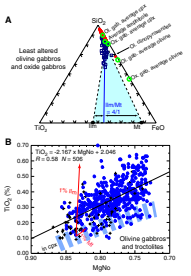

bros is 4:1 with small scatter. However, two least-altered samples plot well to the right of the main trend of oxide gabbros. These are olivine clinopyroxenites—cumulates rich in Fe-Mg silicates rather than plagioclase—with a very small proportion of oxide minerals. Such rocks are minor in abundance in the core (Dick et al., 2000). However, they demonstrate that to whatever extent any sample contains FeO in silicate minerals, it will plot closer to the right sideline of the ternary. Since most oxide gabbros do not do this and instead fall along a single, well-defined trend, this means that they have close to cotectic proportions of Fe-Mg silicates and plagioclase and that the oxide minerals they contain are effectively a pure cumulus addition to the rocks (cf. Natland and Dick, 2001), with ilmenite exceeding magnetite in the minimum proportion of 4:1.

Since olivine gabbros and troctolites hug the right sideline of the ternary close to the SiO_2 corner, however, their bulk compositions are determined almost entirely by silicate minerals. Plagioclase plots virtually at the SiO_2 corner of the ternary, of course, and olivine and orthopyroxene fall almost exactly along the sideline. Of the principal silicates, only average clinopyroxene has a small amount of TiO_2 (0.61%). Average amphibole has only a bit more TiO_2 than this (1.14%). Both plot between the oxide gabbros and the SiO_2 corner of the ternary, thus they do virtually nothing to deflect the more titanian and iron-rich trend among oxide gabbros. That trend instead is controlled almost entirely by the total amount and fixed proportion of ilmenite to magnetite in those rocks.

The TiO_2 contents of olivine gabbros and troctolites also correlate with MgNo (Fig. **F32B**), even though TiO_2 is sensitive both to the proportion of plagioclase in the rocks and to the presence of even a very small amount of ilmenite. The correlation thus indicates that most of these rocks contain nearly cotectic proportions of plagioclase to Fe-Mg silicates (Shipboard Scientific Party, 1999b) and almost no magmatic ilmenite or magnetite. The average normative proportion of plagioclase in these rocks, for example, is 57 ± 7, a very tight clustering. As shown in Figure **F32B,** ilmenite itself can cause only a trifling shift in bulk-rock MgNo, and there is clearly insufficient magmatic magnetite to do this if it is consistently intergrown with four times its abundance of ilmenite. Instead, the rocks are adcumulates, with extremely low proportions of material crystallized from residual interstitial liquid from which the late-crystallizing oxide minerals could have precipitated (Natland et al., 1991; Natland and Dick, 2001). The oxide minerals therefore constitute no more than a few tenths of a percent of the mode of olivine gabbros and troctolites. The very low modal proportions of magmatic oxides in such rocks are a consequence of the extreme efficiency of expulsion of residual liquids during the compaction, deformation, and final stages of crystallization of these rocks.

There are thus two broad classes of rock among the gabbros of Hole 735B, one with significant and in some cases very abundant magmatic oxides and the other almost entirely without magmatic oxides. The two correspond to the division between those rocks providing susceptibility peaks and peak regions on the one hand and those with background magnetic susceptibilities on the other.

Figure **F33A** shows the relationship between TiO_2 contents of gabbros from Hole 735B drilled during Leg 176 and their magnetic susceptibility, in each case measured at one point within the length of a sample taken from whole-round core and analyzed by XRF on board

F33. Magnetic susceptibility vs. TiO_2 and MgNo, p. 65.

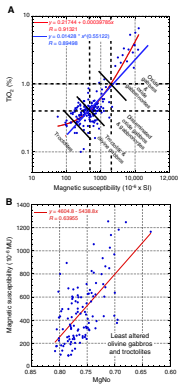

JOIDES Resolution. Each XRF sample was usually a slab or quarter-round piece of core ~5 cm long. The figure is a log-log diagram, chosen in order to amplify the scale of variability among samples with low magnetic susceptibility and low TiO_2 contents, mainly olivine gabbros and troctolites. Both linear and power-law regressions have correlation coefficients of r = ~0.9. On a log-log diagram, the linear regression is curved and the power-law regression is a straight line. The two virtually coincide for rocks having TiO_2 contents between 0.2% and 1.0%.

Magmatic ilmenite, in which most of the TiO_2 in oxide gabbro resides, does not have a high magnetic susceptibility. However, since ilmenite is intergrown with high-susceptibility magnetite in a consistent proportion of about 4:1, this clearly provides the strong correlation between magnetic susceptibility and TiO_2 contents among these rocks. Of course, the strength of the overall correlation is provided mainly by oxide gabbros. Considering gabbros with <0.7% TiO_2, a linear correlation is weaker (r = 0.58). As just demonstrated, however, most of the variability in TiO_2 contents among olivine gabbros is controlled by clinopyroxene, not the oxide minerals, because the rocks are adcumulates. Troctolites have very little clinopyroxene and both lower TiO_2 contents and lower magnetic susceptibility than olivine gabbros (Fig. **F33A**). Thus all rock types contribute to the overall strong correlation, even though the amount of intergrown magmatic ilmenite and magnetite in olivine gabbros and troctolites is inconsequential.

Olivine gabbros and troctolites also show a fairly strong correlation between magnetic susceptibility and bulk MgNo of the rocks (Fig. **F33B**). Here, some of the scatter about the correlation results from the different volumes and geometries of rock material sampled by the Bartington sensor and for XRF analysis. Perhaps there is also a slight effect of variable but small amounts of intergrown magmatic oxides. Some other factor, however, overrides these effects among olivine gabbros and troctolites and provides the correlation. One of the other types of magnetite in the rocks mentioned earlier must be responsible. Since least-altered rocks were used to establish the correlations, magnetite associated with secondary amphibole is probably not important, although it may also contribute somewhat to the scatter about the correlation in Figure **F33B** and to some variability in susceptibility along the entire section drilled.

Magnetite exsolved from primary silicates, including plagioclase, is therefore left as the oxide mineral most likely causing the principal variability of background measurements of magnetic susceptibility among olivine gabbros and troctolites. The correlation between MgNo and magnetic susceptibility just among these rocks suggests that the proportion of such magnetite depends on the composition of the silicate minerals being higher in rocks with more iron-rich pyroxenes (similarly olivine) and more sodic plagioclase.

In almost all troctolites and olivine gabbros, tiny dark inclusions are present in all three of the principal silicates, olivine, pyroxene, and plagioclase. Some are secondary inclusions arrayed along fractures (Fig. **F34A**–**F34F**), some are along cleavage planes, and some follow crystallographic partings (Fig. **F34E**–**F34G**), but on the usual scale of observation they were rarely noted in shipboard descriptions. Migrating fluids or melts may have precipitated the inclusions along the fractures; alternatively, these were produced by reaction with those fluids. The other two types are present along cleavage planes and partings. They more likely formed by simple exsolution. Tiny opaque grains are also present at

F34. Photomicrographs of magnetite, p. 66.

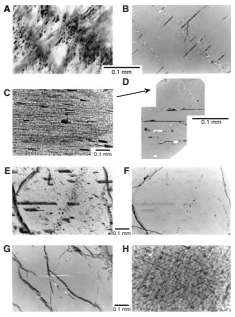

grain boundaries between plagioclase neoblasts and also evidently formed by exsolution. The tiny inclusions are usually completely surrounded by host or adjacent silicates in the 30-m thickness typical of thin sections; only those few intersecting the polished surfaces of the thin sections were brought out as pin-point reflective surfaces by routine polishing (Fig. **F34B, F34D, F34F, F34G**). Magnetite inclusions in plagioclase are usually rodlike in form, parallel to crystallographic axes, and pale brown in color, which is appropriate for very tiny magnetite grains. In some plagioclases, exsolved magnetite forms spectacular grids paralleling crystallographic axes (Fig. **F34H**).

Plagioclase may contribute significantly to the total amount of magnetite in olivine gabbros and troctolites. Plagioclase phenocrysts in abyssal tholeiites from the Indian Ocean contain as much as 0.2%–1.2% FeO, increasing as An decreases (Fig. **F35**). Presumably similar amounts of FeO originally partitioned into plagioclases of gabbro cumulates of Hole 735B. At similar An values, plagioclase in gabbros from Hole 735B now contains only 0.04%–0.30% FeO. The feldspar therefore appears to have lost between 0.2% and 0.6% of iron as FeO during subsolidus reequilibration, with the greater amount being lost from more sodic plagioclase. By themselves, the electron-probe analyses do not say where the missing iron went, but from petrography, it probably is now tied up in exsolved magnetite either within the crystals or at the interfaces between them. There should also be more exsolved magnetite in plagioclases of the more differentiated olivine gabbros than in those of troctolites. Acicular iron oxide exsolved from plagioclase has described from some layered intrusions and elsewhere (Sobolev, 1990; Tegner, 1997; Selkin et al., 2000).

F35. FeO vs. An for plagioclase phenocrysts, p. 68.

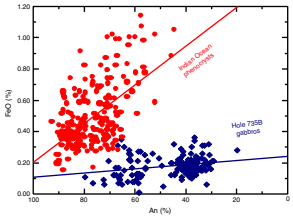

MgNo, however, is a ratio and independent of the variations in the modal proportion of plagioclase to olivine and pyroxenes. For it to correlate with magnetic susceptibility among troctolites and olivine gabbros, either the amount of exsolved magnetite in a given rock does not differ between Fe-Mg silicates and plagioclase, or it does, but the proportion of plagioclase in the rocks is nearly constant, and exsolution has proceeded to the same degree in all rocks. Average modal proportions of olivine gabbros measured during Leg 176 (Shipboard Scientific Party, 1999b) are ol/plag/cpx = 9.8/59.2/29.2. These are very close to experimentally determined proportions (11/59/30) (Grove and Baker, 1984; Grove et al., 1992; Toplis and Carroll, 1995). The proportion of normative plagioclase (57 ± 7, as mentioned earlier) is virtually the same as the proportion of plagioclase in the mode. In troctolites, the cotectic proportions are ol/plag = 30/67, also very similar to the modal proportions measured in such rocks during Leg 176. There is thus no simple way of telling whether plagioclase or Fe-Mg silicates have more exsolved magnetite. Both mineral groups have some, so they both must contribute to the signal of magnetic susceptibility of these rocks.

In summary, whether or not there is more exsolved magnetite in Fe-Mg silicates than in plagioclase, the overall amount of it correlates with a cryptic compositional parameter of the olivine gabbros and troctolites, namely their MgNo, and this provides a signal of magnetic susceptibility increasing with the extent of differentiation of these rocks. Second, because most the rocks also have nearly cotectic proportions of silicate minerals, this also provides a somewhat weaker correlation between magnetic susceptibility and the bulk TiO_2 content of the rocks, this being provided by their nearly fixed proportion of clinopyroxene. In rocks with >0.7% TiO_2 contents, the susceptibility signal is domi-

nated by magmatic ilmenite and magnetite, intergrown in nearly fixed proportions in the rocks.

Cryptic variation is a term coined by Wager and Deer (1939) to describe variations in gabbro composition that are independent of the modal proportions of minerals. Mineralogically, the Fo content of olivine, En/Fs of pyroxenes, and An content of plagioclases are all cryptic parameters. So also in a general way are bulk-rock MgNo and normative An/(An+Ab). If a cumulus mineral assemblage is quite pure with a small proportion of material crystallized from trapped residual liquid, then its mineralogical and even bulk-chemical cryptic parameters can be related to the liquid compositions that produced the cumulates. At issue now is whether magnetic susceptibility is a measure of one of the most important cryptic parameters of the gabbros from Hole 735B, namely MgNo. We know that the high magnetic susceptibilities of oxide gabbros reflect their proportion of magmatic oxides. This is not a cryptic property of the rocks. What about olivine gabbros and troctolites?

One test is to find out whether susceptibility correlates with the variability of a silicate mineral, for example, the Fo content of olivine. Figure **F36A** plots compositions of olivine vs. magnetic susceptibility from the Leg 176 portion of the core (olivine data from Dick et al., **Chap 10,** this volume). Although there are weak linear and power-law correlations, magnetic susceptibility still spans two orders of magnitude at some olivine compositions (e.g., Fo_{70}). The two do not correlate. Thus there are many susceptibility peaks representing oxide gabbros in which the oxide minerals have apparently simply been added to an underlying and preexisting matrix of olivine gabbro. Some of these, identified in the core descriptions, contain so many magmatic oxides that they were not even identified as olivine gabbro. There are several cases of two samples only a few centimeters apart in the core, one being an oxide gabbro that provided a spike in magnetic susceptibility of several thousand $\times 10^{-6}$ MU, the other being an olivine gabbro with background magnetic susceptibility of only ~100×10^{-6} to 300×10^{-6} MU. Yet the olivine in the oxide gabbro is even more forsteritic than in the adjacent olivine gabbro. On the contrary, some rocks with olivine as iron-rich as Fo_{55} have very low magnetic susceptibility.

This result is so widespread that it can be used to outline a general argument about the petrogenesis of the rocks cored during Leg 176. First, the oxide minerals overall had to crystallize from liquids more differentiated—more iron rich—than the liquids that produced even the most iron-rich olivine in any of them (Fo_{46}). Such liquids are represented by some of the even more differentiated oxide gabbros from the upper 500 m of the hole, drilled during Leg 118, which have olivine as fayalitic as Fo_{30} (Ozawa et al., 1991). Second, iron-rich liquids almost always were efficiently expelled from the intercumulus matrix of all gabbros that crystallized olivine ranging from Fo_{84} to Fo_{46} to produce adcumulates with very little iron-rich interstitial melt remaining. Third, not only did the expelled liquids aggregate and reintrude the section en masse at those places that now show up as *peak regions* in magnetic susceptibility, some of them nearly 2 m thick, but they also injected the intercrystalline porosity structure of primitive gabbros at hundreds of places up and down the core, producing a host of narrow spikes in magnetic susceptibility but without significantly changing the mineralogy of their new hosts. Preexisting olivines, for example, were not completely destroyed by reaction with the penetrating melts. Reaction with the injected liquids may have left those olivines embedded in the common

F36. Magnetic susceptibility vs. olivine composition, p. 69.

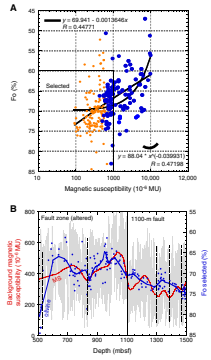

orthopyroxene coronas seen adjacent to them in many of these rocks. In this way, the original cryptic variability of the olivine was maintained, even if the rock itself became infested with oxide minerals and cannot now be identified as an olivine gabbro. Some very unusual rock types, such as the disseminated-oxide troctolite mentioned earlier, resulted from this process.

As complicated as this might seem, all is not lost. The reaction process may have occurred in portions of rock that are discrete enough that we can still consider the cryptic variation of olivine among just olivine gabbros and troctolites, even including some rocks that experienced oxide enrichment, and compare it with the background magnetic susceptibility. Figure **F36B** shows both background magnetic susceptibility and average composition of olivine per sample vs. depth. The plotted olivine compositions are the same as those within the box labeled "Selected" in Figure **F36A.** They are screened to include all olivine compositions more magnesian than Fo_{60} with magnetic susceptibility $<1000 \times 10^{-6}$ MU. This removes rocks as differentiated as olivine gabbronorites from the comparison. Among all remaining rocks, it assumes that the differential between background susceptibilities and 1000×10^{-6} MU resulted from addition of a small proportion of oxide minerals to the rocks, without destroying the host olivine completely. In other words, the rocks originally had a lower proportion of oxide minerals, and after freezing, would have produced magnetic susceptibilities within background limits. Instead, they lay in the path of a percolating, iron-rich melt. Figure **F36B** includes 10% weighted curves for both magnetic susceptibility and olivine compositions, scaled so that the two curves are superimposed.

Because vertical scales were chosen so that the amplitudes of fluctuations along the two weighted curves are similar, the scatter of olivine compositions falls almost entirely within the band of background magnetic susceptibility. Although there are far fewer olivine compositions than measurements of magnetic susceptibility, when similar window averages are used then some of the similarities of the two weighted curves appear to be significant. The first is that the fault at 1100 mbsf, marked by a sharp drop in background susceptibility among the rocks deeper than this, is also reflected in more forsteritic olivine compositions. There are also similar general fluctuations in the two curves, notably rises in amplitude between 900 and 1100 mbsf, downturns in both curves to very low susceptibilities and high Fo contents at ~830 mbsf, and perhaps a small upturn in both curves at ~1350 mbsf. Note that the downturn in the olivine curve at ~820 mbsf probably would not exist without inclusion of forsteritic olivine from just two samples. This underscores the difficulty of determining the true pattern of cryptic mineralogical variation in this complicated core from mineral data using samples spaced on the average 1–2 m apart.

Between 500 and 700 mbsf, the two curves do not correspond. Partly this resulted from selected sampling of troctolites used for microprobe analysis at ~510 mbsf. These provided several magnesian olivines, but adjacent, more differentiated, and typical gabbros from this part of the core were not sampled. From 550 to 650 mbsf, core recovery was somewhat low because of the presence of fractured and hydrothermally altered rock in two closely spaced fault zones. The alteration particularly affected olivine; those samples in which it was preserved may not represent the typical lithologies in this part of the core.

I conclude, somewhat guardedly, that background magnetic susceptibility in general reveals the pattern of cryptic variability among olivine

gabbros and troctolites along most of the core recovered during ODP Leg 176. Since almost all of these rocks are adcumulates, this means that expulsion of intercumulus melts, the residual from which the oxide minerals precipitated, was both efficient and fairly uniform throughout the core. Some of the local scatter in background magnetic susceptibility, but not its weighted variability on a scale of 50 m or more, may indicate variations in the percentage of interstitial melt that was present when the oxide minerals crystallized. Although the core was riven with many late-stage oxide-rich seams, magnetic susceptibility reveals the occurrence and width of those seams and the maximum extent of the core that was refertilized with iron-rich melt. All such rocks have been screened from Figure **F36B.** The figure is thus a map of the distribution of adcumulates in the core rocks from which interstitial melt was efficiently squeezed, amounting to nearly 63% of the section. It also gives a general idea of how differentiated those rocks happen to be. Some fairly strongly differentiated gabbronorites are also adcumulates with low percentages of oxide minerals and background levels of magnetic susceptibility. These are included in Figure **F36B.**

For oxide-bearing and oxide-rich gabbros, the utility of magnetic susceptibility as a geochemical index is much more straightforward. Simply considering TiO_2 contents, a crude breakdown is quite meaningful. Thus olivine gabbros and troctolites have <0.7% TiO_2; disseminated-oxide gabbros have 0.7% < TiO_2 < 2.0%; and oxide gabbros have >2.0% TiO_2. The bulk of analyzed samples within these limits have clearly different magnetic susceptibilities. Presence or absence of the different silicate minerals allowed discrimination of particular lithologies. In gabbros with <0.7% TiO_2 content, most of the TiO_2 resides in clinopyroxene and is simply influenced by olivine, orthopyroxene, and plagioclase, which have very low TiO_2 contents, acting as dilutants. The proportion of clinopyroxene to these other minerals, however, oscillates only a small amount from cotectic proportions, and this ultimately allows us to use magnetic susceptibility as a geochemical log even among these rocks.

Above 0.7% TiO_2 contents, however, the trend produced simply by the low-TiO_2 silicate minerals is deflected by an increase in the mode of oxide minerals (Shipboard Scientific Party, 1999b). The proportion of TiO_2 in the oxide minerals exceeds the amount tied up in clinopyroxene. Addition of cumulus ilmenite and magnetite becomes paramount and is independent of the underlying composition of silicate minerals. Natland and Dick (2001) describe this as a process of accumulation of the two oxide minerals as they precipitated in small-scale porosity structure in a matrix, or mush, of silicate minerals during flux of highly differentiated liquids rich in iron and titanium. The effectiveness of formation of cumulus oxide minerals was strongly controlled by patterns of porosity structure that developed in response to deformation of the rocks. Some aspects of this have been developed in this paper.

The Average Composition of the Core

The linear regression of Figure **F33A** can be used to estimate aspects of the bulk composition of the core. This obviously applies only to the three general classes of gabbroic rocks just mentioned. Neither Figure **F33A** nor **F33B** includes compositions of felsic veins (quartz diorites to granites) or hybrids between felsic veins and country rocks (diorites).

However, these comprise only ~0.3% of the core; they do not significantly affect the result outlined below.

Dick et al. (2000) calculated average compositions for each 500-m portion of Hole 735B. Their procedure corrected the lengths of lithologic intervals for instances of both low recovery and >100% recovery and used average compositions of each lithologic type, weighting them properly for differences in density. Recovery of >100% occurs when the drill recores a stump of rock left from a prior core and then adds a full 9.7 m of additional rock to it. I wished to check the validity of this approach using magnetic susceptibility, given that this measurement allows a greatly refined estimation of the proportions of rocks having different compositions throughout the core recovered during Leg 176. My analysis only concerns TiO_2 contents, since this oxide is one that I can relate most simply and directly to magnetic susceptibility. In the end it fairly strongly validates the estimates of Dick et al. (2000).

The procedure I used for magnetic susceptibility was to obtain the average value per core, relate this as quantitatively as possible to the TiO_2 contents of analyzed rocks, and consider that the average estimated TiO_2 contents represent the depth range for that core given in the site report (Shipboard Scientific Party, 1999b, table T1). The average TiO_2 content of each core was calculated using the linear regression in Figure **F33A.** For the density correction, I calculated a linear regression for the relationship between normative density calculated from bulk XRF compositions (based on Niu and Batiza, 1991 with some additional mineral densities from Deer et al., 1992) and TiO_2 contents. The relationship for 323 chemical analyses is $D = 0.68 \times TiO_2 + 3.013$ ($r = 0.87$). The range of normative densities is 3.013–3.120 g/cm^3, slightly higher than measured densities for minicores because as measured on deck, the latter usually include tiny cracks and other microporosity structure, reducing their densities. Only relative differences in normative density among samples have any bearing on this calculation, however, and normative densities follow differences in measured densities very closely. The average density-corrected TiO_2 content for each core was then divided by the total depth range under consideration (part or all of the 1003.2 m cored during Leg 176) and the values summed over that interval to provide the average TiO_2 content for the interval.

The average TiO_2 content calculated in this way for the interval from Cores 176-735B-88R through 153r (504.8–1005.3 mbsf) is 0.71%, nearly the same as the value (0.70%) obtained by Dick et al. (2000) for lithologies from 500 to 1000 mbsf. From Cores 176-735B-154R through 210R (1005.3–1508.0 mbsf), the average is 0.41%, a bit lower than the 0.50% obtained for the lowermost 500 m of the hole by Dick et al. (2000). The values for the two parts of the hole should correspond to differences in other correlative attributes of composition (Mg#, Ca#, etc.) cited by Dick et al. (2000) as being related in general to the degree of differentiation of basaltic liquids from which these cumulates crystallized. The deepest 500 m of the hole, and certainly the body of rocks below the fault at 1100 m, is a slightly more primitive body of gabbro than suggested by the estimate based on identification of lithologic intervals in the shipboard descriptions. Given the uncertainties implicit in either of the estimates by lithology or magnetic susceptibility, I consider that the overall agreement is quite good and that the estimates of Dick et al. (2000) for TiO_2, all the other oxides, and the several trace elements are not likely to differ significantly from a more extensive treatment based on magnetic susceptibility.

DISCUSSION

One consequence of the development of high-resolution measurements of core properties by ODP using the MST and some other techniques has been the gradual relinquishment of the primacy of visual core descriptions in evaluation of core lithology. Descriptions of igneous rocks have thus far escaped this fate, largely because of low recovery. For whatever technical reason, however, rotary coring with large bits penetrated massive and unfractured gabbro in Hole 735B like butter, relatively speaking, and recovered so much of it that, for the first time, high-resolution techniques can be applied to at least this one igneous lithology at this one place. This bodes very well for future deep drilling in the lower ocean crust, even if it means that the eyes of igneous petrologists turn out to be less trustworthy than, say, measurement of magnetic properties of the rocks.

The gabbros of Hole 735B have extraordinary lithologic complexity. This was evident on the first description of them during Leg 118, and in this respect Leg 176 did not disappoint. Many potential relationships among the rocks, anticipated both in comparison to ophiolites and to layered intrusions, simply did not show up (Natland and Dick, 2001). Instead, other kinds of relationships—to fractures, faults, patterns of alteration, and zones of deformation—became important, if not indeed all-important. The full extent of this complexity, however, is revealed less by core descriptions than by integrating the descriptions with the high-resolution measurement of magnetic susceptibility. One result of this, however, is that the initial basis for interpreting the chemical stratigraphy of the gabbros (e.g., Shipboard Scientific Party, 1999b; Dick et al., 2000) is inadequate. The existence of five "plutons" drilled during two legs and definable on the basis of, for example, MgNo vs. depth, with each contributing to a substantial thickening of the ocean crust at this location, is no longer tenable in view of the breakdown between "background" olivine gabbros and troctolites and "peak" disseminated-oxide and oxide gabbros. Whereas XRF analyses suggest that each of the three plutons penetrated during Leg 176 is increasingly differentiated upward, in fact each instead represents the consequence of sampling "representative" lithologies for chemical analysis, with intrusive oxide-bearing and oxide-rich seams becoming more prominent with elevation in each "pluton." However, this is entirely accidental. Fluctuations in "background" compositions have nothing to do with the location of oxide gabbros; thus, they should be treated separately as rocks that correspond to an underlying, fundamental, and very different igneous stratigraphy. These rocks were later, and in uncertain sequence, intruded and modified on an intimate scale by much more differentiated liquids. The deeper primitive gabbros may have contributed to those later liquids by a continuing process of differentiation, with expulsion of buoyant interstitial liquids upward during compaction and deformation (Natland and Dick, 2001), or the later liquids may have come in from somewhere else altogether (Dick et al., 2000).

Concurrently, although the core as a whole can be treated as a sequence or series of igneous units with composition as the fundamental variable, perhaps instead the core should be treated as a series of *structural* units, in which the attributes of crystal/plastic deformation in the presence of interstitial melts (Fig. **F25**) figure at least as strongly as bulk composition. Oxide gabbros are intimately interleaved with more primitive olivine gabbros and troctolites. The relationships between the two

are equally intimately connected to the *late-stage* high-temperature deformation of the rocks. *All* of the oxide gabbros should be conceptually stripped out of the section before the underlying intrusive relationships among olivine gabbros and troctolites—in particular all of the contacts and variations in grain size and texture *just* among these lithologies are considered, if we want to understand the *initial* stages of construction of ocean crust at this slowly spreading ridge. That is the foremost lesson of this initial evaluation of the high-resolution igneous and deformational stratigraphy of Hole 735B. This is what was done in the evaluation of chemical stratigraphy for the synthesis of this volume (Natland and Dick, **Synthesis Chap.,** this volume).

CONCLUSIONS

The principal results of this study are as follows:

1. Magnetic susceptibility is an extremely useful and precise means of evaluating the lithology and stratigraphy of gabbro recovered in whole-round core.
2. The distribution of high-susceptibility oxide gabbros on a background of low-susceptibility olivine gabbros and troctolites in Hole 735B is far more intricate than is indicated by designation of lithologic intervals on the core description barrel sheets.
3. Oxide gabbros on the whole experienced more extreme crystal-plastic deformation than olivine gabbros and troctolites.
4. Felsic veins and vein nets are strongly but not exclusively associated with oxide gabbros, but usually formed after episodes of crystal-plastic deformation.
5. The distribution of seams of oxide gabbro is unrelated to the distribution and composition of the olivine gabbros and troctolites that they intrude.
6. The low magnetic susceptibility of olivine gabbros and troctolites by themselves is still sufficient to reveal compositional differences among these rocks.
7. The pattern of magnetic susceptibility among olivine gabbros and troctolites is related to the amount of magnetite exsolved from silicate minerals, including plagioclase, and this in turn depends on the average stage of differentiation of these rocks.
8. There are several minima in the downhole pattern of background magnetic susceptibility of olivine gabbros and troctolites that may be places where fairly large volumes of primitive magma inflated the lower ocean crust at or near the ridge axis.
9. The block of olivine gabbro and troctolite below a fault zone at 1100 mbsf is more primitive, on the average, than similar lithologies above the fault. It is less deformed, has fewer seams of oxide gabbro, and has more widely separated felsic veins.
10. Magnetic susceptibility is a useful geochemical log, with the measurements correlating especially strongly with bulk-rock TiO_2 contents reflecting a consistent proportion of magmatic ilmenite to magnetite in the rocks.
11. Taking magnetic susceptibility as an index of TiO_2 contents over the whole of the core obtained during Leg 176 confirms estimates for the bulk composition of the section based on lithologic intervals obtained by Dick et al. (2000).

ACKNOWLEDGMENTS

The Leg 176 shipboard technical and scientific parties prepped, prodded, described, and photographed the cores, and they made almost all the measurements that form the basis of this paper. I especially thank Ralph Stephen and Andrew Kingdon for pushing the cores through the MST and for consultations at various points on how to evaluate the data listings and get them into my computer. Gerry Iturrino and Sarah Haggas obtained the whole-round core scans. Eiichi Kikawa and Jeff Gee patiently explained the mysteries of magnetic susceptibility. Later, Henry Dick kindly provided his compilation of mineral data, which clarified one of the great complexities of the relationship of magnetic susceptibility to the cores. Maurice Tivey and Jeff Gee both provided careful and thoughtful reviews of the manuscript. Additional comments were made by Editorial Review Board member Dick Von Herzen. This research used samples and/or data provided by the Ocean Drilling Program (ODP). ODP is sponsored by the U.S. National Science Foundation (NSF) and participating countries under management of Joint Oceanographic Institutions (JOI), Inc. The study was supported by a postcruise grant from the United States Science Support Program (USSSP), administered by JOI, Inc.

REFERENCES

Bowen, N.L., 1920. Differentiation by deformation. *Proc. Natl. Acad. Sci.,* 6:159–162.

Bowen, N.L., and Schairer, J.F., 1935. The system MgO-FeO-SiO_2. *Am. J. Sci.,* 29:151–217.

Collinson, D.W., 1983. *Methods in Rock Magnetism and Palaeomagnetism: Techniques and Instrumentation:* London (Chapman and Hall).

Deer, W.A., Howie, R.A., and Zussman, J., 1992. *An Introduction to the Rock-Forming Minerals* (2nd Ed.): New York (John Wiley and Sons).

Dick, H.J.B., Meyer, P.S., Bloomer, S., Kirby, S., Stakes, D., and Mawer, C., 1991. Lithostratigraphic evolution of an in-situ section of oceanic Layer 3. *In* Von Herzen, R.P., Robinson, P.T., et al., *Proc. ODP, Sci. Results,* 118: College Station, TX (Ocean Drilling Program), 439–538.

Dick, H.J.B., Natland, J.H., Alt, J.C., Bach, W., Bideau, D., Gee, J.S., Haggas, S., Hertogen, J.G.H., Hirth, G., Holm, P.M., Ildefonse, B., Iturrino, G.J., John, B.E., Kelley, D.S., Kikawa, E., Kingdon, A., LeRoux, P.J., Maeda, J., Meyer, P.S., Miller, D.J., Naslund, H.R., Niu, Y., Robinson, P.T., Snow, J., Stephen, R.A., Trimby, P.W., Worm, H.-U., and Yoshinobu, A., 2000. A long in situ section of the lower ocean crust: results of ODP Leg 176 drilling at the Southwest Indian Ridge. *Earth Planet. Sci. Lett.,* 179:31–51.

Dick, H.J.B., Natland, J.H., Miller, D.J., et al., 1999. *Proc. ODP, Init. Repts.,* 176 [CD-ROM]. Available from: Ocean Drilling Program, Texas A&M University, College Station, TX 77845-9547, U.S.A.

Dixon, S., and Rutherford, M.J., 1979. Plagiogranites as late-stage immiscible liquids in ophiolite and mid-ocean ridge suites: an experimental study. *Earth Planet. Sci. Lett.,* 45:45–60.

Fenner, C.N., 1929. The crystallization of basalts. *Am. J. Sci.,* 18:225–253.

————, 1931. The residual liquids of crystallizing magmas. *Mineral. Mag.,* 22:539–560.

Grove, T.L., and Baker, M.B., 1984. Phase equilibrium controls on the tholeiitic versus calc-alkaline differentiation trends. *J. Geophys. Res.,* 89:3253–3274.

Grove, T.L., Kinzler, R.J., and Bryan, W.B., 1992. Fractionation of mid-ocean ridge basalt (MORB). *In* Morgan, J.P., Blackman, D.K., and Sinton, J.M. (Eds.), *Mantle Flow and Melt Generation at Mid-Ocean Ridges*. Geophys. Monogr., Am. Geophys. Union, 71:281–310.

Hunt, C., Moskowitz, B.M., and Banerjee, S.K., 1995. Magnetic properties of rocks and minerals. In *Rock Physics and Phase Relations*. AGU Ref. Shelf 3, 189–204.

Kikawa, E., and Pariso, J.E., 1991. Magnetic properties of gabbros from Hole 735B, Southwest Indian Ridge. *In* Von Herzen, R.P., Robinson, P.T., et al., *Proc. ODP, Sci. Results,* 118: College Station, TX (Ocean Drilling Program), 285–307.

Natland, J.H., and Dick, H.J.B., 1996. Melt migration through high-level gabbroic cumulates of the East Pacific Rise at Hess Deep: the origin of magma lenses and the deep crustal structure of fast-spreading ridges. *In* Mével, C., Gillis, K.M., Allan, J.F., and Meyer, P.S. (Eds.), *Proc. ODP, Sci. Results,* 147: College Station, TX (Ocean Drilling Program), 21–58.

————, 2001. Formation of the lower ocean crust and the crystallization of gabbroic cumulates at a very slowly spreading ridge. *J. Volcanol. Geotherm. Res.*, 110:191–233.

Natland, J.H., Meyer, P.S., Dick, H.J.B., and Bloomer, S.H., 1991. Magmatic oxides and sulfides in gabbroic rocks from Hole 735B and the later development of the liquid line of descent. *In* Von Herzen, R.P., Robinson, P.T., et al., *Proc. ODP, Sci. Results,* 118: College Station, TX (Ocean Drilling Program), 75–111.

Niu, Y.-L., and Batiza, R., 1991. In situ densitiers of MORB melts and residual mantle: implications for buoyancy forces beneath mid-ocean ridges. *J. Geol.,* 99:767–775.

Ozawa, K., Meyer, P.S., and Bloomer, S.H., 1991. Mineralogy and textures of iron-titanium oxide gabbros and associated olivine gabbros from Hole 735B. *In* Von Herzen, R.P., Robinson, P.T., et al., *Proc. ODP, Sci. Results,* 118: College Station, TX (Ocean Drilling Program), 41–73.

Pariso, J.E., Scott, J.H., Kikawa, E., and Johnson, H.P., 1991. A magnetic logging study of Hole 735B gabbros at the Southwest Indian Ridge. *In* Von Herzen, R.P., Robinson, P.T., et al., *Proc. ODP, Sci. Results,* 118: College Station, TX (Ocean Drilling Program), 309–321.

Selkin, P.A., Gee, J.S., Tauxe, L., Meurer, W.P., and Newell, A.J., 2000. The effect of remanence anisotropy on paleointensity estimates: a case study from the Archean Stillwater Complex. *Earth Planet. Sci. Lett.*, 183:403–416.

Shipboard Scientific Party, 1989. Site 735. *In* Robinson, P.T., Von Herzen, R., et al., *Proc. ODP, Init. Repts.,* 118: College Station, TX (Ocean Drilling Program), 89–222.

————, 1999a. Explanatory notes. *In* Dick, H.J.B., Natland, J.H., Miller, D.J., et al., *Proc. ODP, Init. Repts.,* 176, 1–42 [CD-ROM]. Available from: Ocean Drilling Program, Texas A&M University, College Station, TX 77845-9547, U.S.A.

————, 1999b. Site 735. *In* Dick, H.J.B., Natland, J.H., Miller, D.J., et al., *Proc. ODP, Init. Repts.,* 176, 1–314 [CD-ROM]. Available from: Ocean Drilling Program, Texas A&M University, College Station, TX 77845-9547, U.S.A.

Sobolev, P.O., 1990. Orientation of acicular iron-ore mineral inclusions in plagioclases. *Int. Geol. Rev.*, 32:616–628.

Tegner, C., 1997. Iron in plagioclase as a monitor of the differentiation of the Skaergaard Intrusion. *Contrib. Mineral. Petrol.*, 128:45–51.

Toplis, M.J., and Carroll, M.R., 1995. An experimental study of the influence of oxygen fugacity on Fe-Ti oxide stability, phase relations, and mineral-melt equilibria in ferro-basaltic systems. *J. Petrol.,* 36:1137–1170.

Usselman, T.M., and Hodge, D.S., 1978. Thermal control of low-pressure fractionation processes. *J. Volcanol. Geotherm. Res.,* 4:265–281.

Wager, L.R., and Deer, W.A., 1939. Geological investigations in Greenland, Part 3. The petrology of the Skaergaard Intrusion, Kangerdlugssuaq, East Greenland. *Medd. Groenl.,* 105.

Figure F1. Magnetic susceptibility vs. depth from the Leg 118 downhole log, modified after Pariso et al. (1991). LU = lithologic unit, D = zones of strong deformation (hatched) (from Shipboard Scientific Party, 1989).

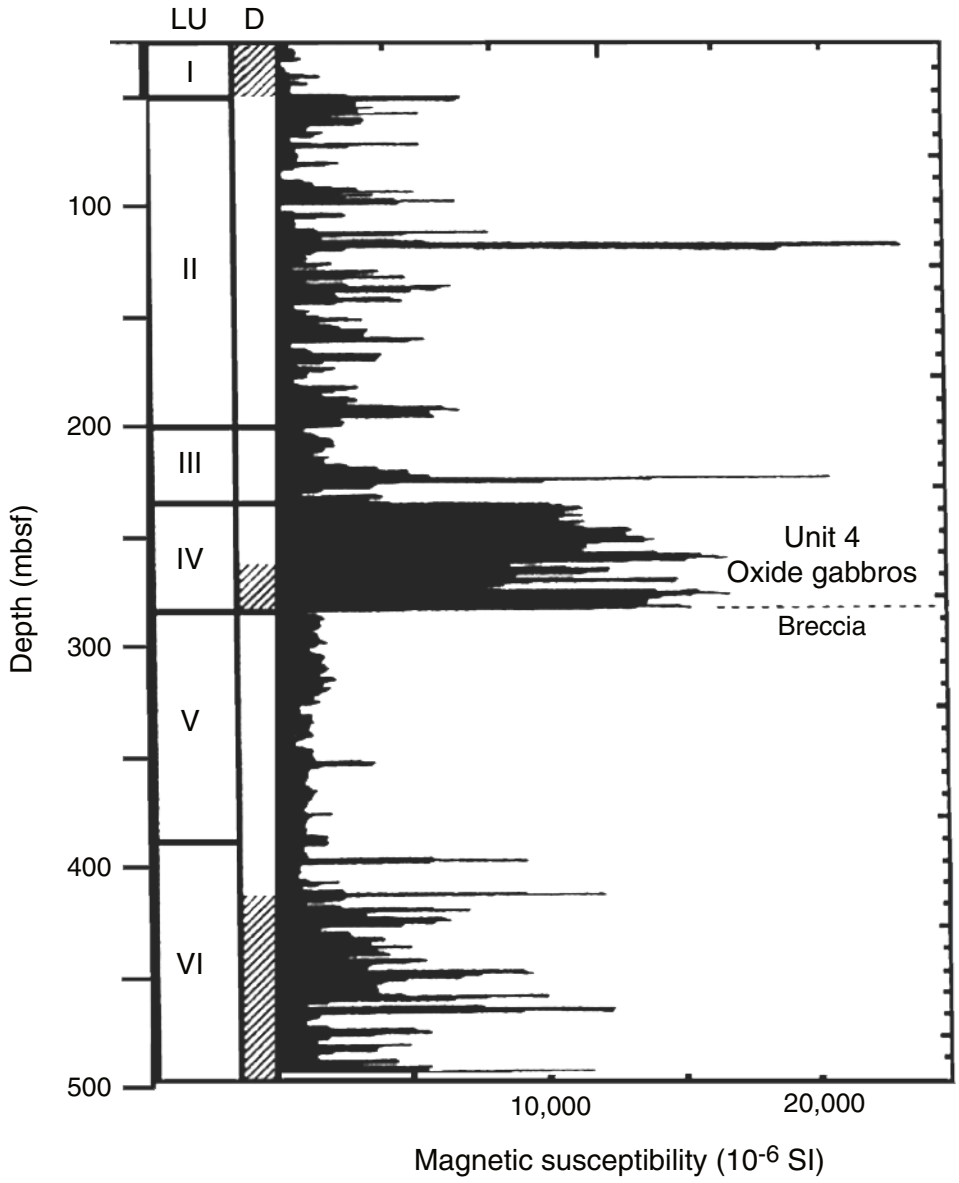

Figure F2. Example of the effects of gaps at piece edges (shaded) and machine saturation on spikes in magnetic susceptibility in core from Sections 176-735B-139R-1 and 139R-2 from 872.3 to 873.0 mbsf. Piece and interval numbers plus lithologic identifications are given on the right, as is the location of a felsic vein. The corrected magnetic susceptibility is given by asterisks linked by the dashed line. Background measurements are indicated by dots on the flat portions of the curve at the top and bottom of the figure. See text (**"Conventions, Protocols, and Editing of the Data File,"** p. 4) for additional explanation.

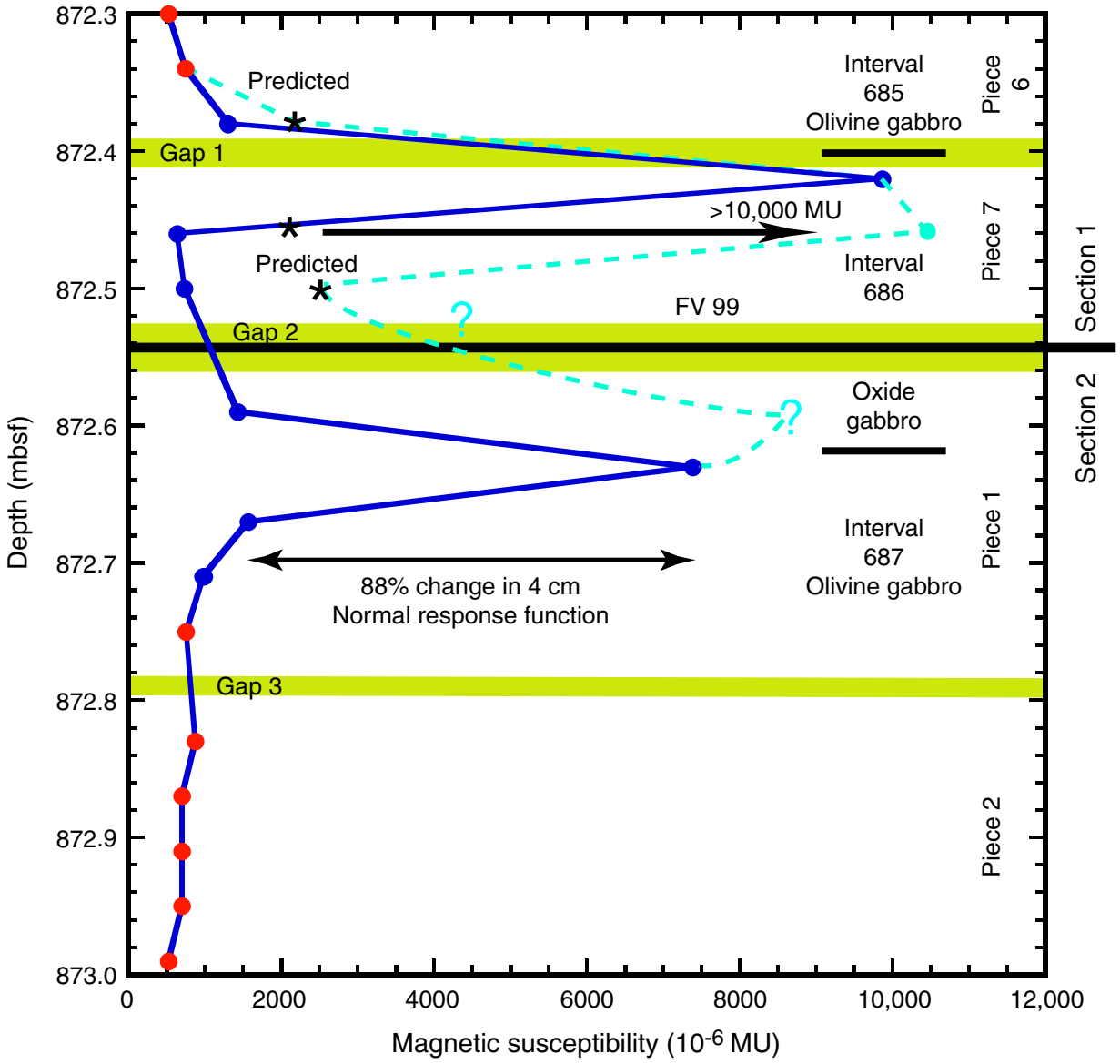

Figure F3. Magnetic susceptibility of minicores vs. magnetic susceptibility of the corresponding interval measured by the Bartington sensor on the MST. The linear regression (equation 1) is slightly curved on this log-log variation diagram, whereas the power-law regression (equation 2) is a straight line.

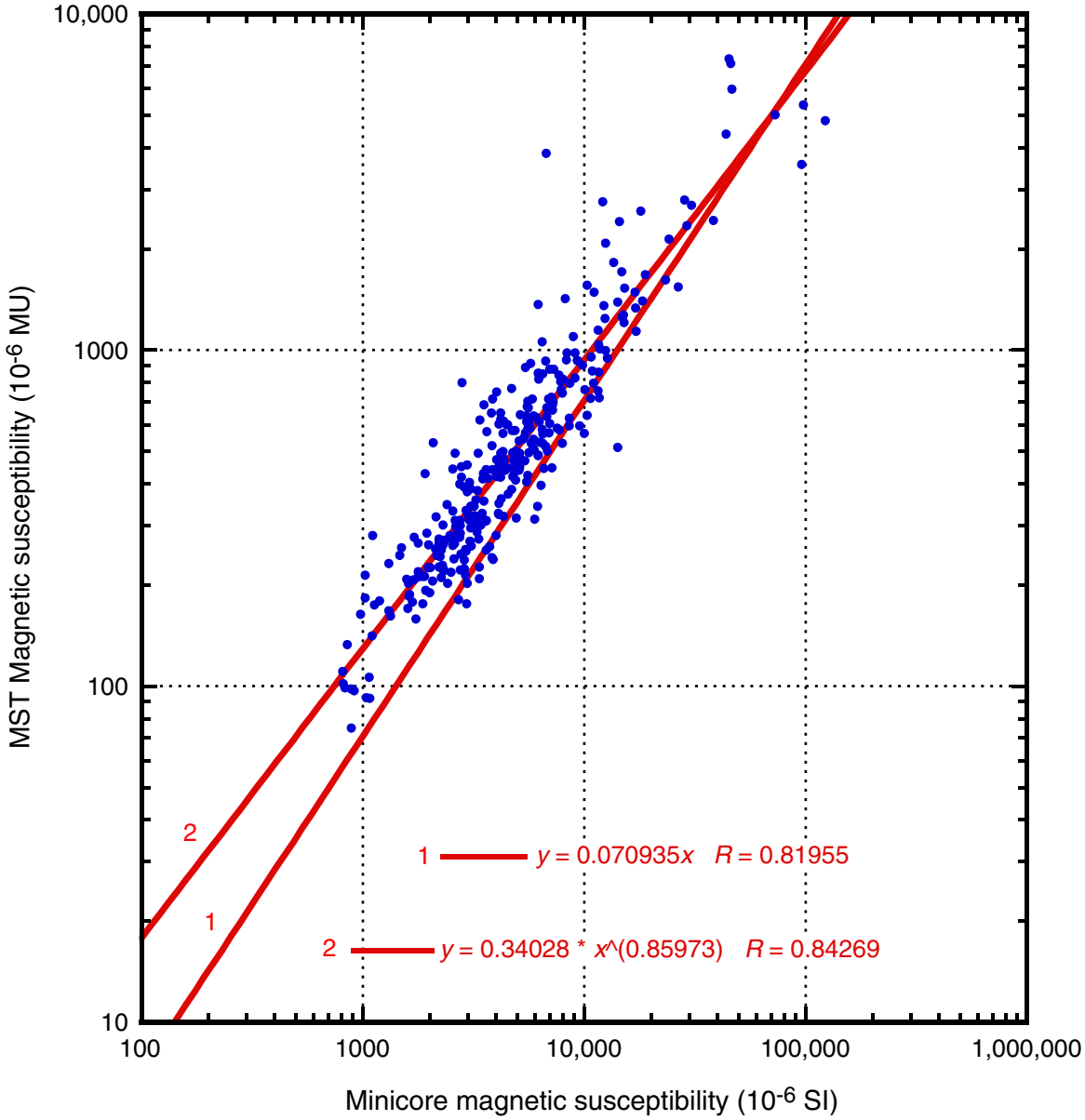

Figure F4. MST magnetic susceptibility vs. depth, edited as described in the text. The scale at the top is in SI units, corrected by the factor of 0.66 from the scale in machine units (MU) at the bottom, as discussed in the text. The thick line gives a smoothed fit to the data, binned over 20-m intervals, as calculated using the plotting program, Kaleidagraph.

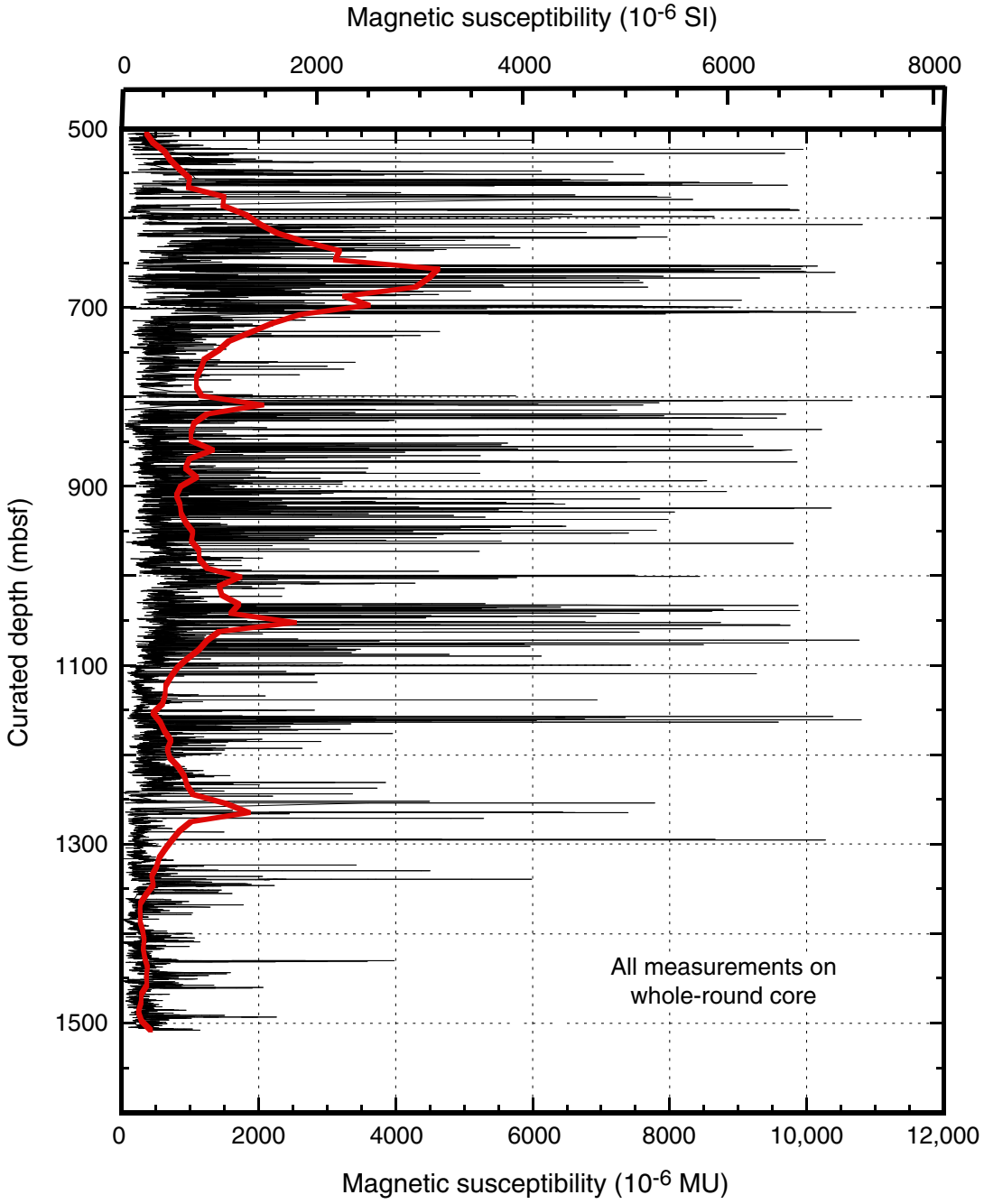

Figure F5. Magnetic susceptibility vs. depth for a typical peak region between 703 and 706.5 mbsf. Background values are shown as solid dots. Lines are drawn between each data point that has not been edited. The corresponding lithologic units and rock identifications are to the right, as taken from the igneous rock description forms in the site report (Shipboard Scientific Party, 1999b). DOOG = disseminated-oxide olivine gabbro.

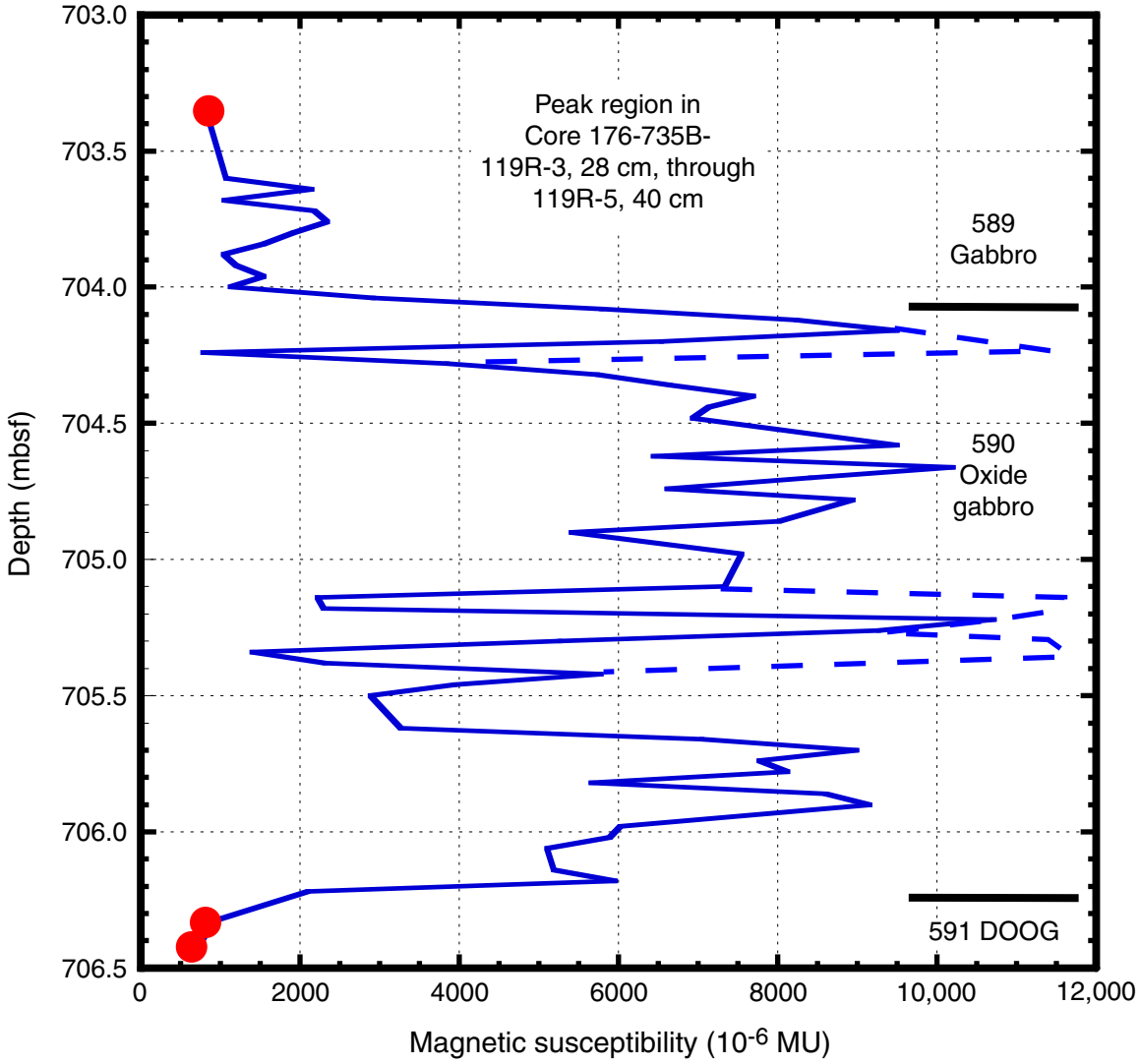

Figure F6. Magnetic susceptibility vs. depth for two peak regions between 652 and 662 mbsf. Background values are in red. Lines are drawn between each data point that has not been edited.The corresponding lithologic units and rock identifications are to the right, as taken from the igneous rock description forms in the site report (Shipboard Scientific Party, 1999b).

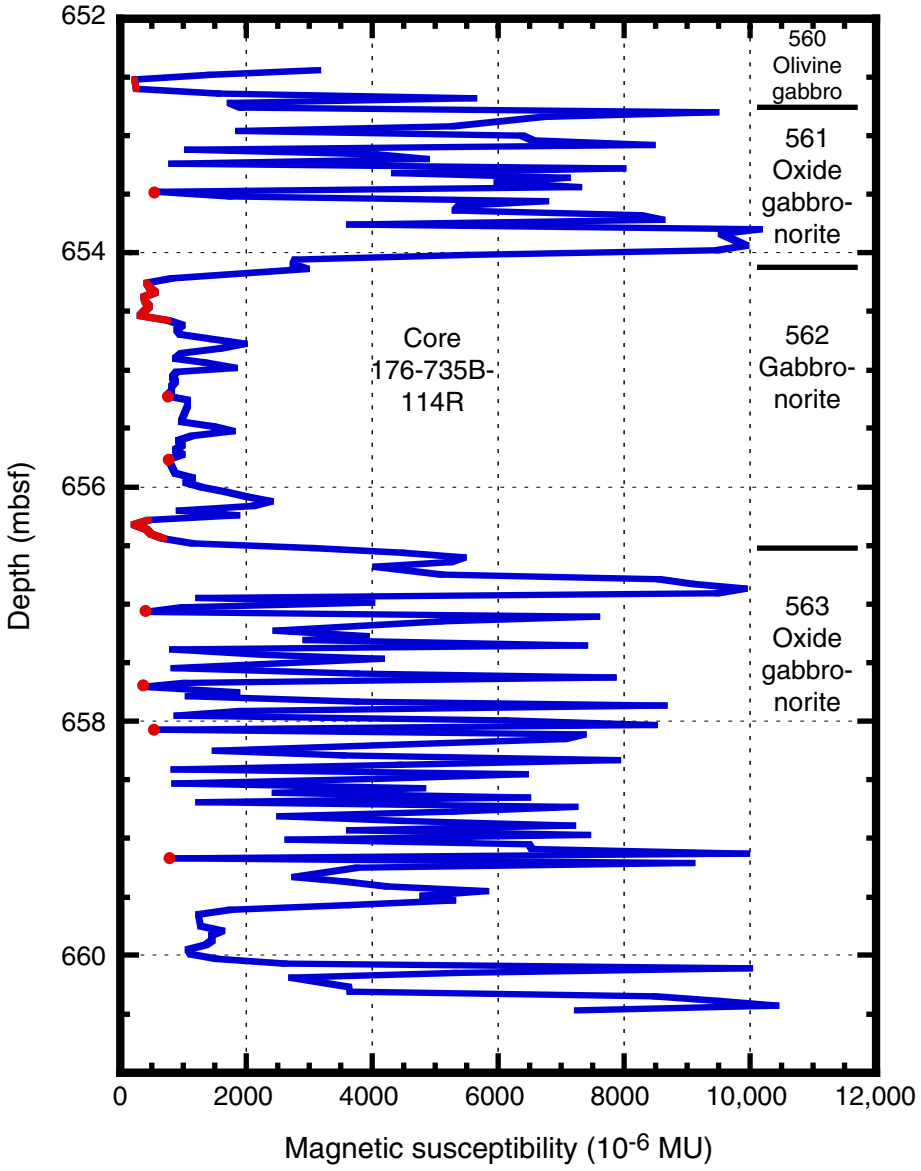

Figure F7. Magnetic susceptibility vs. depth between 1071 and 1084 mbsf. Background values are in red. Lines are drawn between each data point that has not been edited. The corresponding lithologic units and rock identifications are to the right, as taken from the igneous rock description forms in the site report (Shipboard Scientific Party, 1999b). Sequential felsic veins (FV) are given by number in order of depth, from Vein-log.xls, given in supplemental material to the site report. Others without numbers are from the core descriptions.

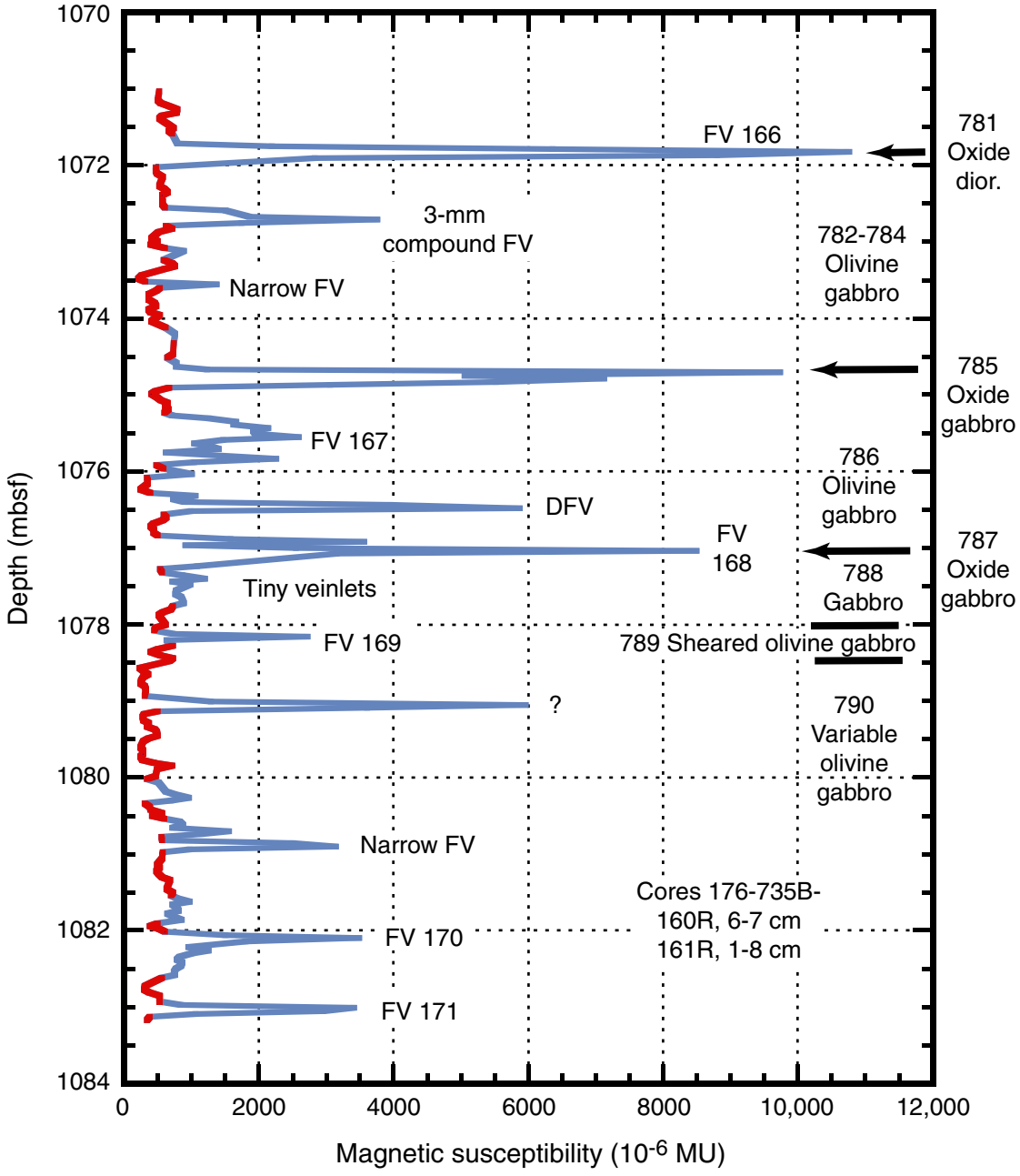

Figure F8. Thicknesses of peaks and peak regions having magnetic susceptibility >2000 × 10^{-6} MU vs. depth, from 500 to 1500 mbsf. The average width (13.4 cm) is given by the solid vertical line.

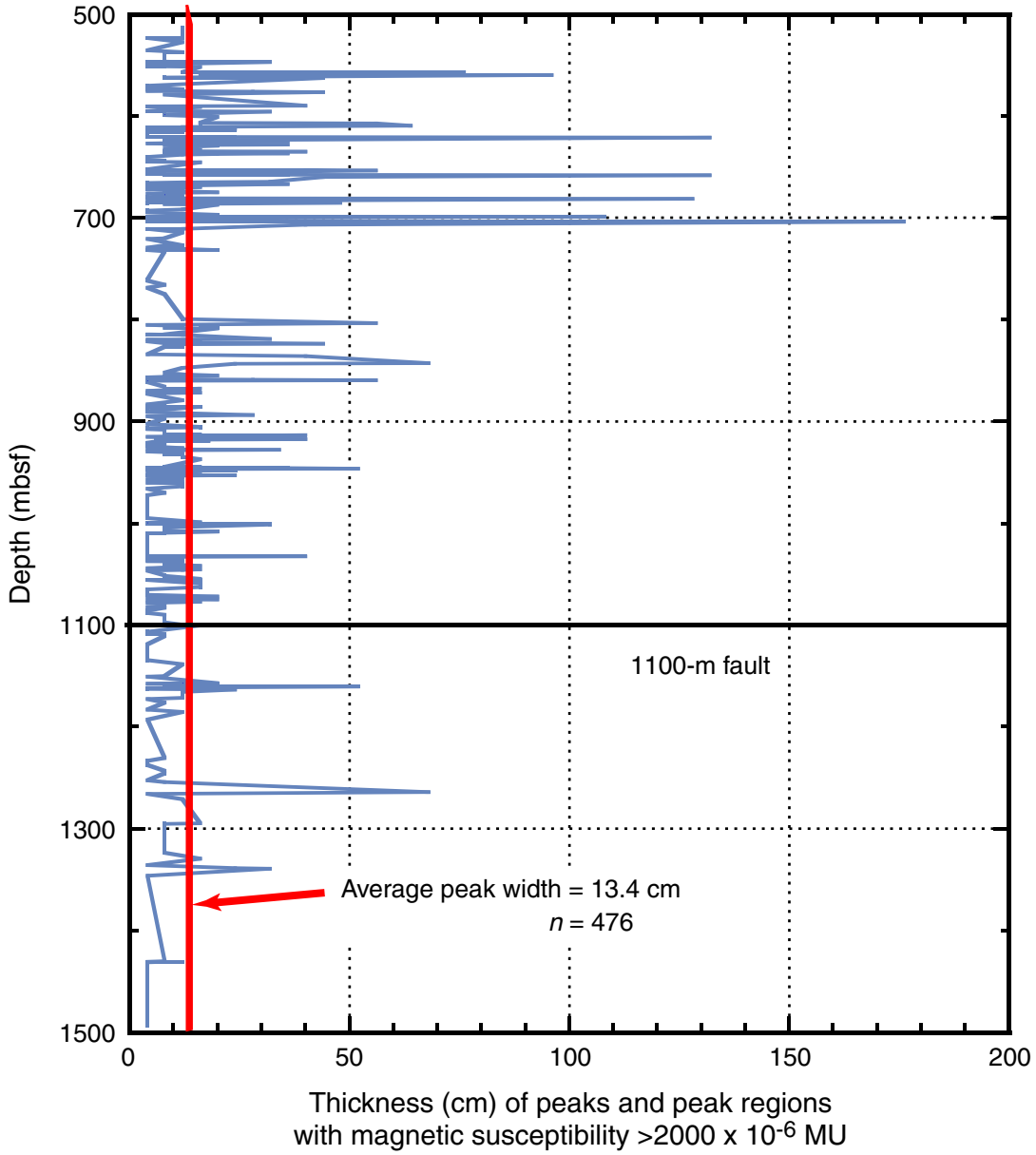

Figure F9. Percent of measurements of peaks and peak regions of magnetic susceptibility per 20-m interval vs. depth (thin line) from 500 to 1500 mbsf. This divides the plot into percent peaks (left) and percent background measurements (right). The thick curve smoothes the data over 10% of the data (200 m).

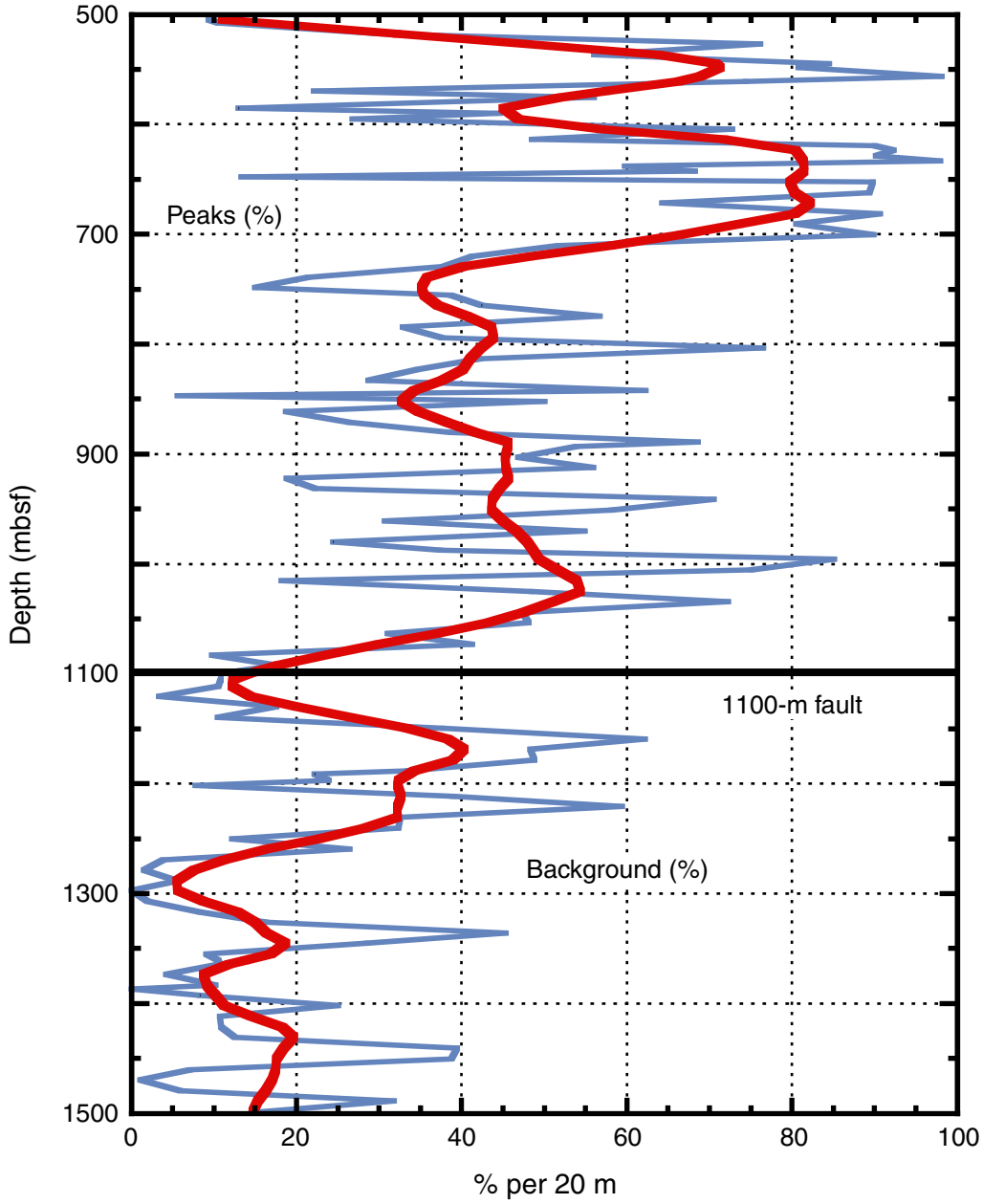

Figure F10. Background magnetic susceptibility vs. depth from 500 to 1500 mbsf. The two curves are (1) smoothed over 10% of the data (smoother) and (2) interpolated (more peaks). The break in background magnetic susceptibility at 1000 mbsf is given by the bold black line, indicated as the 1100-m fault. The dashed lines correspond to minima in the smoothed curve and appear to divide the core into major blocks (3 and 4) of olivine gabbro and troctolite, with internal fluctuations in magnetic susceptibility (A, B, etc.). There are two other blocks of olivine gabbro in the upper 500 m of the hole.

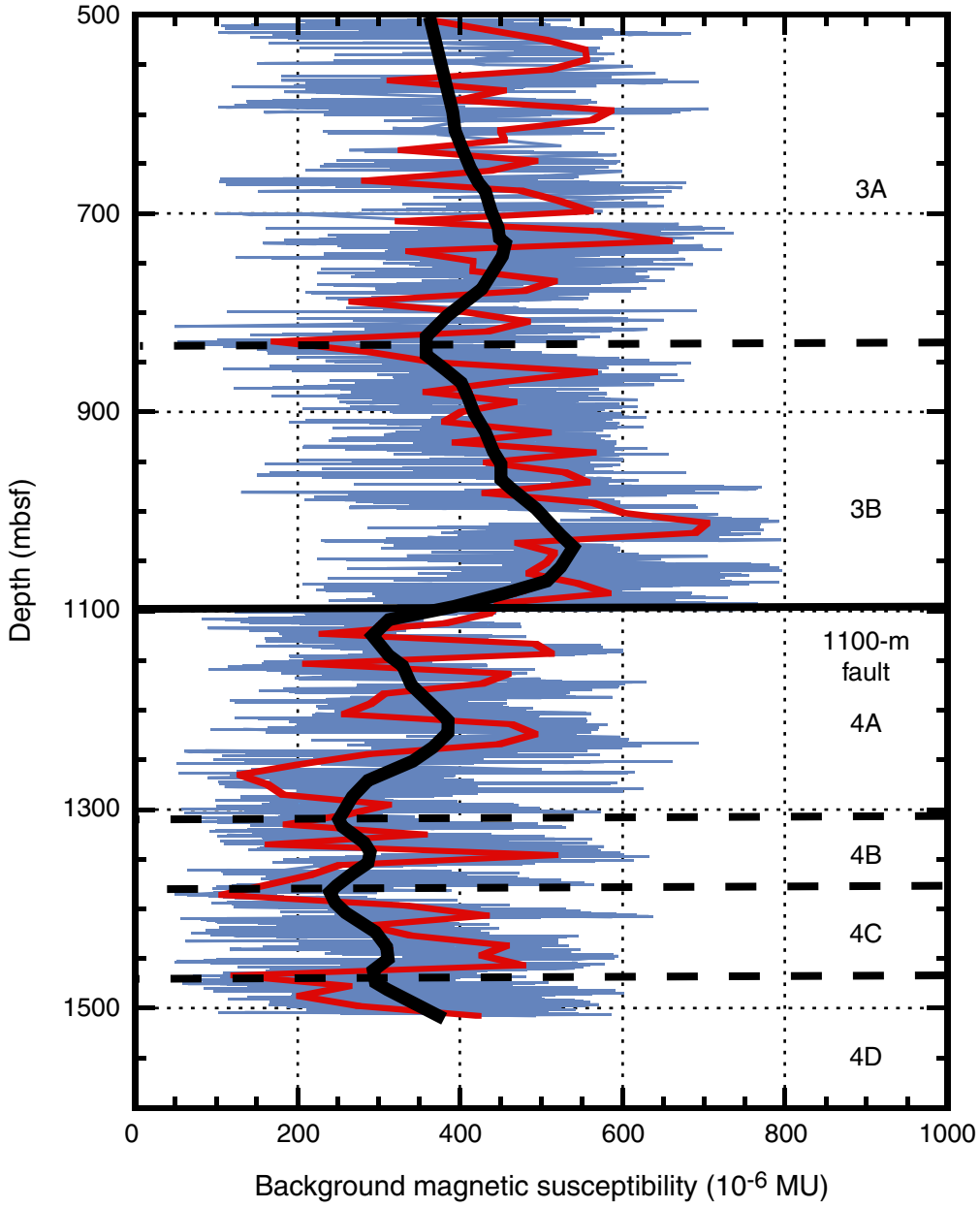

Figure F11. Average background magnetic susceptibility by core vs. depth from 500 to 1500 mbsf. This weights the data by cored interval rather than by recovery. The drop in magnetic susceptibility at 1100 mbsf is indicated by the black line, identified as the 1100-m fault. The thick curve is smoothed over 10% of the number of cores and resembles the smoother curve in Figure F12, p. 44. Magnetic susceptibility (× 10^{-6} SI) for all of Hole 735B, merging the downhole log from 20 to 490 mbsf (Leg 118) and the measurements obtained during Leg 176 using the MST and corrected to SI units using the factor 0.66, as discussed in the text (504–1508 mbsf). The three highest minicore measurements for each leg are also plotted. Susceptibility units as defined in the text are indicated to the right.

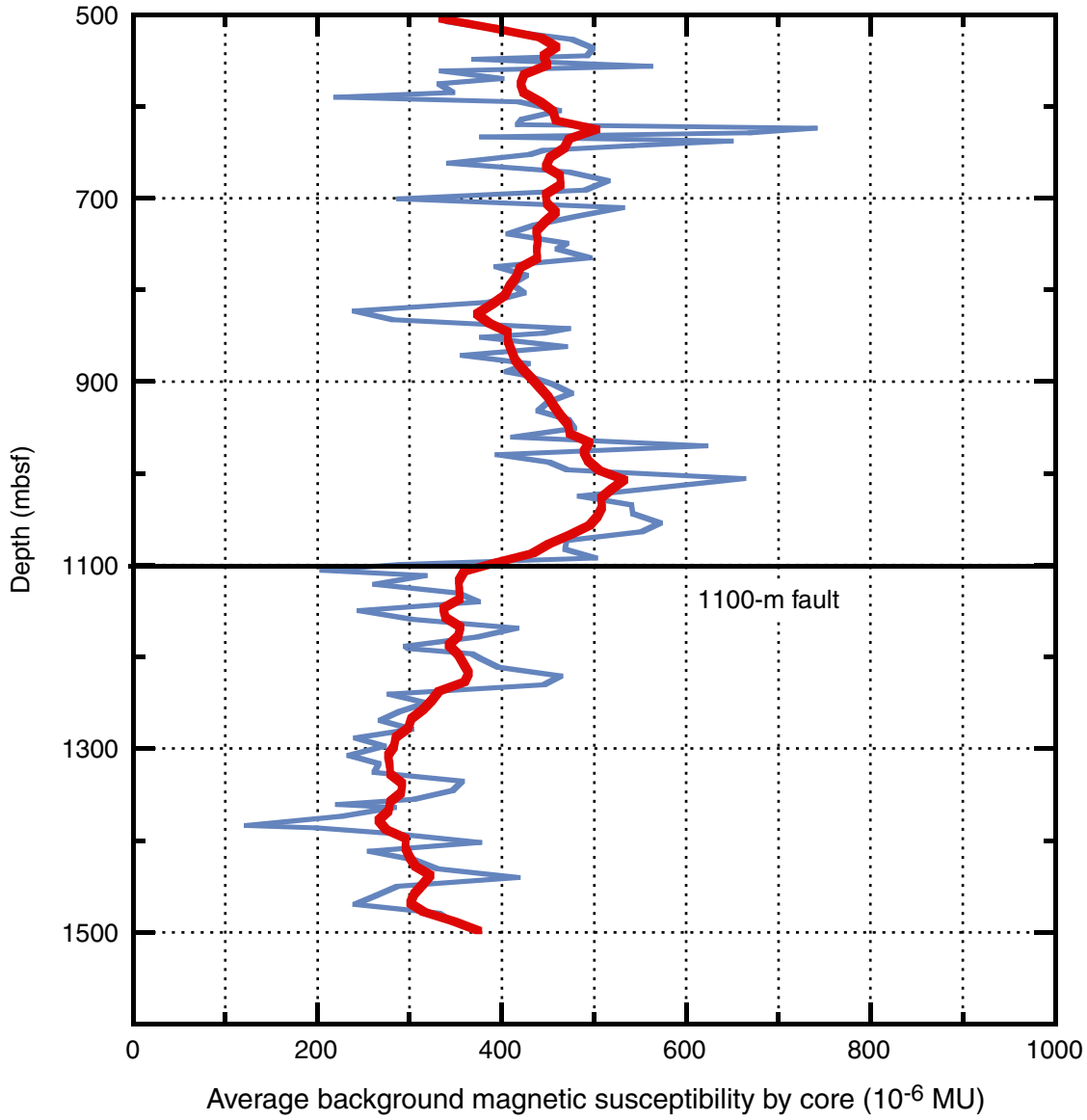

Figure F12. Magnetic susceptibility (10^{-6} SI) for all of Hole 735B, merging the downhole log from 20 to 490 mbsf (Leg 118) and the measurements obtained during Leg 176 using the MST and corrected to SI units using the factor 0.66, as discussed in the text (504–1508 mbsf). The three highest minicore measurements for each leg are also plotted. Susceptibility units as defined in the text are indicated to the right.

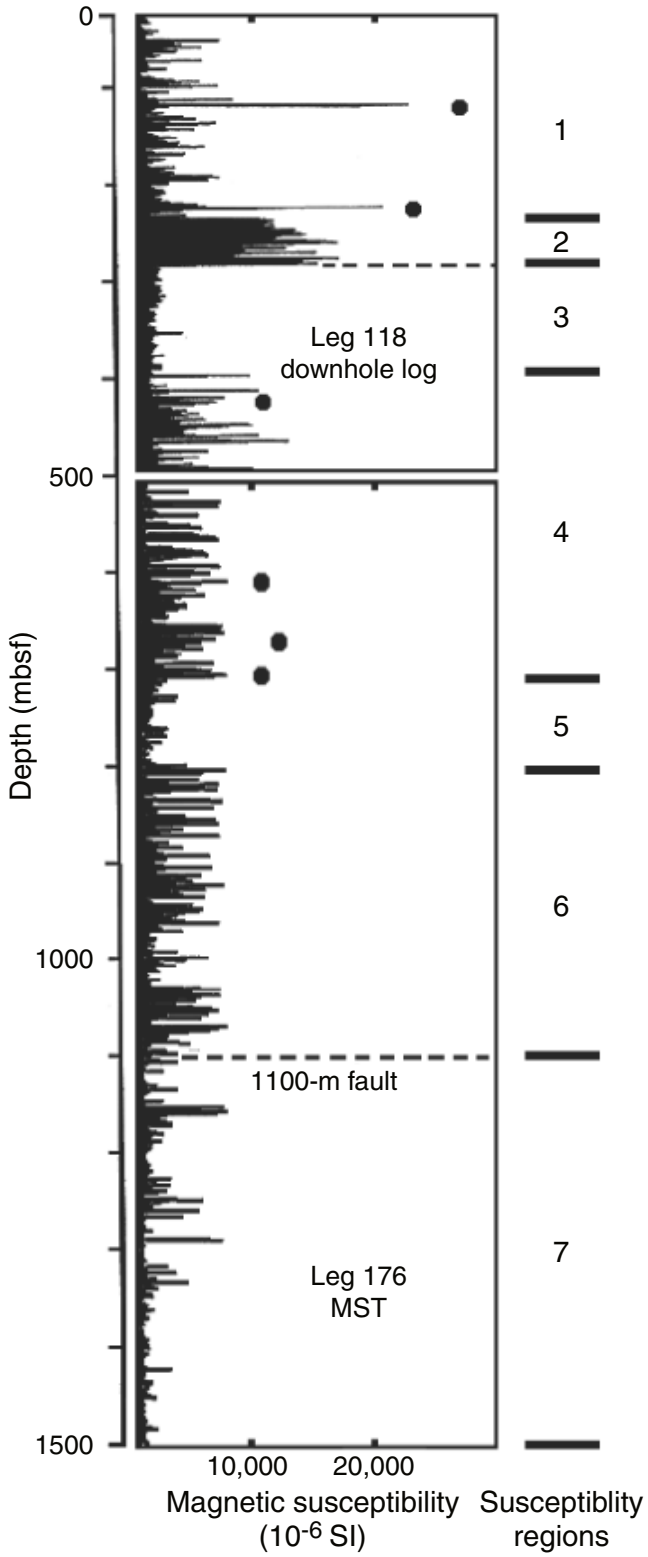

Figure F13. Right: percent of measurements with magnetic susceptibility >2000 × 10^{-6} MU (curve with lower values) and of the percent of measurements above background (curve with higher values) from 500 to 1500 mbsf in 20-m intervals, and of the percent of minicore measurements with magnetic susceptibility >2000 × 10^{-6} MU from 0 to 500 mbsf (continuation of blue curve). Left: percent of core described as oxide gabbro, oxide gabbronorite, and oxide olivine gabbro, given as lithologic intervals from 0 to 1500 mbsf, also in 20-m intervals. Note the similarity between the curve with lower values on the left and the curve on the right. BG = background.

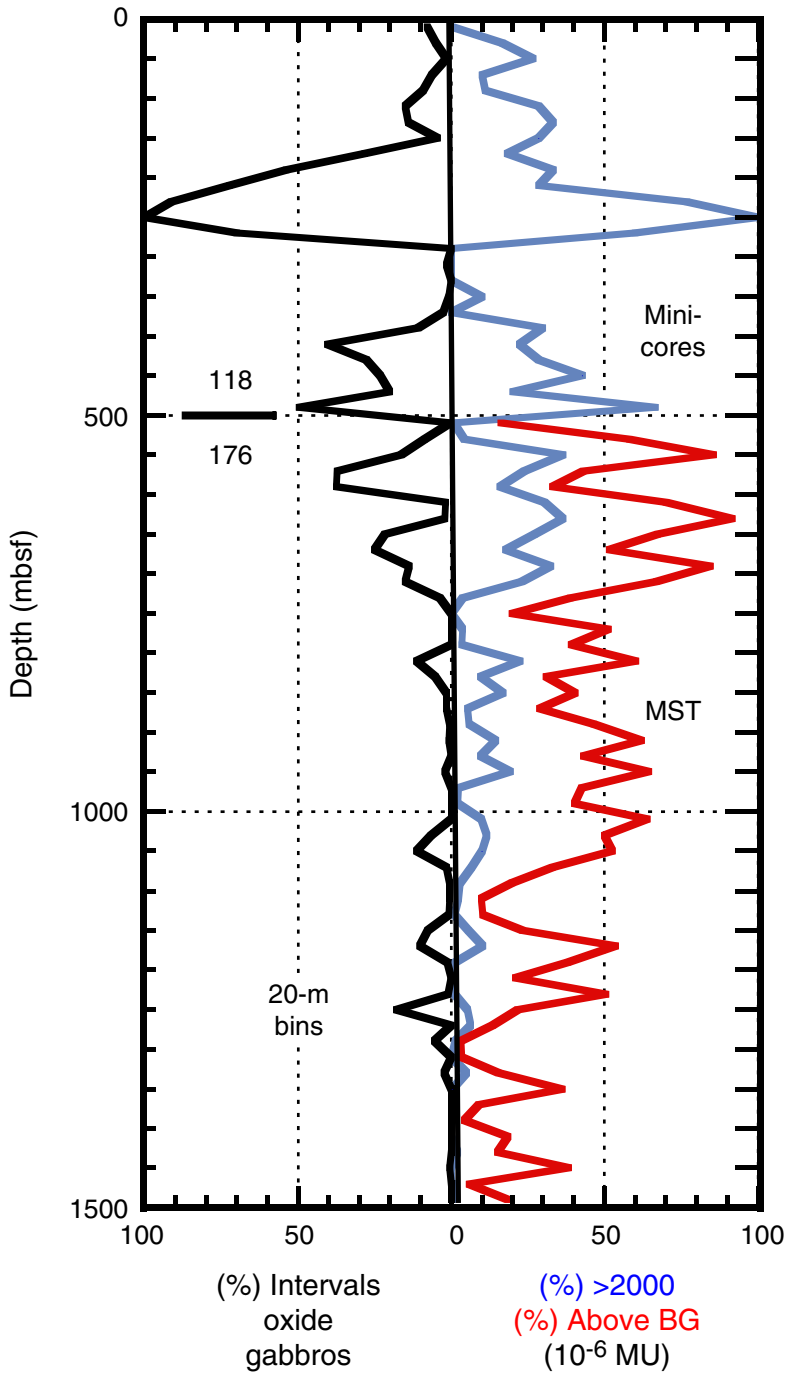

Figure F14. Magnetic susceptibility vs. depth for a peak region between 652.5 and 654.5 mbsf, spanning portions of Sections 176-735B-114R-1 and 11R-2. Lithologic intervals and rock identifications are given to the right. Background measurements are dots and bolder line on the left side of the curve. The plot is compared to a larger image for Pieces 6A–F, from the corresponding core photograph (far left), with strong contrast enhancement showing the distribution of oxide-rich portions of the core (black). The central image is compressed and widened (3×) to correspond to the vertical depth scale of the plot of magnetic susceptibility. Other pieces are added to show how the oxide-rich portions of the core correspond to susceptibility peaks. Small arrows next to the image on the left indicate boundaries to oxide-rich portions of the core that are aligned and steeply dipping in the same direction.

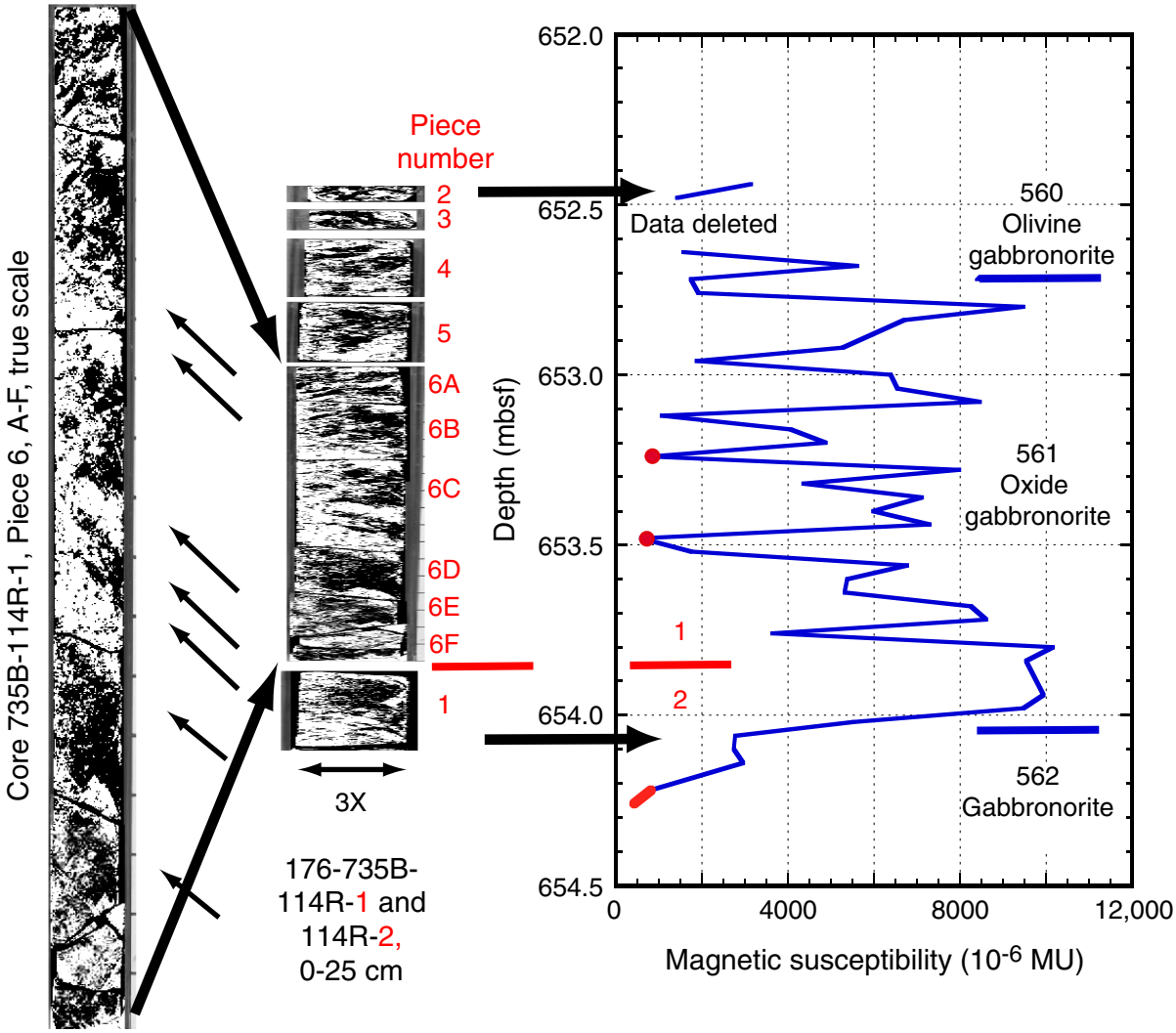

Figure F15. Magnetic susceptibility vs. depth for a peak region between 1008.1 and 1009.1 mbsf, spanning interval 176-735B-157R-3, 37–140 cm. Background measurements are the flat parts of the curve on its left side. Lithologic intervals and rock identifications are given on the far left. This is compared with an unrolled core scan and a sketch indicating tops and bottoms of subintervals, which are numbered to the right of the core scan and in the plot of magnetic susceptibility. Some contrast enhancement has been applied to the core scan. Numbers in parentheses on the plot of susceptibility vs. depth give the deformation intensity. Peaks in magnetic susceptibility correspond to subintervals 3 and 6, pointed out by arrows adjacent to the core-scan image. XRF/TS = X-ray fluorescence/thin section.

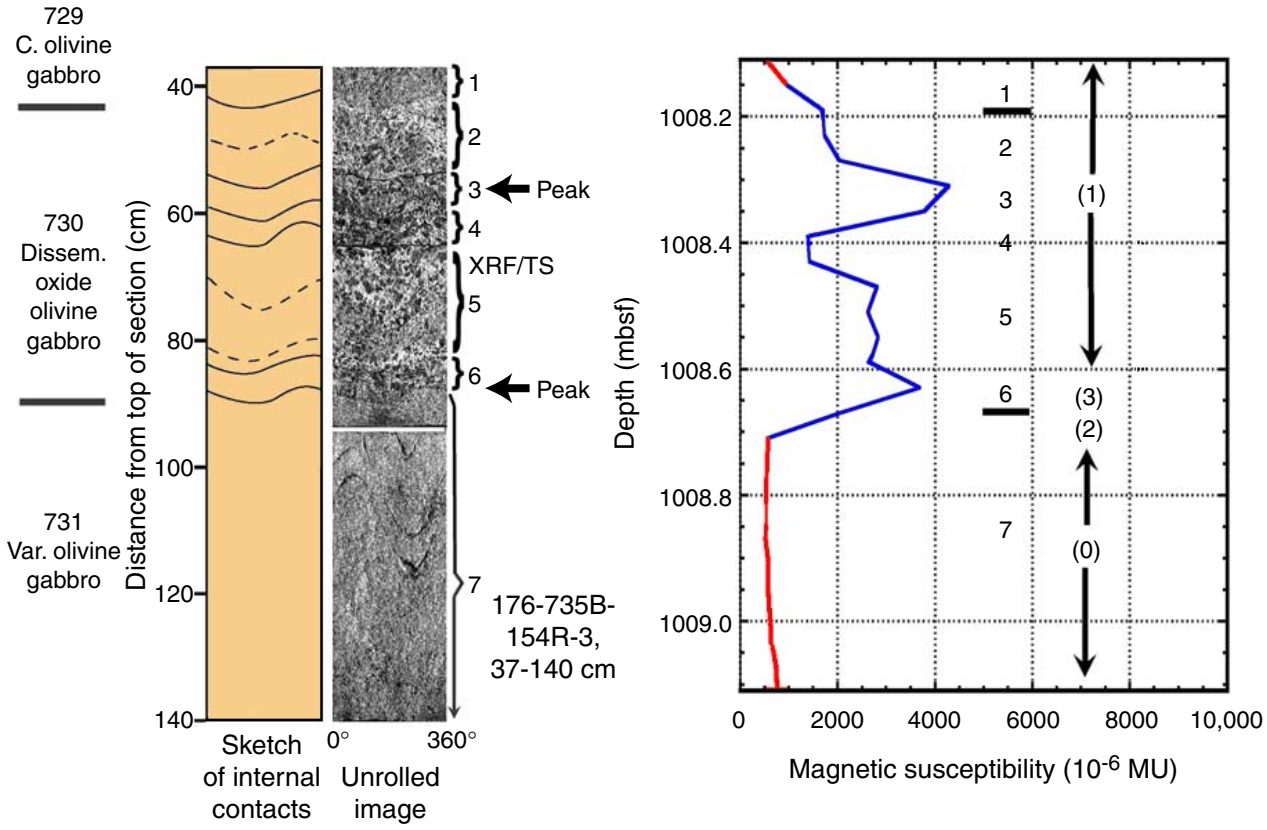

Figure F16. Magnetic susceptibility vs. depth for a peak region between 1032.6 and 1033.3 mbsf, spanning interval 176-735B-156R-7, 0–70 cm. Background measurements are given by the dot and the flat part of the curve below 1033.2 mbsf. Lithologic intervals and rock identifications are given on the right side of the plot and deformation intensities on the far right. These are compared with an unrolled core-scan image and the corresponding core photograph, the latter widened by 2×. Some contrast enhancement has been applied to both images. On the left is a sketch of subinterval contacts within lithologic interval 742 from the unrolled image.

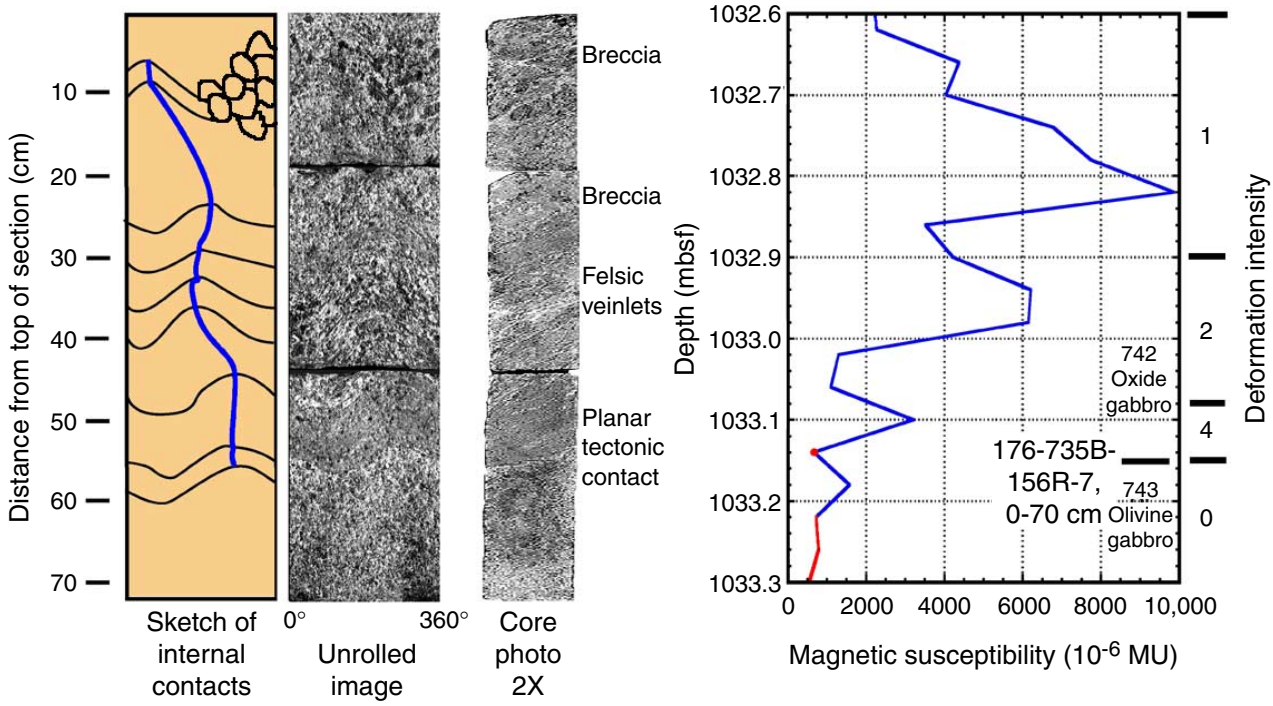

Figure F17. A prominent felsic vein in interval 176-735B-90R-1, 37–63 cm. The close-up photograph on the left is compared with a plot of magnetic susceptibility vs. depth for the corresponding interval. The vein has lower magnetic susceptibility than the immediately surrounding rock, although the surrounding rock itself has magnetic susceptibility slightly higher than local background measurements.

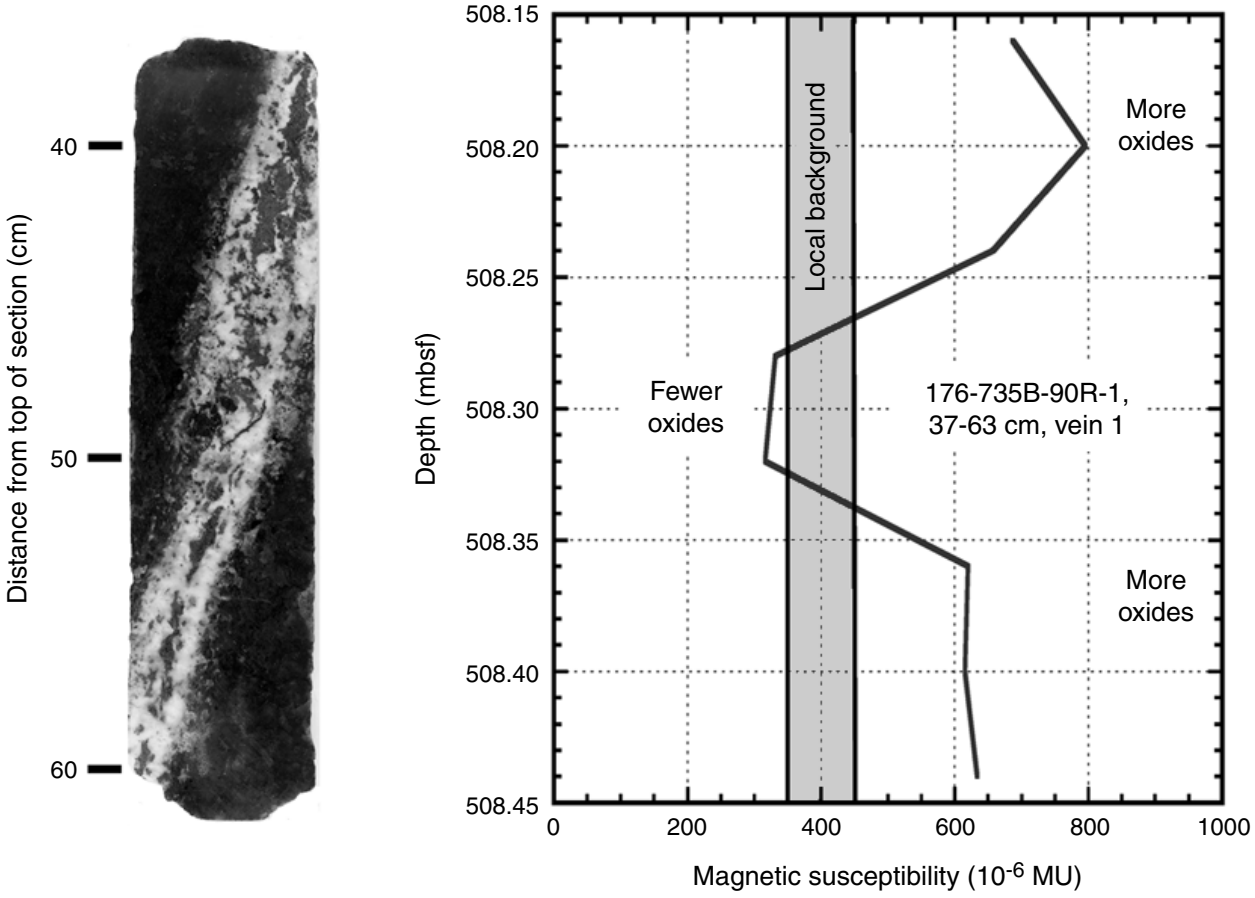

Figure F18. Felsic material filling fractures and surrounding angular fragments, Core 176-735B-110R-4, 10–50 cm. The image on the left is an unrolled core scan. A close-up image of the flat surface of the split piece of rock, and of one above it, is to the right of the core scan. These are compared with the a plot of magnetic susceptibility vs. depth of the same interval of rock. Background measurements are given by the dots.

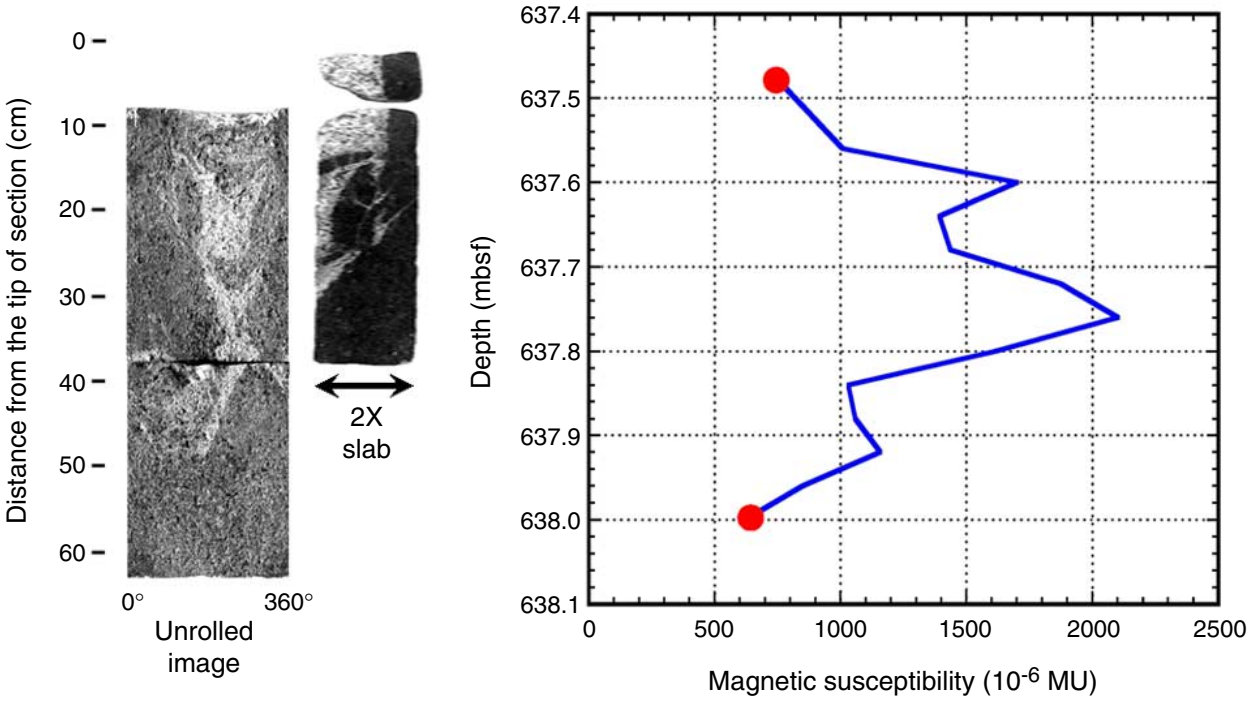

Figure F19. Close-up photograph (upper left) of interval 176-735B-143R-2, 101–115 cm, showing a felsic vein (white) with oxide-rich gabbro (dark) at ~905 mbsf in Hole 735B. The deformation intensity is to the right of the close up. The close up is linked to measurements of magnetic susceptibility vs. depth at 4-cm intervals (upper right) corresponding to a portion of lithologic interval (LI) 693. The magnetic susceptibility inset shows the individual susceptibility peak among several others in a 7-m section of core. The lower panels focus on the nearly horizontal felsic vein and show by means of successive enhanced-contrast selection of the dark oxide minerals, the association of coarse ilmenite and magnetite with the vein and strong foliation of the rock near the vein.

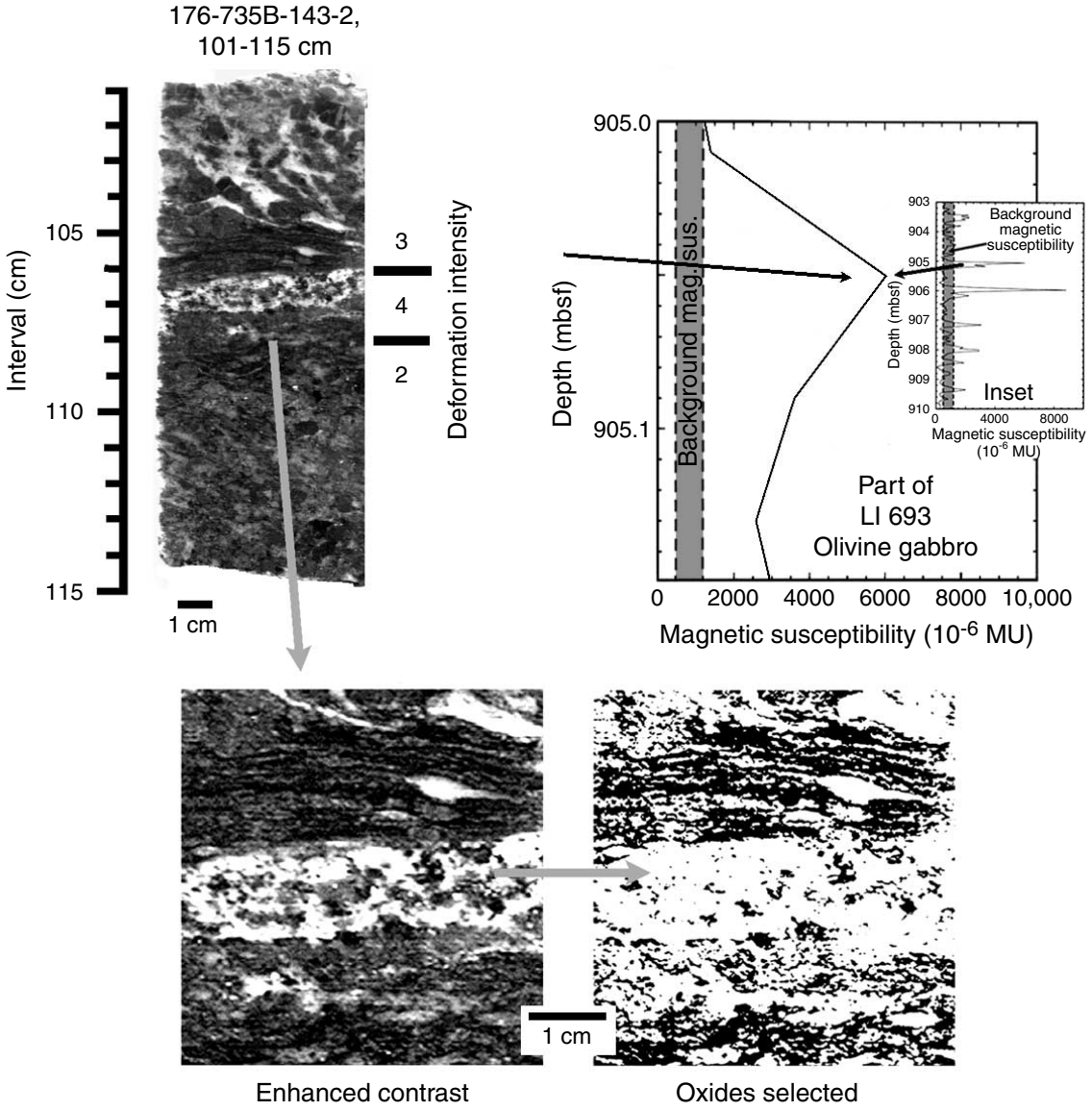

Figure F20. A core photograph of a deformed oxide gabbro seam in Section 176-735B-149R-3 (left) that produced a strong spike in magnetic susceptibility (right). The deformation intensity is strongest (grade 4; mylonitic) just at the peak in intensity of magnetic susceptibility. The contrast of the photograph is somewhat enhanced to reveal the presence of a deformed felsic vein between 52 and 55 cm in the section and felsic veinlets in the deformed troctolite (lithologic interval 718) just above the oxide-gabbro mylonite. The latter was not identified as a separate lithologic interval in the core descriptions. The inset is a scanned image of a slab sample of this portion of the section. In the plot on the right, background measurements are the flat parts of the curve on its left.

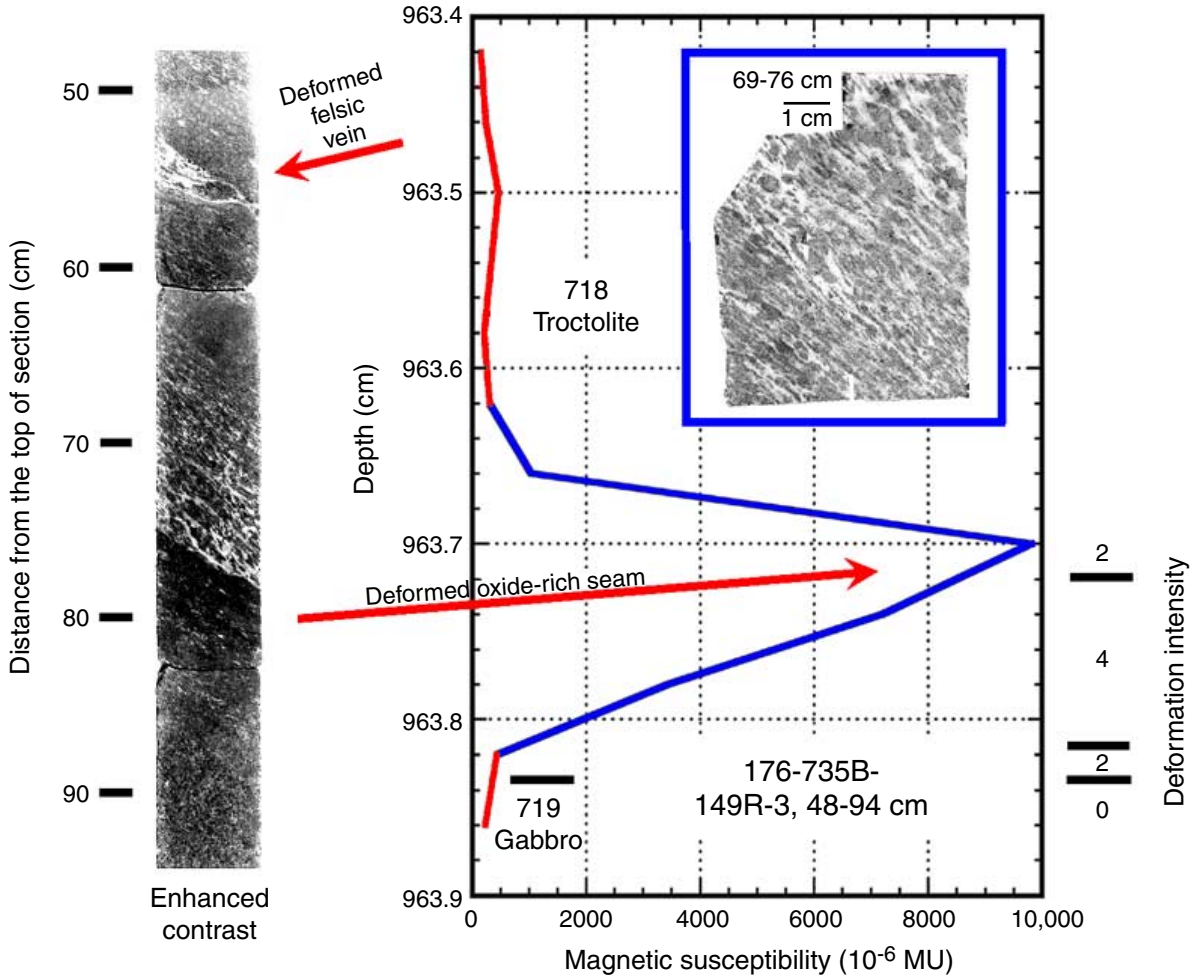

Figure F21. A narrow mylonite/ultramylonite zone in interval 176-735B-107R-1, 20–30 cm. The unrolled image of the whole-round core and a core photograph of the split surface of the rock are on the left. Contrast in both is somewhat enhanced to heighten detail. Two small blow-ups of portions of the core photograph show details of the mylonite zone and the coarse, nearly pegmatitic olivine gabbro just below it. There are felsic streaks in the mylonite, the base of which corresponds to a small increase in magnetic susceptibility (plot at right). In the plot, background measurements are the flat parts of the curve on its left. Deformation intensities (DI) are indicated to the right.

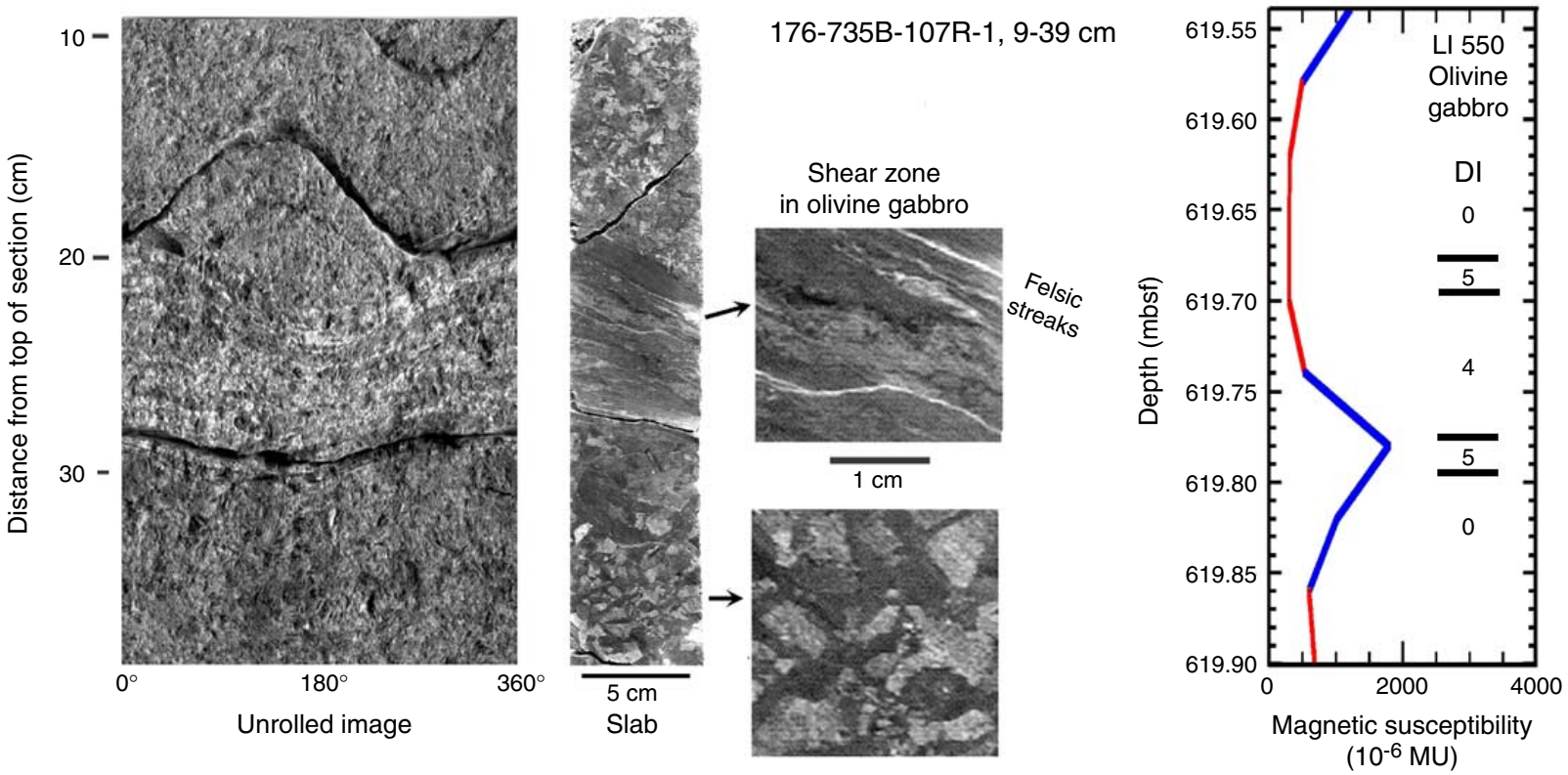

Figure F22. A portion of the core photograph for interval 176-735B-131R-1, 0–37 cm, an oxide gabbro that provided three peaks in magnetic susceptibility. **A.** No contrast enhancement; the double-headed arrow gives the interval for an analyzed slab sample reported by Snow et al. (**Chap. 12,** this volume). **B.** Same image with greater contrast, showing both oxide-rich material (black) and swirls of felsic material (white). **C.** Same image, with oxides selected. **D.** Same image, with felsic swirls selected. **E.** Magnetic susceptibility vs. depth. The analyzed rock has 4.34% TiO_2 from the oxide minerals and 76 ppm Zr, from the felsic swirls.

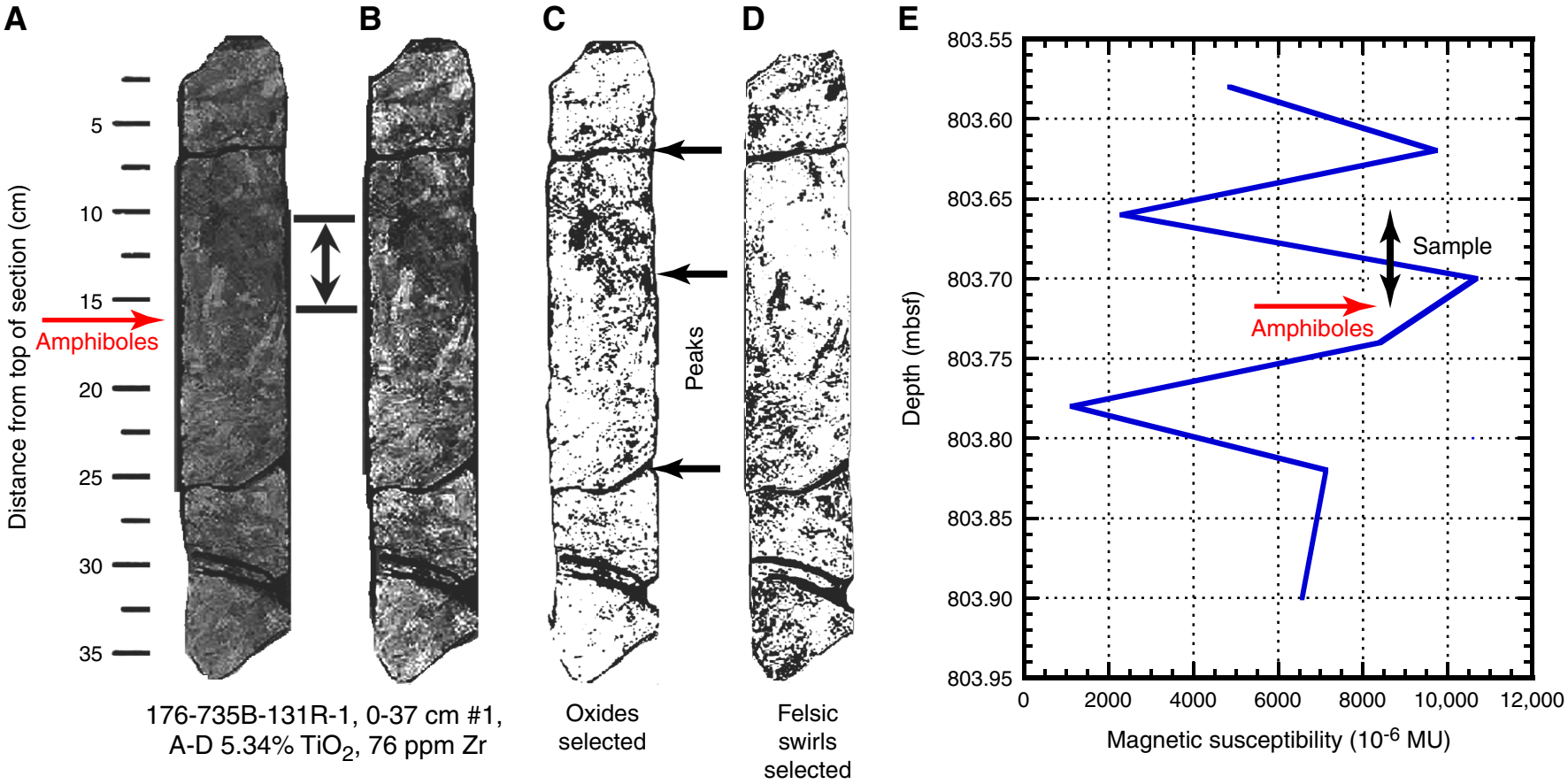

Figure F23. A–F. Scanned images of slab samples with felsic veinlets or vein nets cementing breccias from Hole 735B. Core numbers are given above each sample. Contrast has been somewhat enhanced in each case, to highlight both felsic veins (white) and occurrences of oxides (dark gray to black). Deformation intensities are given by the numbers to the right of, and magnetic susceptibilities are below, each image.

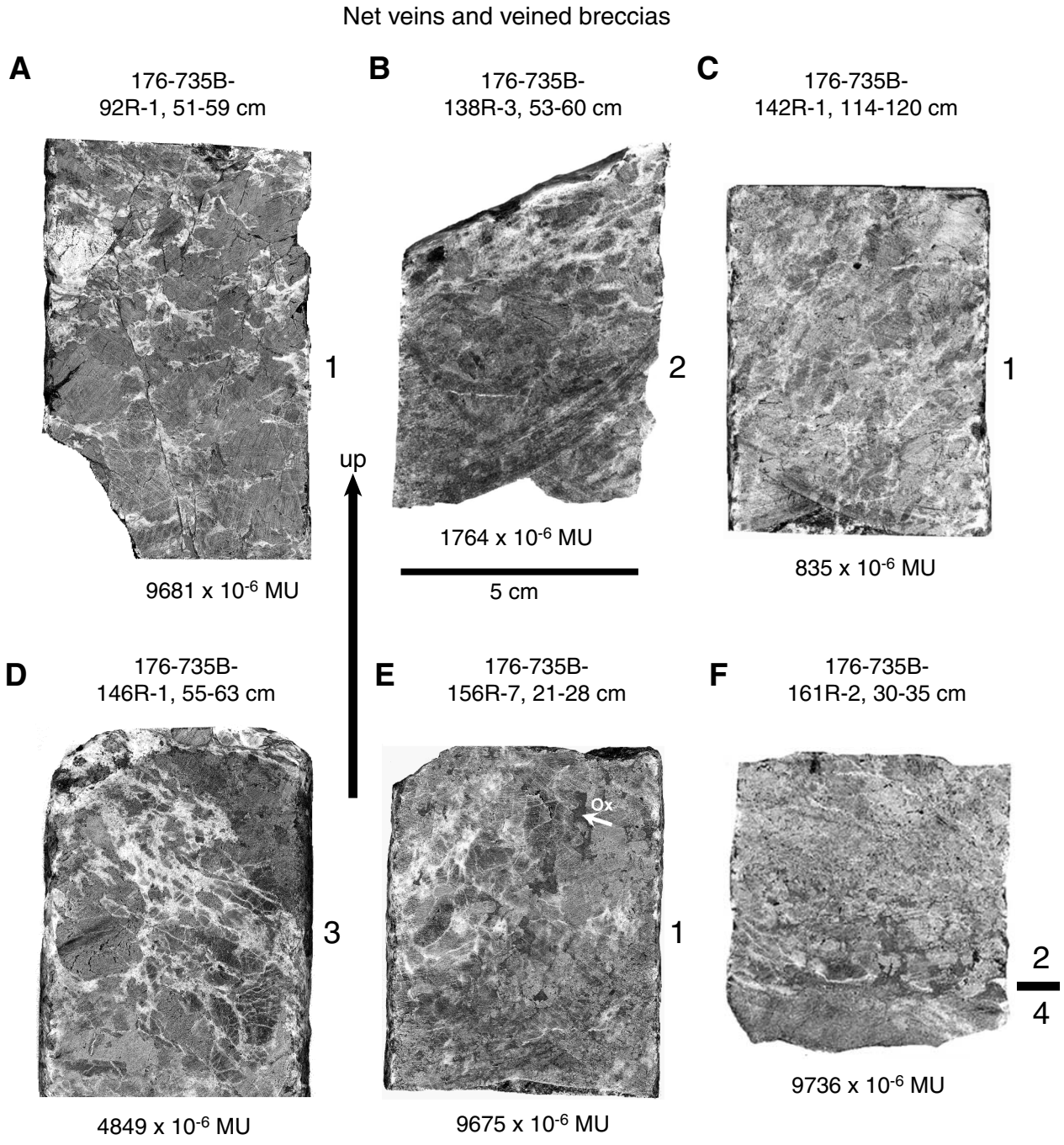

Figure F24. A coarse pegmatitic breccia with high magnetic susceptibility from interval 176-735B-107R, 0–50 cm. The unrolled core scan and corresponding photograph of the split surface of the rock are on the left. A portion of the latter showing details of the breccia is blown up at the bottom. The corresponding magnetic susceptibility is plotted vs. depth on the right. Lithologic intervals and lithologic identifications are indicated on the diagram. DOOG = disseminated oxide olivine gabbro.

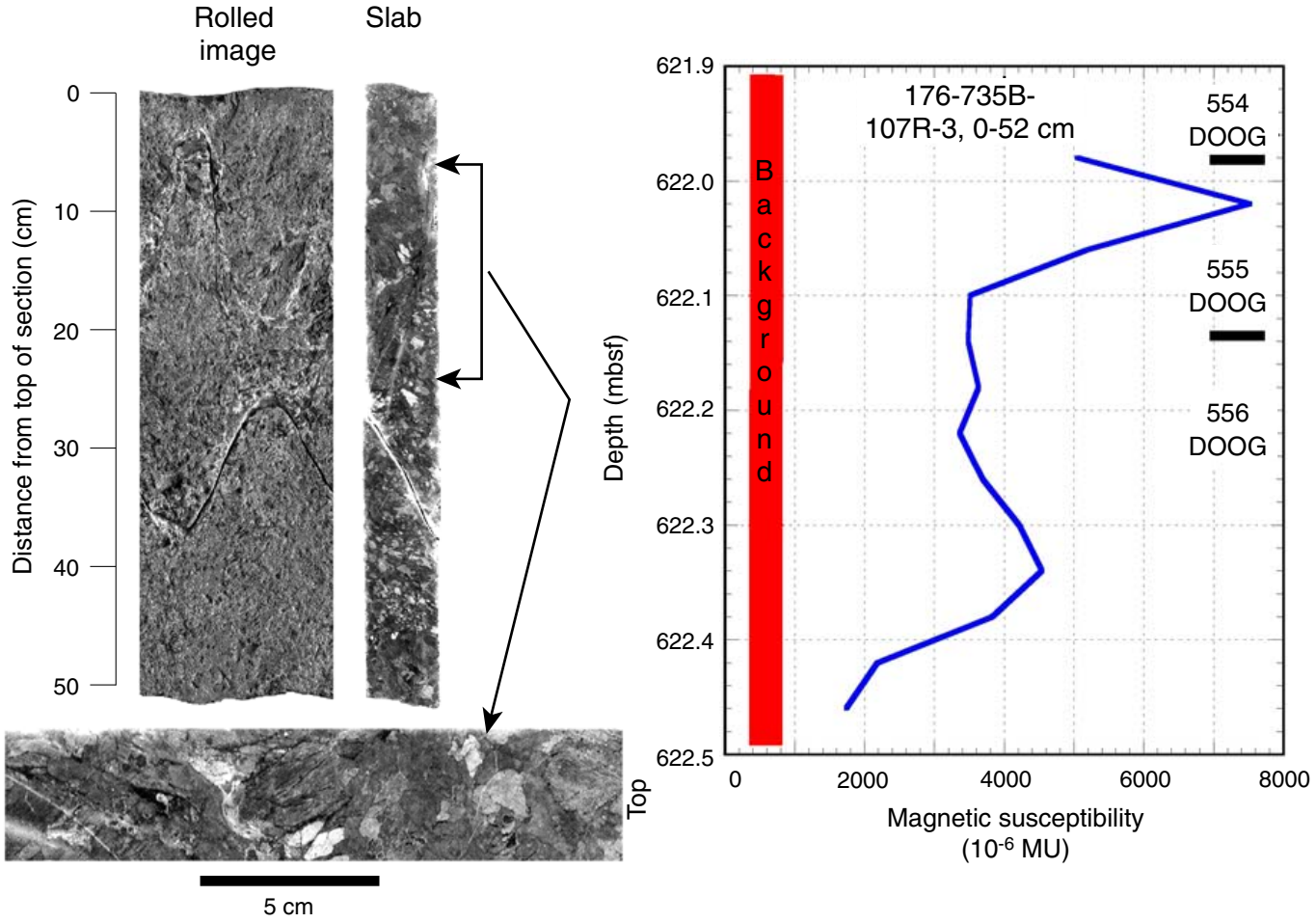

Figure F25. A histogram giving number of veins vs. their magnetic susceptibility in bins of 400×10^{-6} MU. In each case, magnetic susceptibility was taken as the maximum value in the interval of rock crossed by the vein. Of 203 veins noted in the vein-log spreadsheet, 196 occur in whole-round core. Of these, 79 (40.3%) are in core with background levels of magnetic susceptibility ($<800 \times 10^{-6}$ MU), and 117 are in peaks or peak regions ($>800 \times 10^{-6}$ MU) corresponding to oxide gabbros. Of the latter, 52 veins (26.5%) occur in oxide gabbros ($>2000 \times 10^{-6}$ MU).

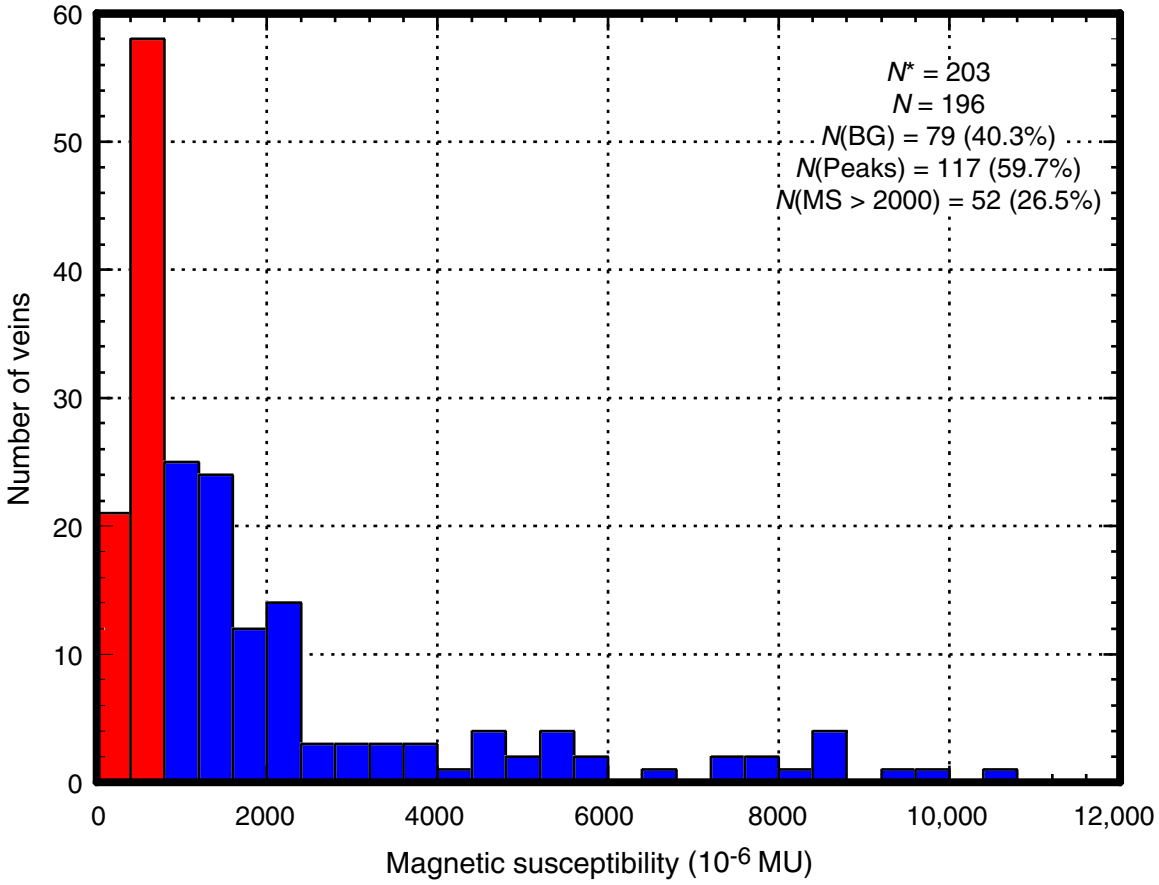

Figure F26. Comparison of 10% least-squared weighted curves of magnetic susceptibility vs. depth, from 5000 to 1500 mbsf, for background measurements, peaks, and peak regions without felsic veins and peaks with veins as labeled. The result of the curve fit is to plot a best fit smooth curve through the center of the data. Here it shows that felsic veins have comparable or even higher magnetic susceptibility than oxide gabbro seams (peaks) without such veins. The fault at 1100 mbsf is shown by the vertical black line.

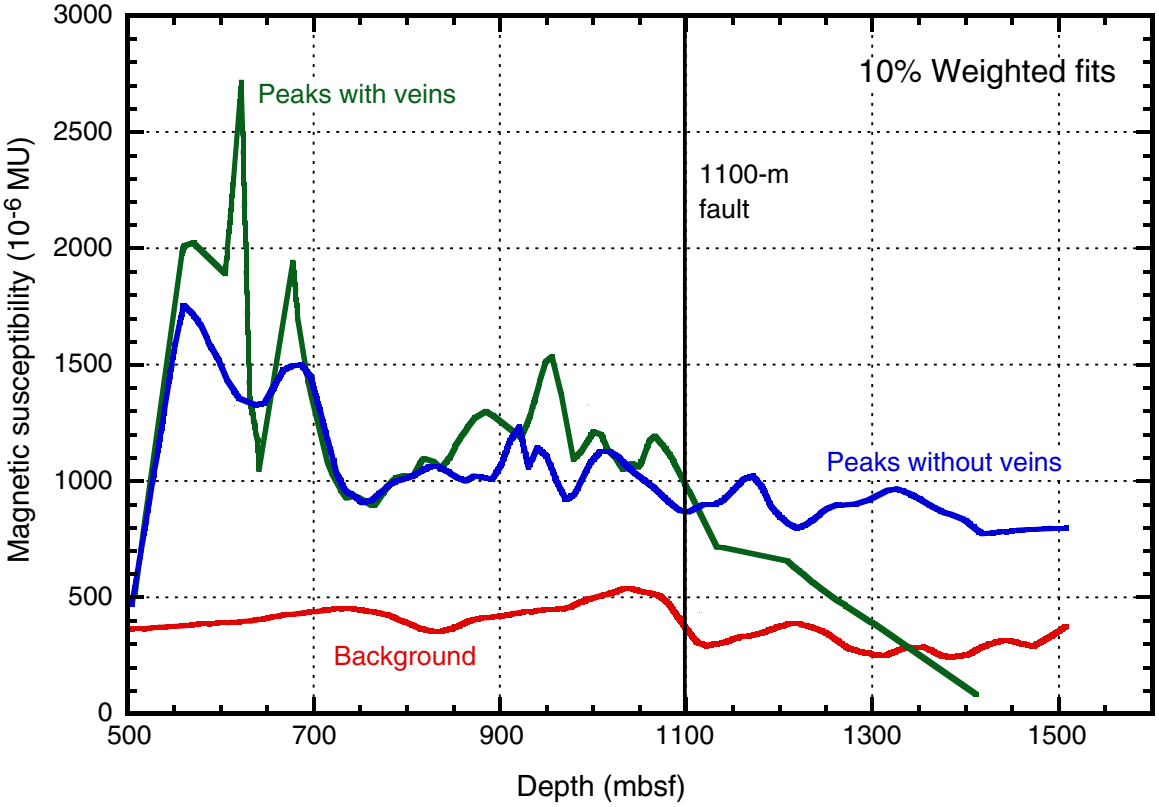

Figure F27. A. Vein number, sequenced from the vein-log spreadsheet (supplementary material to the site report (Shipboard Scientific Party, 1999b) vs. depth from 500 to 1500 mbsf, showing the contrast in vein frequency above and below the fault at 1100 mbsf. **B.** Felsic vein volume per 10 m of core vs. depth, also from the vein-log spreadsheet.

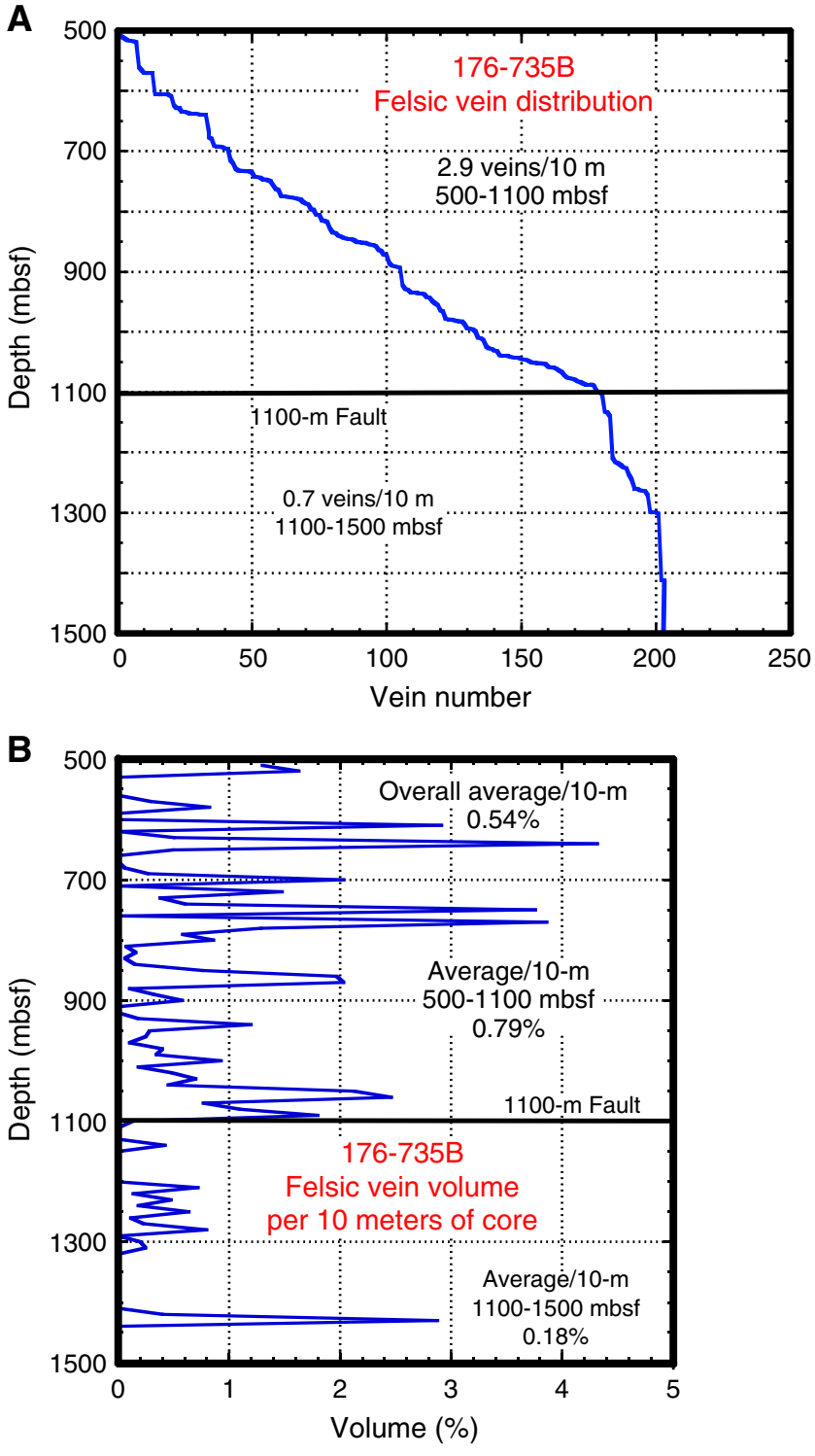

Figure F28. Comparison of magnetic susceptibility (right) with crystal-plastic deformation intensity (left) for a portion of core from 944.5 to 964 mbsf plotted vs. depth. On the right, peaks and peak regions are contrasted in color or shade with lower background measurements. Lithologic intervals by number and rock identifications are also indicated on the right, as are occurrences of three felsic veins (FV). Large squares give locations of samples taken for rock analysis (from Shipboard Scientific Party, 1999b, Niu et al., **Chap. 8,** this volume; Snow et al., **Chap. 12,** this volume). Small squares give locations of thin sections shown in Figure **F29,** p. 61. On the left, deformation categories are 0 = undeformed; 1 = slightly deformed; 2 = banded or gneissic; 3 = porphyroclastic; 4 = mylonitic; and 5 = ultramylonitic. Deformation categories are averages for given intervals, giving the diagram its stepwise character. Arrows on the left identify strongly deformed rock corresponding to susceptibility spikes on the right.

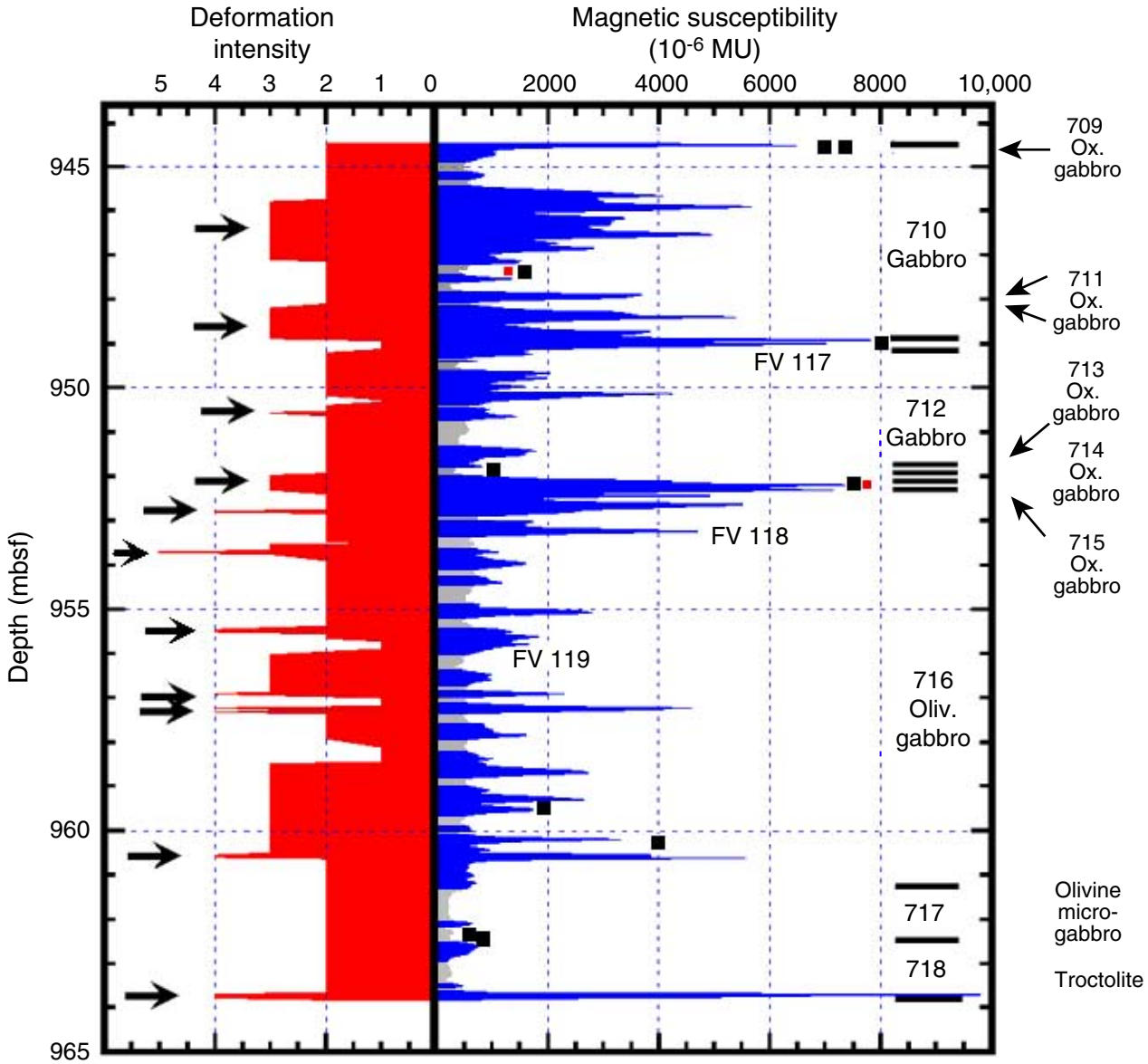

Figure F29. Scans of oversized thin sections from two intervals of deformed rock given by the red dots in Figure F28, p. 60. **A.** Sample 176-735B-147R-6 (Piece 2A, 45–51 cm), gneissic gabbro, lithologic Interval 710. **B.** Sample 176-735B0148R-1 (Piece 3B, 127–132 cm), porphyroclastic oxide gabbro. Both sections are oriented in the same way with arrows pointing toward the top of the core. Note the darker clinopyroxene (gray) and greater abundance of oxide minerals (black) in B than in A. **C, D.** The oxides from the two respective thin sections of A and B are selected (black). Alignment of oxides along planes of foliation is evident in both.

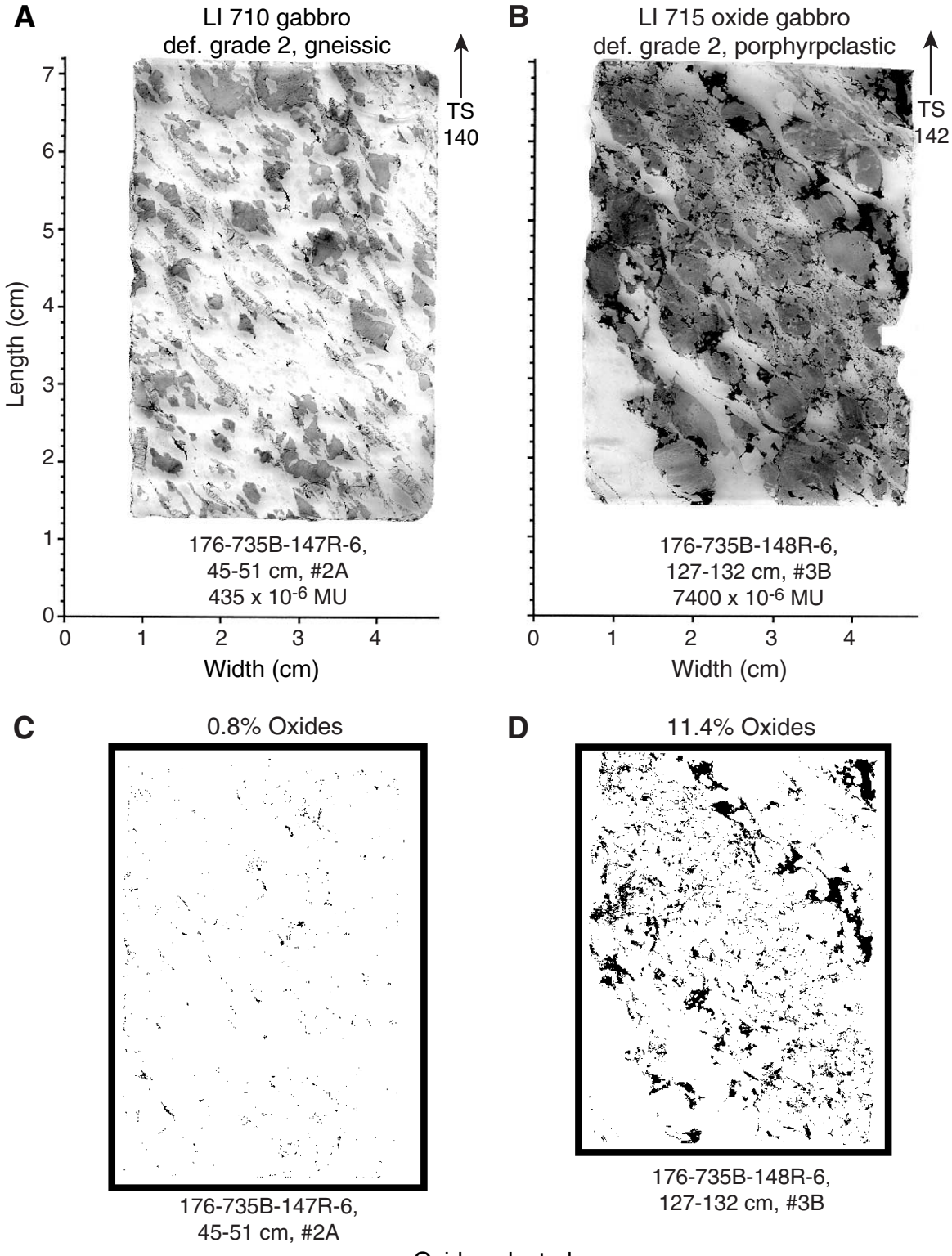

Figure F30. Portions of Sections 176-735B-147R-3 and 147R-4, showing the upper contact of the deformed region of core from Figure F29, p. 61. The unrolled scanned image and the corresponding core photograph of the split surface of the rock are on the left. Magnetic susceptibility vs. depth is on the right. Inclined contacts between lithologic units are indicated by arrows next to the core photograph. Lithologic intervals, rock lithologies, and intensities of deformation are given on the diagram of susceptibility vs. depth.

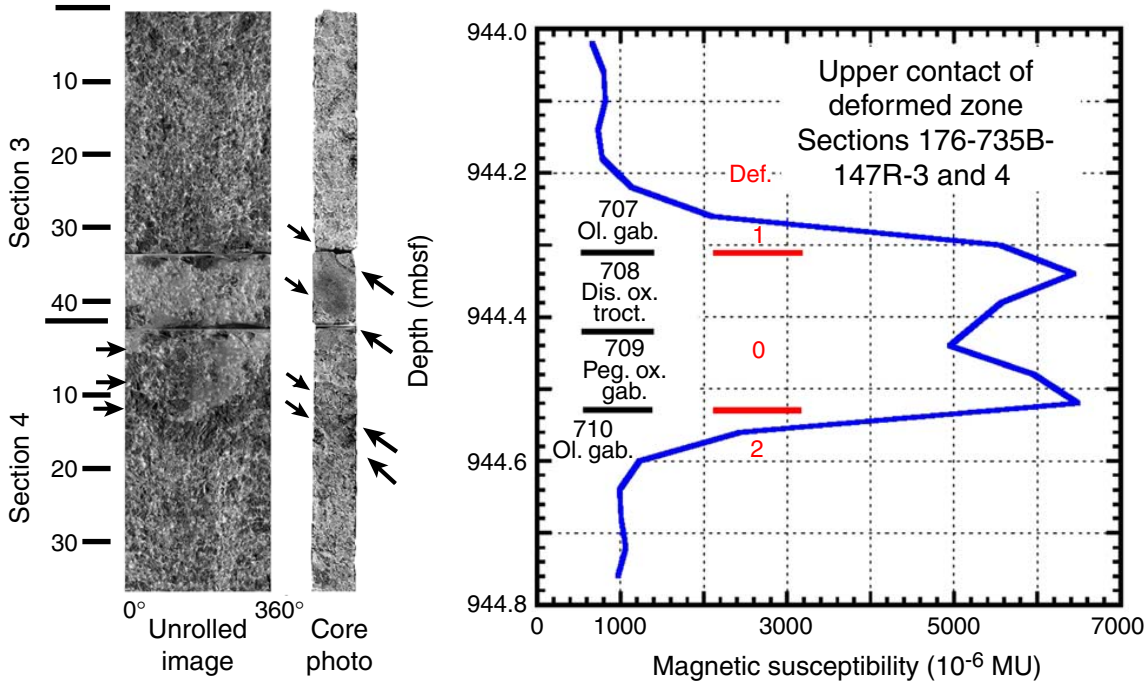

Figure F31. Magnetic susceptibility histogram for strongly deformed rock. The histogram represents the values of susceptibility measurements corresponding to deformation grades 2–5 in bins of 400×10^{-6} MU. Peaks represent 65.9% of the measurements and background measurements 34.1%. Strong peaks corresponding to oxide gabbros ($>2000 \times 10^{-6}$ MU) are 32.4% of the measurements.

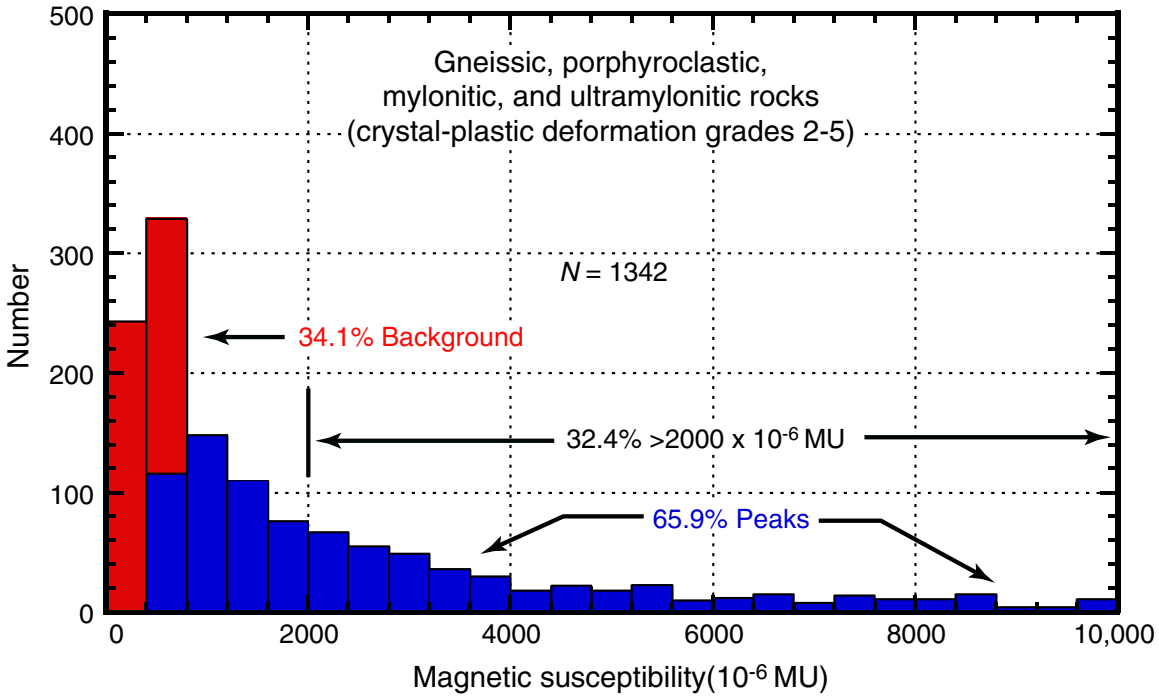

Figure F32. Chemical relationships between gabbros and minerals from Hole 735B. **A.** Ternary FeO-SiO_2-TiO_2 diagram for gabbros and minerals of Hole 735B. Small dots = olivine gabbros and troctolites; squares = oxide gabbros; large open circles = average clinopyroxene, amphibole, and olivine for olivine and oxide gabbros; large dots = average ilmenite and magnetite. Data sources are Dick et al. (**Chap. 10,** this volume) and Natland et al. (1991). The shaded triangle links average olivine gabbro with ilmenite and magnetite. A solid line is drawn from the upper apex of the triangle through the oxide gabbros to a point on the baseline of the triangle. The lever rule applied to this line shows that the proportion of ilmenite to magnetite in oxide gabbros, corresponding to the ratio of the respective lengths of the longer and shorted double-headed arrows, is 4:1. This assumes all FeO is contained in the oxide minerals, whereas some of it is in olivine and pyroxenes. The ratio thus gives the minimum proportion of ilmenite to magnetite in oxide gabbros. Petrographic estimates range from 3:1 to 5:1. **B.** MgNo (= Mg/[Mg + Fe^{2+}] with Fe^{2+} determined by titration of least altered olivine gabbros (dots) and troctolites (pluses) vs. their TiO_2 contents. Data are from **"Appendix B,"** p. 46, of Natland and Dick (**Synthesis Chap.,** this volume). TiO_2 shows a weak correlation to MgNo (solid line; linear regression correlation coefficient = 0.58) even in troctolites, which have very little clinopyroxene. Among silicates, TiO_2 is only present in significant amounts in clinopyroxene (0.6% average throughout the core). The amount of TiO_2, which increases with decreasing MgNo, that is accommodated in modally fluctuating amounts of clinopyroxene (average = 29%) is indicated by the dashed shaded line. The effects of adding 1% separately of average ilmenite and magnetite (Natland et al., 1991) to a typical troctolite are given by the curved arrows. Almost all TiO_2 thus has to be accommodated in small amounts, but no more than 1%, of ilmenite in any of these rocks. Adding ~0.4 ± 0.3% of ilmenite on a background of modally variable clinopyroxene thus accounts for the weak correlation. This would be accompanied only by ~0.01% of intergrown magnetite (see text for discussion).

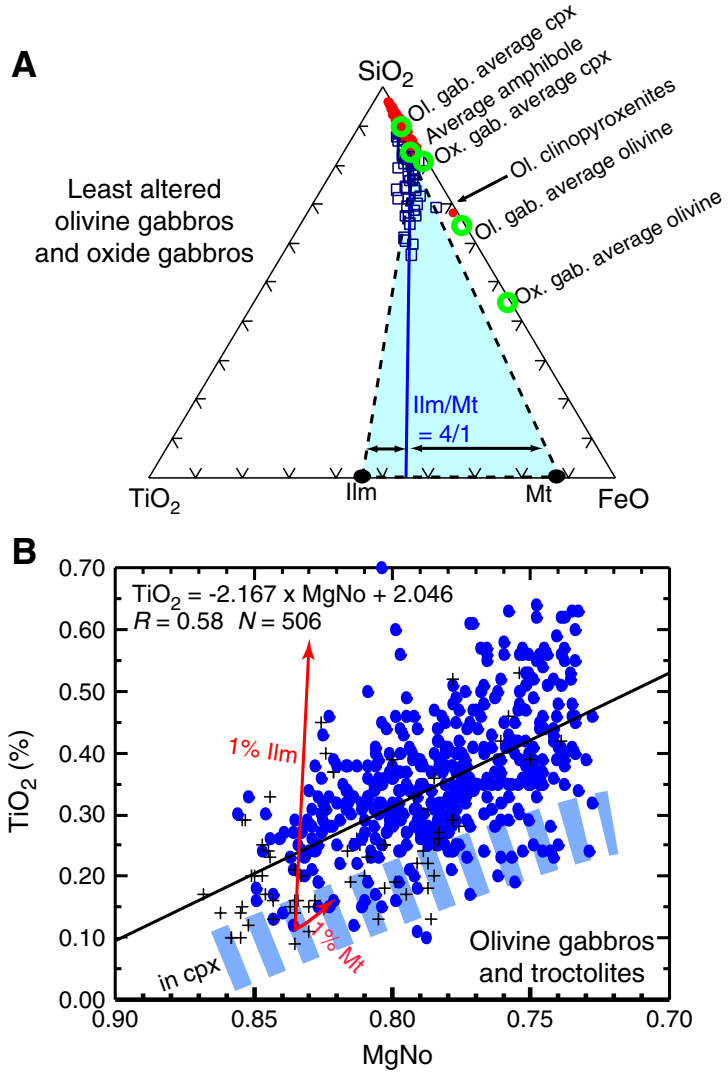

Figure F33. A. Log-log diagram of magnetic susceptibility ($\times 10^{-6}$ MU) vs. TiO_2 for all gabbros of Hole 735B. Both linear and curving power-law regressions are shown. Diagonal black lines divide the rocks into principal lithologic types. TiO_2 values are from shipboard XRF data (Shipboard Scientific Party, 1999b). Magnetic susceptibility is taken as the value closest to the center of the ~5-cm-long sample taken for each sample **B.** MgNo (= Mg/[Mg+Fe^{2+}] with Fe^{2+} determined by titration) from shipboard analyses vs. magnetic susceptibility ($\times 10^{-6}$ MU) for least altered olivine gabbros and troctolites (TiO_2 <0.7%) from Hole 735B. A linear correlation (r = 0.64) is shown by the line.

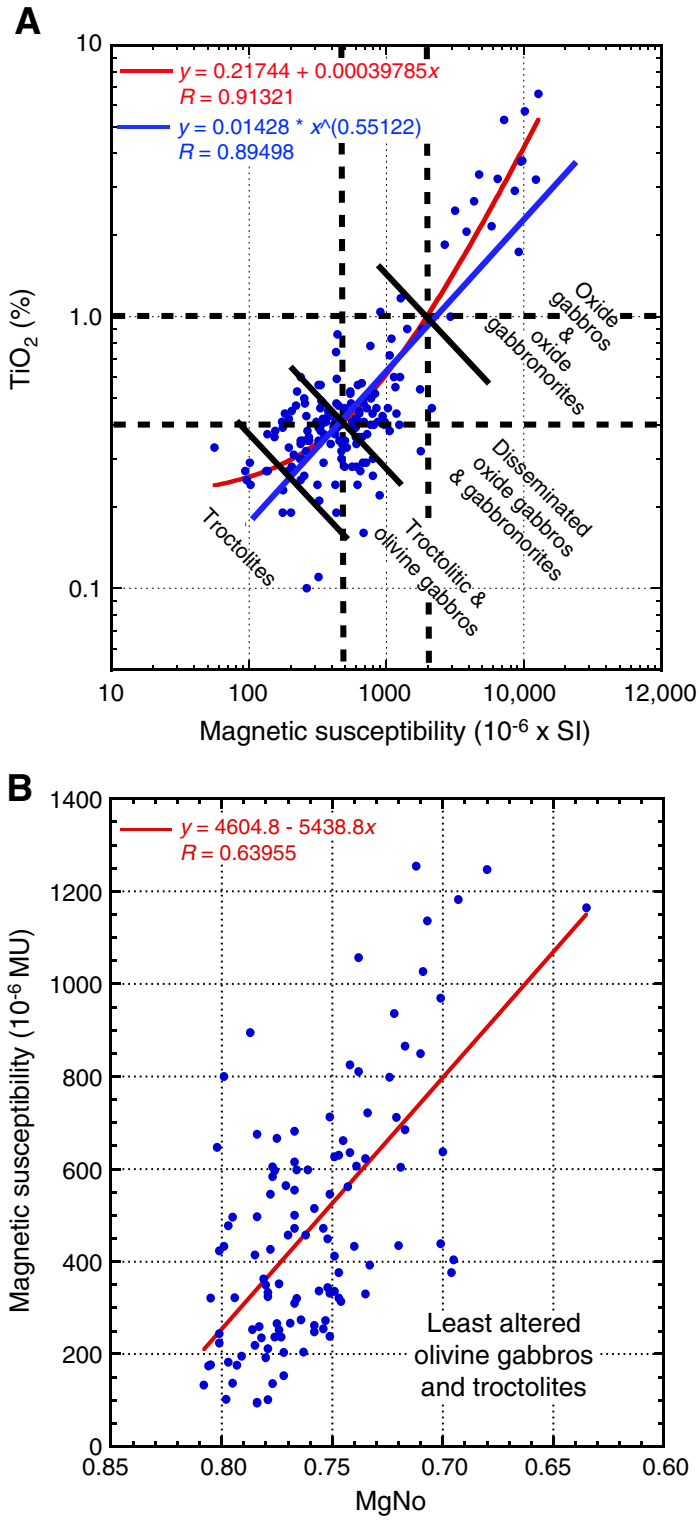

Figure F34. Photomicrographs of magnetite produced by exsolution from silicates in gabbros of Hole 735B. TiO_2 amounts from XRF data and values for magnetic susceptibility below are from the site report (Shipboard Scientific Party, 1999b). Photomicrograph identifications in brackets giving role and photo number (e.g., 7–19) are from the photolog file in the supplemental material portion of the Leg 176 *Initial Reports* volume (Dick, Natland, Miller, et al., 1999). **A.** Sample 176-735B-155R-1 (Piece 2, 10–13 cm) in transmitted light (photo 7–19). Olivine gabbro, lithologic interval 731, TiO_2 = 0.40%, magnetic susceptibility = 810 [10–13 cm. Exsolved oxides concentrated in cleavage adjacent to orthogonal cracks in clinopyroxene. **B.** Same view as A in reflected light (photo 7–20). **C.** Same sample as A exsolved oxides along cleavage in another clinopyroxene (photo 7–12). **D.** Same view as C in reflected light (photo 7–14). The arrow points from a swirl of tiny oxides in C toward the more magnified corresponding swirl in D. **E.** Sample 176-735B-158R-5 (Piece 4, 135–141 cm) in transmitted light (photo 7–25). Leucocratic disseminated oxide olivine gabbro, lithologic interval 769, TiO_2 = 1.04%, magnetic susceptibility = 902×10^{-6} MU. Exsolved oxides in partings in olivine. The partings are oblique to the plane of the thin section. A train of secondary inclusions is oblique to the partings. **F.** Same view as E in reflected light (photo 7–26). The train of secondary inclusions consists of rows of tiny open pits without oxide minerals. The partings in E appear in this view as tiny rows of oxides where they intersect the polished surface of the mineral. **G.** Sample 176-735B-155R-4 (Piece 1, 1–4 cm) in reflected light (photo 7–23). Olivine gabbro, lithologic Interval 732, TiO_2 = 0.28%, magnetic susceptibility = 659×10^{-6} MU. Oxide minerals are in partings in the olivine. **H.** Sample 176-735B-137R-3 (Piece 2A, 34–38 cm) in transmitted light (photo 8–08). Olivine gabbro, lithologic interval 679, TiO_2 = 0.35%, magnetic susceptibility = 237×10^{-6} MU. Magnetite rods exsolved from plagioclase. Also shown in Shipboard Scientific Party, 1999b, figure 18. (**Figure shown on next page.**)

Figure F34 (continued). (Caption shown on previous page.)

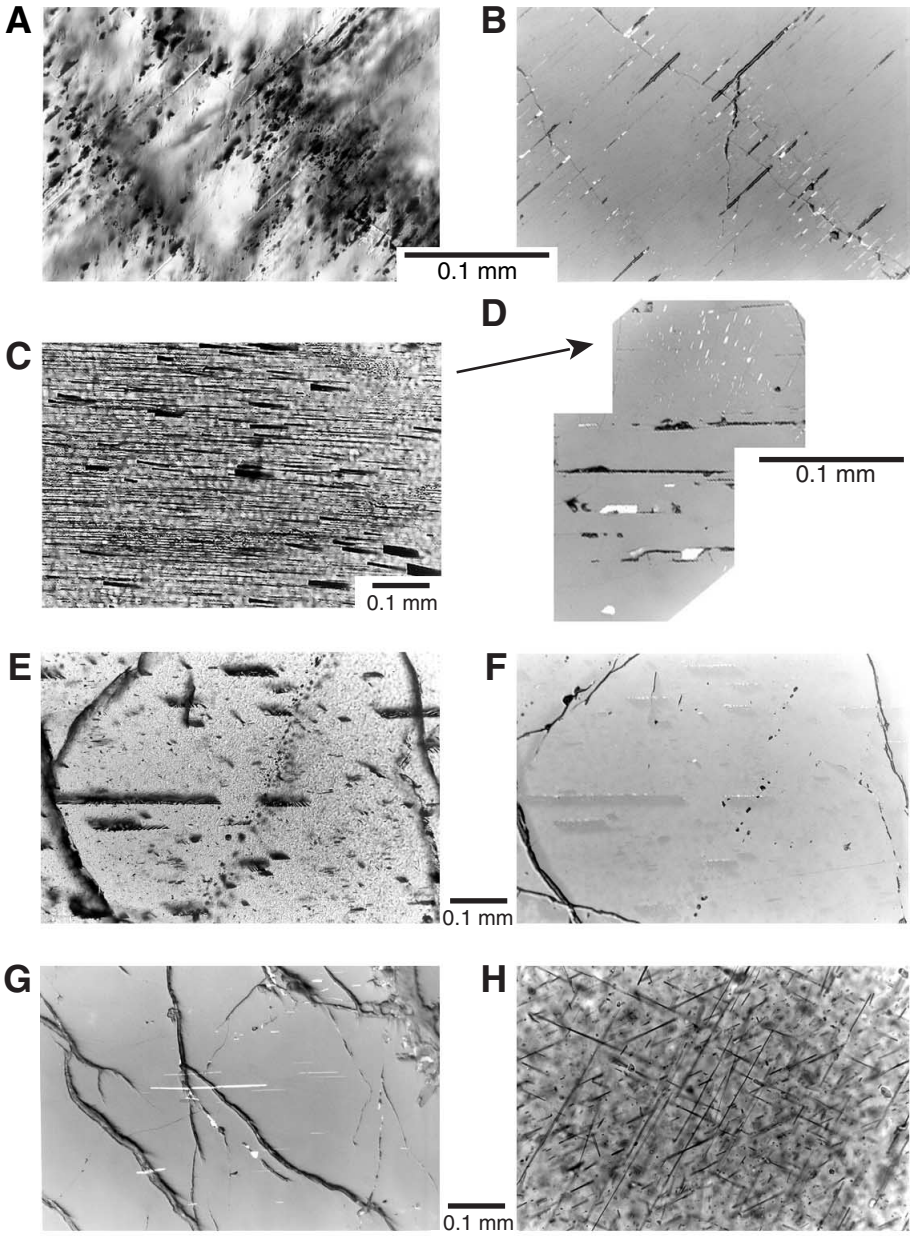

Figure F35. Comparison of FeO contents vs. An for plagioclase phenocrysts in abyssal tholeiites from the Indian Ocean (dots) and in gabbros of Hole 735B (diamonds). Data are from Dick et al. (**Chap. 10,** this volume) and J. Natland (unpubl. data). Solid lines give linear regressions through each group of data.

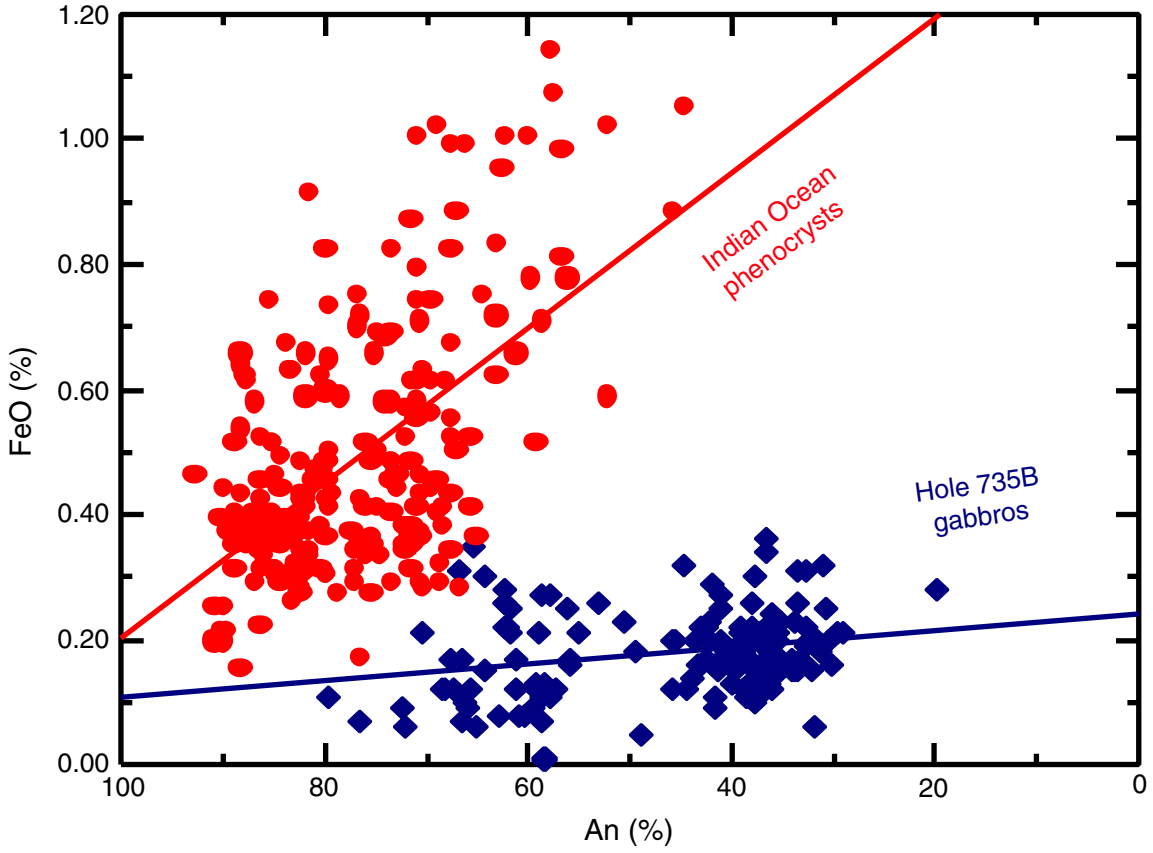

Figure F36. A. Magnetic susceptibility (× 10^{-6} MU) vs. compositions of olivine (Fo%) at corresponding intervals. Data are divided into samples from intervals with background magnetic susceptibility (small dots) and those above background from peaks and peak regions (large dots). Linear and power-law curves are also shown. These have poor correlation coefficients (r = 0.45 and 0.47, respectively). The box encloses selected samples with Fo > 60 and magnetic susceptibility < 1000 × 10^{-6} MU, as discussed in the text. **B.** Background magnetic susceptibility (gray) from Figure F10, p. 42, and Fo contents of olivines selected in A (dots) plotted vs. depth. Curves smooth magnetic susceptibility over 10% of the data (MS), and olivine compositions over 5% of the data (olivine). The fault at 1100 mbsf is shown by the solid vertical line. The dashed vertical lines correspond to minima on the susceptibility curve. The smoothed curves correspond reasonably well except in the zone of fractured altered rock and low recovery from 500 to 650 mbsf. The abrupt change in magnetic susceptibility at the base of the fault zone at 1100 mbsf corresponds to a less distinct downhole increase in Fo contents of olivine at the same depth.